Gdańsk University of Technology
Faculty of Civil and Environmental Engineering
Department of Hydraulic Engineering

Mgr inż. Marlena A. Gronowska-Szneler

DIMENSIONING OF VORTEX SEPARATORS

PhD DISSERTATION

Supervisor: Prof. dr hab. inż. Jerzy M. Sawicki

Gdańsk, 2015

Table of contents

AIM AND SCOPE OF THE DISSERTATION ... 5

1. SOURCES AND QUALITY OF STORM WASTEWATER ... 9

1.1. General remarks ... 9

1.2. Formation of storm run-off ... 9

1.3. Characteristics of urban catchments ... 12

1.4. Quality of storm wastewater collected over urban catchments ... 14

1.4.1. Law requirements ... 14

1.4.2. Sources of pollutants ... 15

1.4.3. Qualitative and quantitative composition of pollutants ... 18

2. DEVICES FOR STORM WASTEWATER TREATMENT ... 21

2.1. General remarks ... 21

2.2. Physical impurities in storm wastewater ... 22

2.3. Mechanical means of wastewater treatment ... 23

2.3.1. Principle of operation of devices for sedimentation ... 24

2.3.2. Principle of mathematical description of particle trajectory ... 26

2.3.3. The concept of vortex separator ... 30

3. CENTRIFUGAL FORCE AS A FACTOR ENHANCING SEPARATION ... 34

3.1. General remarks ... 34

3.2. Description of vortex separator operation ... 35

3.2.1. Fundamental equations ... 35

3.2.2. The need for simplification ... 36

3.2.3. Possibilities of simplification ... 37

4. EXISTING METHODS FOR DIMENSIONING VORTEX SEPARATORS ... 38

4.1. General remarks ... 38

4.2. Description of the methods ... 38

4.3. Verification of the methods ... 41

4.4. Physical analysis of the methods ... 41

4.5. Propositions of corrections ... 43

5. EMPIRICAL DETERMINATION OF LIQUID VELOCITY FIELD ... 45

5.1. Measurements of liquid velocity ... 45

5.1.1. Laboratory test stand ... 45

5.1.2. Location of measurement points ... 48

5.1.3. Measurements methodology ... 49

5.2. Results of measurements 51
5.2.1. General discussion 51
5.2.2. Evaluation of the influence of the Coriolis force 56
5.2.3. Relation between measured and calculated inlet velocities 57

6. DESCRIPTION OF VELOCITY FIELD AND PRESSURE DISTRIBUTION 58

6.1. Choice of the velocity model 58
6.1.1. Analysis of existing possibilities 58
6.1.2. Formulation of general relations 59

6.2. Determination of velocity field model parameters 61
6.2.1. Radial flow 61
6.2.2. Tangential flow 62

6.3. Pressure distribution 68

7. SOLUTION OF THE GENERAL EQUATION OF PARTICLE MOTION 70

7.1. Calculation of the time of particle motion 70

7.2. Determination of the suspended particle trajectory 71

7.3. Practical remarks 73

8. PRACTICAL DESIGN CRITERIA FOR VORTEX SEPARATORS 74

8.1. General remarks 74

8.2. General classification of conditions 74

8.3. The criterion of force balance 75
8.3.1. Description of force balance in vortex separators 75
8.3.2. Determination of the first design criterion 76

8.4. The criterion of the particle time of advection and sedimentation 78
8.4.1. Exact calculation of the time of advection 78
8.4.2. Approximate calculation of the time of sedimentation 79
8.4.3. Approximate calculation of the time of advection 80
8.4.4. Determination of the influence of the centrifugal force on the suspended particle time of advection 82
8.4.5. Determination of the second design criterion 83

8.5. Comparison of the developed design criteria 84

8.6. The influence of the centrifugal force on the difference between suspended particle and carrier liquid velocities 85

9. DETERMINATION OF LIQUID RESIDENCE TIME 86

9.1. General remarks 86

9.2. Measurements methodology 86

9.3. Results of measurements 92

9.4. Comparison of the average residence time and the plug-flow time 94

10. DETERMINATION OF VORTEX SEPARATOR EFFICIENCY 95

10.1. Laboratory test stand 95

10.2. Course of the measurements 97

10.3. Results of the measurements 98

10.4. Design of practical objects 99

CONCLUSIONS 101

ACKNOWLEDGEMENTS 103

NOTATION AND SYMBOLS 104

REFERENCES 106

APPENDIX NO. 1 111

APPENDIX NO. 2 117

APPENDIX NO. 3 127

Aim and scope of the dissertation

"Water is not a commercial product like any other but, rather, a heritage which must be protected, defended and treated as such."

By adopting the Water Framework Directive 2000/60/WE (WFD) the European Parliament and the Council of the European Union established a framework for the protection of inland surface waters, transitional waters, coastal waters and groundwater. Governments of the European Union Member States are obliged to take a new holistic approach to managing their waters with the aim to achieve good status in all waters by the year 2015 and must ensure that this status does not deteriorate in any waters. The WFD defines how this should be achieved through the establishment of environmental objectives and ecological targets for all waters. Poland, as a Member State, must follow the WFD provisions by taking appropriate actions. One of the threats to waters quality are all types of wastewater that is discharged to the environment from municipalities and agglomerations. Following the provisions of law, wastewater must be treated before being introduced to surface waters or ground. The means to fulfil wastewater quality requirements are mechanical methods for wastewater treatment that may be applied separately or combined with other methods (chemical, biological, e.g., a settling tank installed after a biological reactor). Mechanical methods include such devices like screens, settling tanks, grit chambers or separators, which are usually a part of wastewater treatment plants or may also be applied as individual objects. In order to obtain satisfying operation parameters, these devices need to have bigger dimensions. In case of treatment plants, considerable dimensions usually do not pose any problems, with sufficiently vast area for the installation and external funding. On the contrary, individual local devices are problematic. Situated at long distances from cities along roadways, or in urban areas with tight space constraints, they must work alone and without constant supervision. Thus, they should be automatic, efficient, tiny fitting (have smaller dimensions), fracture proof and durable. As a result, such devices are commonly equipped with additional systems enhancing their operation. The most popular devices of such type are separators equipped with special lamella sections that trap suspensions and oils, as well as coalescence inserts that separate oils and remove suspended matter from wastewater. Lamella separators are best to remove suspensions, while coalescence separator are applied to remove oils from wastewater.

Taking into account the law requirements and a limited choice of devices, producers and manufacturers of objects for wastewater treatment seek to find new solutions. One of them is to apply the centrifugal force to enhance the process of separation inside the device. The objects using this force, that have been already introduced on the market, include two types of devices: centrifuges and circulative separators.

Industrial centrifuges, in which the chamber is rotating around a vertical axis, are used for separating solids from liquids, liquid-liquid separation, and liquid-liquid-solid separation. They are characterized by high velocities and generation of several hundreds or thousands of times the earth's gravity. Centrifuges have a vast range of applications, including chemistry, biology, and biochemistry for isolating and separating suspensions; gas centrifuges for uranium enrichment; food processing for refining of vegetable oils and removal of fat from milk; water and wastewater treatment to dry sludges; purification of liquid fuel, air and water on chips and vessels, and many more. Circulative separators are divided into two categories of devices: cyclones and vortex separators that are both characterised by an inlet at a tangent to a cylindrical chamber and an outlet located in the axis of the object.

Cyclones originate from the beginning of the 20th century (White, 1932) and are mainly used as devices for removing dust from air, as well as for water treatment (hydrocyclones). They are characterized by a centrifugal-vertical fluid flow and air fed with high velocities. In cyclones, the centrifugal force directs the suspended particles towards the outer wall away from the central part of the device.

In vortex separators, designed for gravitational removal of suspensions from waste water, liquid is introduced to the chamber at a tangent to the outer wall resulting in a centrifugal-horizontal flow with smaller velocities. Basic research on hydrodynamic vortex separators (HDVS) was described by Smith (1959). A more detailed study on HDVS devices was launched in the 1960s, yielding solutions such as the United States Environmental Protection Agency's Swirl Concentrator or Storm King to remove suspensions from rain water (Andoh and Saul, 2003). At present, some researchers (Cho and Sansalone, 2013) are investigating washout of particulate matter from hydrodynamic separators that are to be integrated into sewer or drainage systems. In spite of having similar construction, cyclones and vortex separators have different levels of efficiency in practical applications, which results from their different dynamics. For instance, the centrifugal force generated by relatively small cyclones that treat air and work under pressure is stronger than that produced by bigger HDVS that work gravitationally and treat waste water. Nevertheless, vortex separators still attract attention as they can make better use of their cubic capacity - dead zones inside the chamber are reduced due to circulation of the liquid, the fact that was quantitatively highlighted by research done by Andoh and Saul (2003).

Taking into account the analogical principle of operation of these two categories of devices, two methods to design cyclones, that are presented in literature (e.g., Mitosek, 1997; Warych, 1998) were applied to design a vortex separator basing on dimensions of separators already in operation. The result indicated that the experiences in cyclones design cannot be applied to vortex separators due to discrepancies in description of force balance and density differences (Gronowska and Sawicki, 2011) and a lack of properly described fluid velocity field. Moreover, the practically oriented methods proposed by various researchers (e.g., Rhodes, 2008; Smith, 1959; Stairmand, 1951; Trawinski, 1969; Veerapen *et al.*, 2005), are questionable. On the contrary, existing models based on Computational Fluid Dynamics, that can be used to simulate operation of the object by determining trajectories of motion of suspended particles (e.g., Dyakowski *et al.*, 1999; Martignoni *et al.*, 2007), also require the equation of particle motion and fluid velocity field and are far too complex to be a technical tool.

Therefore, with a market need for a simple and practical method to design vortex separators, a research problem on a rational model to properly describe operation of these devices arose. **As such the aim of the dissertation was to investigate the velocity field inside a vortex separator and develop formally simple and technically justified design criteria that could be conveniently used in the design process.** The research conducted included a number of steps:

1. Evaluation of the quality of storm wastewater run-off from urban catchments in light of valid law requirements (chapter 1).
2. Review of the devices used for wastewater treatment in wastewater treatment plants and as local objects, as well as introduction of the concept of vortex separator on an example of existing separators in Tczew, Poland (chapter 2).
3. Analysis of the possibility to apply centrifugal force to enhance the operation of vortex separators (chapter 3).
4. Presentation of existing methods of cyclones design (the "movable" and "immovable" critical particle methods) and verification whether these methods for cyclones design can be used to dimension vortex separators (chapter 4).
5. Construction of the laboratory test stand and empirical determination of the velocity field in the laboratory separator with the use of a micro propeller current meter. Graphical presentation of the results (chapter 5).
6. Analysis of the results of velocity measurements and a choice of the velocity distribution model - equations for tangential and radial velocity components. Description of pressure distribution in vortex separators - the concept of the transverse pressure drift (chapter 6).

7. Presentation of general equations of particle motion, description how to use CFD methods to simulate the trajectory of a suspended particle highlighting the need to develop simplified methods (chapter 7).
8. Development of the design criteria basing on the balance of forces acting on a suspended particle inside the vortex separator (the criterion of force balance) and evaluation of the time of suspended particle time of advection and sedimentation (the criterion of the suspended particle time of sedimentation). Comparison of the equations expressing the two criteria (chapter 8).
9. Empirical determination of the time characteristics of vortex separators - tracer measurements using a fluorometric sensor and Rhodamine WT dye. Calculation and comparison of average residence time, modal time and plug-flow time. Graphical presentation of the results (chapter 9).
10. Presentation of sample applications of designing vortex separators using the developed design criteria - construction of the second test stand dimensioned using the criteria. Empirical measurements of the efficiency of the separator prototype based on mass balance of sand samples introduced into the device. Geometrical interpretation of the design criteria (chapter 10).

1. Sources and quality of storm wastewater

1.1. General remarks

Storm wastewater is the product of transformation of atmospheric precipitation into storm run-off. Precipitation occurs when water vapour undergoes condensation in the atmosphere and it may reach the ground both in liquid state - as rain or drizzle, and in solid state - as hail, snow or ice grains. From hydrological point of view, rainfall is the most important form of precipitation. It occurs when ground temperature is above zero. Rainfall depth in Poland is measured within the framework of the State Hydrological and Meteorological Service managed by the Institute of Meteorology and Water Management (IMGW). Information on rainfall is collected in the Central Climatologic Database.

As it contains numerous pollutants, storm wastewaters may be equally or even more problematic for the receiver than municipal wastewater. Storm wastewaters are collected over the catchment area by means of combined or separate sewerage systems. In case of combined sewerage systems, that cover from 30% to 40% of Polish municipal areas (Królikowska, 2011), waters from periodic atmospheric precipitation are directed to wastewater treatment plants together with municipal and industrial effluents, and infiltration waters that also drain during dry weather periods. On the contrary, in separate sewerage systems storm wastewater is not combined with other types of sewage. These systems, developed especially to collect rainwater, are equipped with devices for its treatment prior to discharge to the receiver. The most suitable objects to treat storm wastewater are sedimentation tanks and separators that are described further in the dissertation.

1.2. Formation of storm run-off

A catchment (Fig. 1.1) is an extent of land from which all rainwater drains into one water reservoir, e.g., into a river, a lake or sea. In case of a river basin, the type of catchment most common in Poland, waters flow into the main river, its tributaries and finally into the sea. Catchment area is enclosed by a boundary that separates waters flowing into different river systems. In most cases, catchment boundary is tracked along highly elevated terrain with an assumption that water flows down along the slopes. In every catchment, on the boundary and within the main river bed, a specific point is chosen, called the closing (gauge) cross-section (Szymkiewicz, 1990), through which all rainwater forming storm run-off within the enclosed area exits the catchment as a focused outflow.

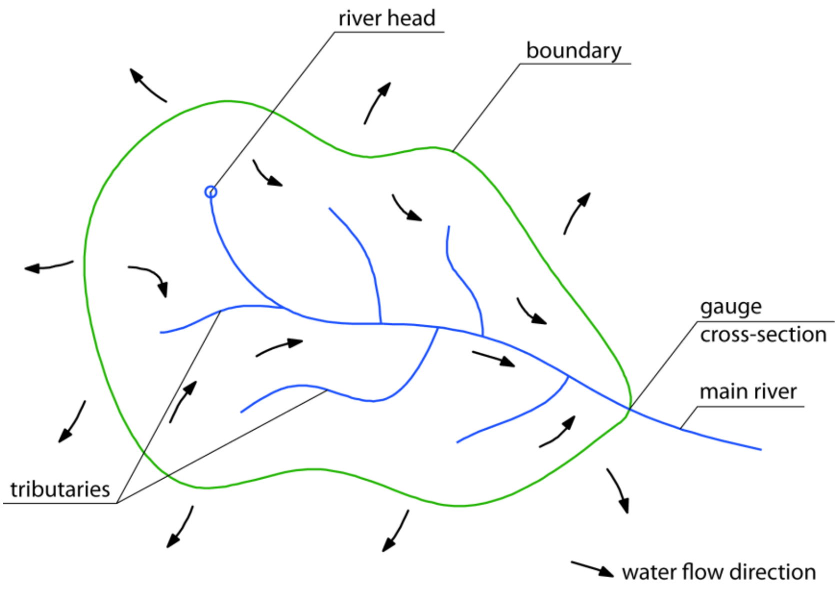

Fig. 1.1. Basic elements of a river basin

From hydrological point of view, catchment is an open physical system as there is a two-directional water flow through its boundary:

– inflow of water in the form of precipitation over the catchment surface;
– partial outflow of water in the form of focused run-off at the gauge cross-section.

In other words, catchment transforms atmospheric precipitation into water outflow from its area.

In order to determine the amount of water that forms storm run-off, distribution of water mass on the catchment surface (water balance) is analyzed. Total precipitation *P(t)* is defined as the average depth of water layer that fell on the catchment area in a unit of time *t* throughout duration of the rainfall. Not all the volume of rainwater contributes to storm run-off as a decent portion is consumed by the “initial water losses” (Szymkiewicz, 1990; Fig. 1.2):

– interception *L(t)* - the amount of water absorbed by plant cover. This process is of significance only in the initial phase of rainfall as every plant is able to absorb a limited volume of water. Furthermore, water absorbed by plants can only be released to the atmosphere in the process of evapotranspiration that is highly limited during rainfall;
– evaporation *E(t)* - the amount of water evaporated from land (including evapotranspiration) and surface waters into the atmosphere;
– depression storage *r(t)* - the amount of water accumulated in local land depressions, especially when soil is low permeable. Water retention occurs in the initial phase of rainfall to diminish completely as surface dips are filled up with water and the process of evaporation is limited;

– infiltration *f(t)* - the amount of water that seeped into the ground thanks to its permeability. In case of a natural catchment which surface is mainly covered by permeable soil, infiltration plays the major role in formation of storm run-off. Water infiltrating into the ground is separated in three different ways: one portion is retained in the ground increasing soil moisture. Soil water retention is particularly high in the initial phase of rainfall when soil is usually dry and able to absorb a relatively high amount of water. This portion is released to the atmosphere in the process of evaporation and plants evapotranspiration. The second part of rainfall (interflow) is stopped by shallow less permeable or impermeable rock formations and discharges onto the ground surface in the form of small periodical springs. The remaining portion of rainwater supplies groundwater flow and penetrates the ground according to rules of filtration.

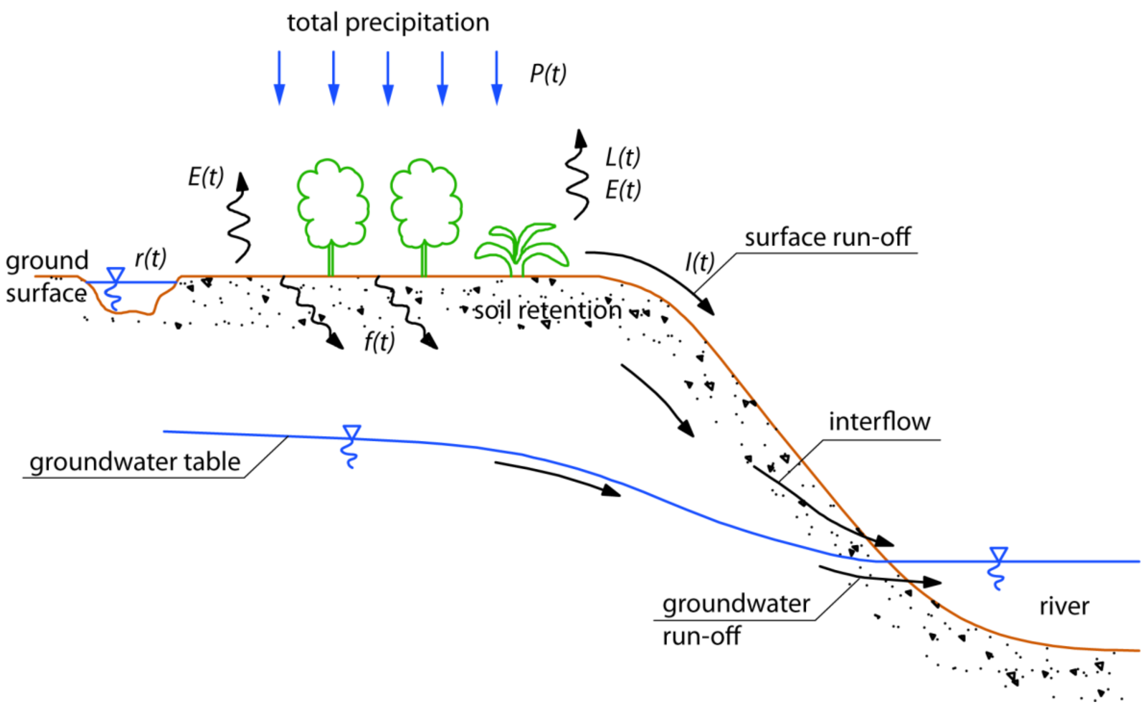

Fig. 1.2. Water distribution over a catchment area (adopted from: Szymkiewicz, 1990)

The remaining volume of rainwater, called the effective rainfall *I(t)*, flows gravitationally according to the slope over the land surface that is either saturated with water or made from impermeable rock formations. Storm run-off may also be seasonally supplied by water from snowmelt and croplands drainage systems.

Taking the described processes into account, water mass balance for a natural catchment looks as follows:

$$P(t)=L(t)+E(t)+r(t)+f(t)+I(t) \tag{1.1}$$

1.3. *Characteristics of urban catchments*

A municipal storm wastewater catchment, further called an urban catchment (Weinerowska-Bords, 2010), is an area separated within the city layout. Water precipitating over a developed area flows into special collectors, usually street storm drains, artificial or natural watercourses, retention reservoirs or other drainage units. As such, urban catchment areas do not intersect with natural catchments boundaries that are set out according to water flow into one receiver.

Moreover, it is impossible to find two identical urban catchments (Babelski, 1999) as they differ by type of land development and use, extent of impermeable and green areas, and most and foremost storm waste water collection systems. Human activities have a massive impact on processes governing water flow within the urban catchment. As a result, in comparison to natural catchments, urban catchments are distinguished by considerable modification of storm wastewater distribution over the catchment area.

In case of a natural catchment, e.g., cropland or forest (Fig. 1.3a), infiltration is the key process in water distribution. In permeable catchments, covered by indigenous soil, about 50% of total precipitation seeps into the ground and almost all remaining rainwater (up to 40%) is absorbed by diverse plant cover. Consequently, storm run-off may be formed only by 10% of the total precipitation. Such a high percent of infiltration in water mass balance results in an elongated time of water flow-through and rainfalls do not cause flash floods.

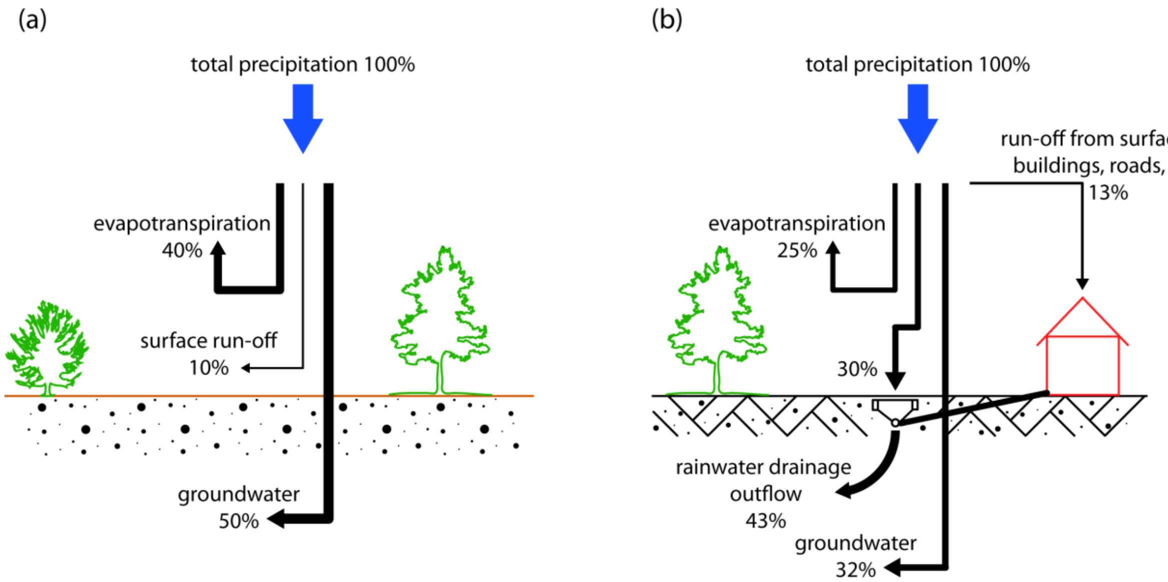

Fig. 1.3. Percentage distribution of rainwater over Ontario catchment in Canada: a) before urbanization; b) after urbanization (adapted from: Rogers, 1994)

On the contrary, from topographical standpoint urban catchments are treated as small impermeable systems (Weinerowska-Bords, 2010). This is a result of a limited size of urban agglomerations, as well as introduction of artificial rainwater drainage systems designed to control water outflow from the catchment. Therefore, the processes determining catchment reaction to rainfall are much more dynamic and rainfall is transformed into outflow much faster than in a natural catchment.

The process of urbanization results in extensive land development - natural surfaces are being replaced by housing, services, industry, transport, etc. Rainwater distribution over the catchment area is modified (Fig. 1.3b) by a number of factors (Szydłowski, 2007; Weinerowska-Bords, 2010):

- changes in topographic features, land cover and land development due to:
    - reduction of plants cover (mainly forests),
    - removal of local retention reservoirs, e.g., ponds and other natural land depressions,
    - regulation of natural watercourses;
- changes in hydraulic conditions of rainwater flow caused by introduction of technical means for rainwater collection, i.a.:
    - construction of artificial channels and street gutters,
    - construction of rainwater drainage systems.

Intensive development of municipal areas is followed by decrease in roughness of storm run-off surfaces and significant sealing of the catchment area. The resulting consequences include (Szydłowski 2007, Weinerowska-Bords 2010):

- 20% reduction in catchment natural capability to retain water resulting in striking decrease or even complete lack of infiltration;
- 15% reduction in interception, evapotranspiration and evaporation processes;
- reduction in depression storage;
- considerable decrease of water flow-through time.

All the aspects listed above disturb the natural water flow by changing participation of particular processes in the hydrological cycle within the urbanized area. Volume of water outflowing from the catchment is increased (Fig. 1.4a) causing a quicker occurrence of storm run-off (time of flood culmination t_c). As the urban catchment reaction time between rainfall and outflow is shorter, flood crest is bigger and occurs faster than in a natural catchment (Fig. 1.4b).

Moreover, an existing rainwater drainage system, in itself, has an impact on the situation under consideration. Regulation of natural watercourses and forced rainwater flow in artificial channels diminishes the time water needs to reach the receiver. This means that local flood risk in municipalities is dangerously high. Additionally, during intensive rainfall even over a limited area, poorly designed or neglected drainage systems may result in rainwater overflow outside the drainage system causing local flooding of houses and infrastructure (Szydłowski 1997).

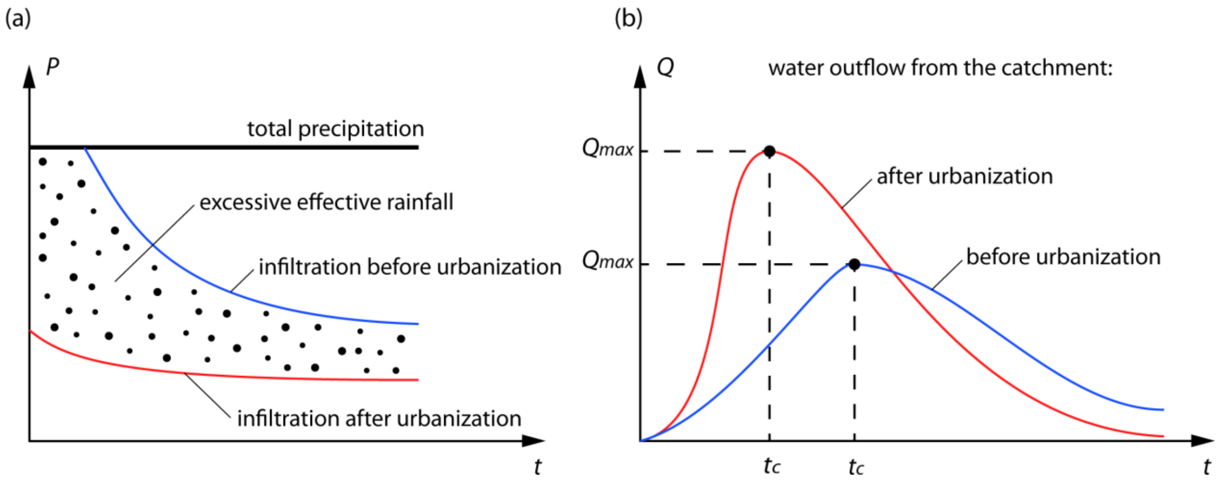

Fig. 1.4. Water outflow from a catchment depending on the state of its urbanization: a) volume of effective rainfall; b) time and volume of flood crest (adapted from: Szymkiewicz, 1990)

Taking into account the relatively small area and consequences of urbanization it was stated (e.g., Weinerowska-Bords, 2010) that the key process responsible for water outflow from the urban catchment is the rainfall itself. Time and spatial variability of rainfall within a separate urban catchment is very high, even to a situation when heavy rain is registered in one district while in the other there is no precipitation whatsoever. Such a distribution of rainfall frequency and intensity is a secondary result of human activities and their impact on the natural hydrological cycle.

1.4. Quality of storm wastewater collected over urban catchments

1.4.1. Law requirements

International law regulations in terms of water management and environmental protection provided by the European Union consider storm run-off from municipal and industrial catchments as a separate category of wastewater that must be adequately managed. Such a statement is based on the quality of rainwater that requires treatment prior to its discharge to the receiver. Mandatory provisions of law oblige water users to treat rainwater as an inseparable element of sustainable development of the municipality, as well as apply solutions that resemble water flow and retention in natural conditions. The requirements stated by the European Union have been transpositioned into two main Polish acts of law concerning water management and their secondary legislation.

According to Art. 4 sec. 2 item c of Prawo Ochrony Środowiska (Environmental Protection Law) rainwater from polluted areas covered with hard surfaces, mainly cities, harbours, airports, industrial and service areas, oil depots, roads, and parking lots, collected by drainage systems, is defined as wastewater. Main indicators characterising the quality of storm wastewater include (Sawicka-Siarkiewicz, 1999) suspended solids, oil derivatives (determined as ether extract), chemical oxygen demand, chlorides (from anti-freezing agents), as well as special indicators depending on the type of the catchment, e.g., heavy metals in case of industrial plants.

The executive act to Prawo Wodne (Water Resources Law) - the Ordinance of the Minister of the Environment of 24 July 2006 lists and describes specific requirements that must be met by wastewater discharged into surface waters or ground. According to par. 19 sec. 1 of the Ordinance rainwater from hard surfaces of polluted areas, industry, storage facilities, oil depots, harbours, airports, cities, railway facilities, roads, parking lots bigger than 0.1 ha, collected by sealed, open or closed drainage systems and discharged into surface waters or ground should not contain more than 100 mg/dm^3 of total suspended solids, as well as no more than 15 mg/dm^3 of oil derivatives. Moreover, according to par. 11 sec. 3 item 4 rainwater should met the same requirements prior to mixing with domestic wastewater, drainage waters from mining operations, cooling waters or process waters from water purification plants.

Concluding, storm run-off generated by rainfall of intensity at least 15 dm^3/s ha that is discharged from the urban catchment into surface waters, ground or mixed with other kinds of wastewater, should undergo treatment on the outflow to the receiver to contain no more than 100 mg/dm^3 of total suspended solids and no more than 15 mg/dm^3 of oil derivatives. Such quality requirements can be met by e.g., installing separators, which are the focus of the dissertation, within the sewerage system.

1.4.2. Sources of pollutants

According to a general statement (e.g., Fidala-Szope, 1980) quality and properties of storm wastewater depend on three fundamental factors:

- parameters of atmospheric precipitation - pollutants carrier;
- characteristics and state of the catchment - pollutants source;
- sewerage system - storm wastewater transportation network.

These three factors are identified with three stages during which rainwater is transformed into storm wastewater (Fig. 1.5).

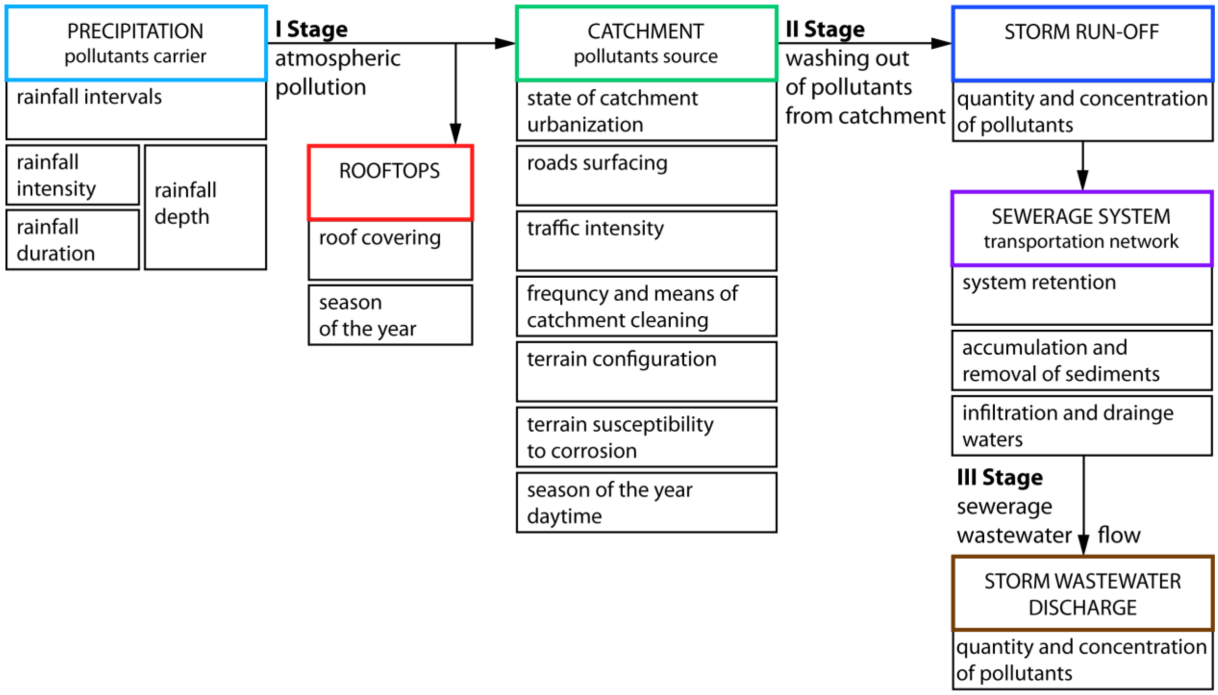

Fig. 1.5. Factors responsible for storm wastewater quality (adapted from: Sawicka-Siarkiewicz, 1999)

First negative changes in water quality (first stage of rainwater pollution) occur when precipitation passes through lower parts of the atmosphere. As water comes in contact with pollutants present in the air, water droplets adsorb solid, liquid and gaseous particles (Tab. 1.1). Chemical composition of rainwater depends mainly on the rate of atmospheric pollution coming from industry and municipalities, as well as climatic and meteorological conditions, e.g., depth, distribution and intensity of rainfall, direction and speed of wind. Most important indicators of spatial pollutants present in atmospheric precipitation include elements responsible for water eutrophication: nitrogen, phosphorous and their chemical compounds used in substances employed in agriculture and farming (Fidala-Szope, 1980; Sawicka-Siarkiewicz, 1999; Szymańska, 1986; Tarnowski and Wira, 2000).

The major part of substances contaminate rainwater as it flows over sewered areas of the catchment (second stage of rainwater pollution). The capacity of rainwater to washout pollutants depends on its three fundamental parameters: intensity, depth, and time of duration. The higher the rainfall intensity, the higher the rainfall washout efficiency. The load of washed pollutants increases with duration of rainfall, thus rainfall depth (Sawicka-Siarkiewicz, 1999). Moreover, elongation of time interval between subsequent rainfalls indentified with time of pollutants accumulation on the catchment surface, results in greater pollution load washed out by rainwater. In case of a few hours time interval between rainfalls, the first rainfall will carry the pollutants away from the catchment surface ant its outflow will be significantly contaminated, whereas, the second rainfall will be far less polluted (Fidala-Szope, 1980). Additionally, pollution load depends also on hydraulic conditions of water flow; flow velocity and terrain slope in particular. The higher the slope, the higher the water velocity, and consequently higher load of washed contaminants; and vice versa.

Tab. 1.1. Types of pollutants present in atmospheric precipitation (based on: Fidala-Szope, 1980; Królikowska, 2011; S.A. Rybicki and S.M. Rybicki, 2001; Sawicka-Siarkiewicz, 1999)

Pollution stage	Contaminants
I Stage **Atmospheric pollution**	– dust and particulates lifted from ground surface, – furnace smokes and industrial fumes, by-products from fuel burning, – radioactive dust, aerosols, tree and flower seeds, microorganisms (bacteria and viruses), – chemical fertilizers, pesticides.
II Stage **Washing out of pollutants from the catchment**	– dry and wet deposition from atmospheric pollution, – rooftops erosion, – organic matter: plant fragments, animal manure, – gravel, sand, silt and clay washed out from ground surface, – products of abrasive wear of roads pavement, road litter, – products of abrasive wear of car tyres, oils, grease, car fuel, exhaust gases, – raw materials, semi-finished products or industrial waste on the terrain of a production plant, – glaze frost removing agents (sand, mineral aggregate), – substances improving crop growth.
III Stage **Sewerage wastewater flow**	– sediments and particulate suspensions dragged from drains bottom.

The amount of pollutants accumulated on the catchment surface depends on a number of factors (Fidala-Szope, 1980; Piotrowski and Roman, 1974; S.A. Rybicki and S.M. Rybicki, 2001; Sawicka-Siarkiewicz, 1999):

- catchment area, land development and use;
- extent of green areas within the city;
- number and type of production plants, applied technology and correctness of operation from environmental protection point of view;
- rate of atmospheric pollution within the catchment boundary;
- soil type and crop management, as well as intensity and means of fertilization;
- damages and accidents, especially road crashes;

- maintenance of hard and unpaved surfaces;
- constructions and repairs, frequency and cleaning of the catchment area;
- areas covered with sewerage systems;
- geological structure of the terrain, as well as range and intensity of erosion;
- duration of snow cover, season of the year.

Furthermore, intensive development of road transport in Poland is followed by significant increase in the amount of pollutants washed out from streets, roads, squares, etc. (Piotrowski and Roman, 1974; S.A. Rybicki and S.M. Rybicki, 2001). Their volume and type depend on roads layout, type of pavements, means of road transport, kind of cargo, intensity of road and pedestrian traffic, means of streets cleaning and removal of glaze frost, reinforcement of road slopes, and also on technical condition of vehicles, type of fuel used or driving techniques, etc.

Quality of storm wastewater flowing through sewerage drains (third stage of rainwater pollution) is influenced mainly by accumulation and removal of sediments from settling tanks and channels, as well as hydraulic conditions of wastewater flow within the system. Additionally, wastewater quality is affected by contaminants carried by drainage and infiltration waters inflowing to the system (Sawicka-Siarkiewicz, 1999).

1.4.3. Qualitative and quantitative composition of pollutants

Storm wastewater collected over urban catchments is generally discharged into surface waters, mainly rivers, streams, springs, lakes, ponds and seas. Receivers most susceptible to pollution include (Osmulska-Mróz, 1991; Piotrowski and Roman, 1974): small watercourses and reservoirs, groundwater lying under permeable rock formations, as well as surface waters important for human economy (water supply for cities and industry, fish ponds, transport of cargo, generation of electrical energy, water sports, etc.). Significance of water requires its quality to be sufficient to support natural biological life in surface waters. That is why, wastewaters discharged into receivers can neither have a negative influence on biological equilibrium nor on economic use of water. Discharge of untreated or improperly cleaned wastewater may reduce oxygen content in water, change water temperature, make water toxic and change its chemical composition, disturbing biological life in the receiver and making water unavailable for use (Piotrowski and Roman, 1974; Zakrzewski and Żabowski, 1963).

The main contaminant of storm wastewater is suspended mineral matter which is the carrier of the majority of other substances present in storm run-off. Tiny fractions of mineral matter adsorb, among others, organic compounds, heavy metals, bacteria and oils, on its surface. Smaller amounts of suspended organic matter originate from marketplaces and green areas, and occur also as fallen leaves in autumn. In general, concentration of suspended matter varies greatly with highest values from several to more than ten thousand mg/dm^3 present in snowmelt run-offs and waters from unmanaged terrain suspected to erosion. According to Dąbrowski (2001) and Królikowska (2011)

1 ha of sealed surface generates 655 kg of suspensions, 630 kg of chemical oxygen demand, 15 kg of hydrocarbons and 1 kg of lead annually, and average specific gravity of suspension ranges from 2.2 to 2.6 g/cm^3.

Storm run-off from industrial sectors may contain pollutants generated during production processes and waste raw materials used for manufacture. These substances include heavy metals, by-products from fuel burning, sulphuric acid, hydrogen sulphide, sulphur dioxide, etc., that are harmful to human health and the environment. According to S.A. Rybicki and S.M. Rybicki (2001), for average atmospheric pollution in Poland, 13700 kg of total nitrogen, 472 kg of total phosphorous, 24000 kg of sulphates, 33.8 kg of lead and 3.17 kg of cadmium are deposited on water surface of a 1000 ha reservoir annually.

Contaminants originating from road traffic, mainly suspensions, lead, grease and oils, phosphates, all forms of nitrogen, chromium, copper, nickel, zinc, cadmium and mercury, accumulate on road surfaces, roadsides and nearby terrain. These substances are then washed out by rainfall and end up in surface waters. Their proportions and loads differ depending, among others, on the state of technological development. Concentrations of pollutants in storm run-off from highways and expressways have a wide range of values (S.A. Rybicki and S.M. Rybicki, 2001), e.g., amount of suspensions can oscillate between 5÷800 g/m^3 (mean value 136 g/m^3, and allowable value 100 mg/dm^3), chemical oxygen demand 5÷700 gO_2/m^3 (mean value 98 g/m^3), ether extract 5÷25 g/m^3 (mean value 6.8 g/m^3, and allowable value 15 mg/dm^3).

Groundwaters that are insufficiently isolated from surface run-off can also become polluted by rainwater. Groundwater quality depends on geological structure of terrain, soil permeability and rate of water infiltration through the soil. During storm run-off from roads, suspensions, organic substances, have metals, sulphates and chlorides may seep into the ground (S.A. Rybicki and S.M. Rybicki, 2001).

Research conducted on quality of outflow from different rainwater sewerage systems in Poland indicate the danger caused by discharging storm wastewater into receivers (Tab. 1.2). Average concentrations of suspension in rainwater collected over specified catchments exceeded the allowable value (100 mg/dm^3) for storm wastewater discharged into surface waters and ground provided by the Ordinance of the Minister of the Environment listed in subsection 1.4.1. On the other hand, average values of ether extract reached the allowable value (15,0 mg/dm^3) in two cases out of four. According to Fidala-Szope (1980) and Królikowska (2011) the ratio of annual loads of contaminants in storm wastewater and loads in untreated municipal sewage ranges between several to more than tens of percent depending on the quality indicator. Thus, the pollution loads carried by rainwater to the receiver may be noticeably big.

Tab. 1.2. Sample results of storm wastewater measurements from different Polish catchments (based on: Garbarczyk, 1997; Osmulska-Mróz, 1991; Sawicka-Siarkiewicz, 1999; Tarnowski and Wira, 2000)

Measurement date/year	Type of catchment	ChZT* [mgO$_2$/dm^3]	pH	Suspended solids [mg/dm^3]	Ether extract [mg/dm^3]
1999	housing estates Warszawa	5.0 - 2950.0	5.1 - 9.8	7.0 - 6430.0	0.0 - 117.6
13.07.1999	„Górny Brzeg” Szczecin	557.4	6.5	621.0	-
02-03.1996	downtown Białystok	219.0	7.2	258.0	43.0
1988-1991	expressway Gdańsk-Warszawa	157.3	-	164.6	12.8
1988-1990	expressways Poland	362.2	-	291.8	14.2

* ChZT - chemical oxygen demand

Furthermore, research conducted by author of the dissertation (Gronowska, 2012b) confirms the statement given above. In order to evaluate the quality of storm run-off within the Polish Tri-City agglomeration, series of samples were collected from various points in Gdańsk and Gdynia, Poland, in late autumn 2011. Concentration of suspensions in wastewater samples were in the range from 123.0 mg/dm^3 to 1021.4 mg/dm^3, so exceeded the allowable value of 100 mg/dm^3. Also, results of ether extract determination gave values higher than the allowable limit of 15 mg/dm^3, as they were in the range from 1.3 mg/dm^3 to 179.3 mg/dm^3.

Concluding, determination of a method to design separators that could be installed in rainwater sewerage systems to treat storm wastewater is pursued and well-justified.

2. Devices for storm wastewater treatment

2.1. General remarks

As explained in the previous chapter (subsection 1.4.3) urban catchments should be equipped with systems to drain, treat and discharge rain and snowmelt waters from developed areas into local surface waters. Storm and snowmelt run-off discharged into surface waters undergo the process of water self-purification. With the use of dissolved oxygen and sunlight, microorganisms decompose contaminants into carbon dioxide CO_2, water and simple organic compounds (Zarzycki *et al.*, 2007). These processes are highly beneficial, however, they occur with small intensity. Thus, for the self-purification process to take place, wastewater directed into the receiver must fulfil certain basic requirements (Zakrzewski and Żabowski, 1963):

– wastewater must not reduce oxygen content in water beneath the minimum level;
– wastewater must not contain impurities that, when present in bigger amounts, might toxically interact with indigenous microflora and microfauna;
– wastewater must not disturb the biological equilibrium of the receiver.

When wastewater contains more pollutants than the receiver can neutralize, the processes of self-purification are stopped and surface water undergoes degradation. The impurities that are not removed have a highly negative impact on water (Zakrzewski and Żabowski, 1963). Floating bodies accumulate on water surface or near the shores resulting in an unpleasant visual experience. Moreover, emulsions may form a surface film and block oxygen transfer from air to water. Suspensions settle on the receiver bottom forming layers of sediments. Organic substances undergo putrefaction which disorders natural biological life.

Full treatment or at least preliminary pretreatment of wastewater prior to its discharge into the receiver is an inseparable element of environmental protection. Wastewater treatment involves complete removal or, at the very least, decrease in the amount of contaminants, or their transformation into harmless forms. Technologies intended for wastewater treatment are divided into two general groups (Zarzycki *et al.*, 2007): methods based on biological processes and methods employing physical and chemical processes. An integral part of these two groups are mechanical means of wastewater treatment. Objects designed for storm wastewater treatment are divided into three groups (Cywiński *et al.*, 1983):

– devices for storm wastewater retention, e.g., storage tanks, settling tanks, ponds, installed as a part of the sewerage system;

- individual objects and special devices intended specifically for storm wastewater treatment, e.g., screens, grit chambers, settling tanks, filtration fields, sewage ponds;
- devices being a part of municipal sewage treatment plants, used for sewage treatment during dry weather, and also for storm wastewater treatment during rainfalls, as well as sewage from combined sewerage systems (subsection 1.1).

Taking into account the aesthetics of local surface waters in cities, storm wastewater treatment may sometimes be limited to a set of screens (cleaned manually or mechanically) to stop larger floating bodies, and grease removal tanks. When a higher degree of receiver protection is required, comprehensive methods of treatment are combined with wastewater retention. In order to establish the relation between requirements of the receiver and scope of wastewater treatment, each case needs to be analyzed individually. However, every time storm wastewater treatment must include the removal of physical impurities and oil derivatives by mechanical means.

2.2. Physical impurities in storm wastewater

Physical impurities present in wastewater include insoluble, mineral or organic emulsions and suspensions of different degree of dispersion. Solids may either float on the surface, when their specific gravity is smaller than wastewater, or be suspended in the liquid, when their specific gravity is bigger than wastewater. Depending on the degree of suspension and shape of the particles with given flow velocity, suspended solids remain in wastewater as suspensions or settle at the bottom as sediments. Suspensions may be categorized according to a number of factors. Taking into account the degree of dispersion of particles forming the suspension, two types of suspensions are distinguished (Sawicki, 2007):

- macroscopic suspension (average particle size bigger than the limit size $d_p > 10^{-6}$ m);
- microscopic suspension (average particle size smaller than the limit size $d_p < 10^{-6}$ m).

On the other hand, referring to suspension susceptibility to be removed from the wastewater stream, suspensions are divided into three groups (Zakrzewski and Żabowski, 1963):

- settleable solids that settle at the bottom of the Imhoff cone during first two hours of separation (the Imhoff cone is a laboratory test vessel in the form of a cone turned upside-down used to measure volume of solids, present in water or wastewater, that settled at the bottom after a specified time period);
- non-settleable solids that settle at the bottom of the Imhoff cone after two hours of separation;

– colloids - non-soluble solids of such a degree of dispersion they cannot be separated from wastewater in the process of sedimentation.

Both settleable and non-settleable particles tend to be relatively easy separated from wastewater compared to other types of impurities.

In wastewater technology (Kujawa-Roeleveld *et al.*, 2011), all mineral impurities composed of granular particles that do not undergo decomposition by microorganisms are referred to as so called “grit”. In general, grit is formed by sand, slag, small cobbles, seeds, coffee grounds, eggshell, etc. From petrographic point of view, sand is a naturally occurring granular material composed of finely divided sedimentary rock in the form of loose non-bounded mineral particles. Most common constituent of inland sand is silica (silicon dioxide), usually in the form of quartz. Particle size varies from 0.063 mm to 2 mm and density of quartz sand is circa 2.62 g/cm^3 (Manecki and Muszyński, 2008). According to standard PN-EN ISO 14688:2006 sand is divided into three fractions:

– coarse grained sand: 2.0 mm ≥ d_p > 0.63 mm;
– medium grained sand: 0.63 mm ≥ d_p > 0.2 mm;
– fine grained sand d_p ≤ 0.2 mm.

Sand deposits cover a relatively large part of Polish territory. Being that abundant, sand is used for various purposes, mainly as a basis for glass, concrete, mortar and cement plasters.

2.3. Mechanical means of wastewater treatment

Mechanical methods of wastewater treatment include processed applied to separate physical contaminants according to their properties (Zarzycki *et al.*, 2007), such as: straining, gravitational separation (sedimentation and flotation) and filtration. These processes comprise the preliminary stage of wastewater treatment.

Straining is the first process of mechanical treatment and is used to stop solids of relatively high dimensions d_p > 3 mm (Roman, 1986), that are floating or dragged by wastewater. Sewage containing contaminants is passed through a system of screens which mesh size is chosen appropriately to devices situated next within the treatment system, and then directed to decanters. Solids accumulated on screens, mainly organic substances, e.g., paper, rags, food remains, etc., are removed by scrapers and transported to special containers for disposal.

The process of sedimentation is carried out in settling tanks, as well as grit chambers and separators, in which flow velocity is relatively low. Solid particles and fine suspensions of diameter smaller than d_p < 1-3 mm and heavier than water, settle at the device bottom due to sedimentation (spontaneous falling of suspended particles to the bottom under influence of the gravity force). Cleaned wastewater flows through horizontal overfalls and out from the settling tank, while sediments accumulated in the sedimentation cone are directed for further filtration or thickening.

Flotation is an inverse process to sedimentation, as dispersed contaminants with density smaller than that for water, float to the surface forming a thin film that is removed by special mechanical devices (spontaneous gravitational flotation). Introduction of air into the flotation chamber allows also to remove solids that are heavier than water. These particles are adsorbed on air bubbles, raise to the surface and form a layer of froth (dissolved air flotation). Flotation is often employed to remove grease and oil (that do not mix with water) from wastewater in oil separators.

Filtration is the process during which suspensions removed from wastewater by means of gravitational separation are passed through a filter medium which stops certain contaminants by creating a filter cake. The process of filtration is driven by pressure difference between both sides of the filter. This can be obtained in two ways: either by increasing pressure on the feed side (pressure filter) or by inducing negative pressure on the other side (vacuum filter). The majority of filters applied in wastewater treatment include continuously operating filter press, band filter, vacuum drum-type filter or plate filter. Suspensions separated by means of filtration are directed for disposal.

2.3.1. Principle of operation of devices for sedimentation

As already mentioned, the process of sedimentation of suspension present in wastewater is employed in three types of devices: grit chambers, settling tanks and separators. In grit chambers, both settleable mineral solids (e.g., sand, slag) and indecomposable organic matter (e.g., small pieces of hard coal) can be removed, whereas, in settling tanks and separators - only mineral matter.

Grit chambers are located at the beginning of the technological line of wastewater treatment and play the key role in every urban wastewater treatment plant. Without a grit chamber, grit would be removed from wastewater stream not before preliminary settling tanks and transported with other sediments to the biological treatment section. There, grit would create a difficult to remove cemented mass decreasing cubic capacity and interfering with the operation of treatment units such as anaerobic digesters and aeration tanks. Moreover, removal of grit in grit chambers protects pipes and channels from clogging and pumps from mechanical abrasion and abnormal wear. A properly designed and maintained grit chamber stops heavier mineral suspensions simultaneously fulfilling the principal requirements (e.g., Piotrowski and Roman, 1974):

– particles larger than $d_p > 0.2$ mm are completely removed from wastewater stream (stopped in 100%);
– particles of diameter in the range of 0.1 mm < d_p > 0.2 mm are removed from wastewater stream in 65-75%;
– particles smaller than $d_p < 0.1$ mm may remain in wastewater stream;
– organic matter content in sediment must not exceed 10% by weight (organic particles are responsible for decomposition of sediment collected from the grit chamber).

In order to allow the sedimentation process to occur, grit chambers have the shape of a rectangle of dimensions chosen as to maximally fulfil the conditions listed above. Taking into account the direction of wastewater flow grit chambers may be divided into the following groups (Kujawa-Roeleveld *et al.*, 2011):

– long rectangular grit chambers with horizontal flow;
– aerated grit chambers with helical flow;
– circular grit chambers with vortex flow;
– circular grit chambers with vertical flow.

Settling tanks retain mineral matter formed by tinier particles than in case of grit chambers, and also substances lighter than water (e.g., PVC pieces, fruit skins and fats mechanically collected from wastewater surface) that were not removed from wastewater in devices preceding the settling tank. Settling tanks come in two types, depending on their function and placement within the technological line: preliminary settling tanks that remove suspensions present in inflowing wastewater and secondary settling tanks that stop suspensions formed during biological and mechanical wastewater treatment. Taking into account the direction of flow the following groups of settling tanks are distinguished (Piotrowski and Roman, 1974):

– settling tanks with horizontal flow of theoretically parallel wastewater streams;
– centrifugal (radial) settling tanks with horizontal flow of wastewater streams directed radiant from the centre to the tank perimeter;
– settling tanks with vertical flow from the bottom to the top;
– settling tanks with skewed flow from the bottom to the top.

In practice, settling tanks have the following applications (Roman, 1986):

– local devices:
    - septic tanks for individual estates or groups of buildings that lack combined sewerage systems;

- fuel oil traps for industrial sewage pretreatment prior to its introduction into urban sewerage systems;

– an element of municipal wastewater treatment processes;
– an element of industrial sewage treatment processes;
– pretreatment of storm wastewater at its discharge point to the receiver.

A properly designed settling tank reaches the percentage reduction in the amount of total suspended solids by 30-40% and settleable solids by over 90% with retention time 1.5-2.0 h and without the use of additional chemical agents (Cywiński *et al.*, 1983).

2.3.2. Principle of mathematical description of particle trajectory

Non-homogeneous systems are divided into two categories: solutions and suspensions. In terms of fluid mechanics these categories are distinguished by unit processes that influence motion of the dispersed substance:

– in case of solutions: transport by the solvent (advection) and transport by diffusion;
– in case of suspensions: transport by the carrier liquid (advection) and gravitational motion (does not apply to colloids) caused by density difference between the liquid and the suspended particle (sedimentation or flotation).

Such a division of processes responsible for transport of dispersed substances in liquids requires their specific quantitative description. This fact is also important to technical objects design. In this approach solutions may be considered as physically homogenous continuous media and their motion described by physical quantities, mainly by velocity and concentration of each dissolved substance (phenomenological method - Sawicki, 2007).

In case of suspensions, the situation is different. Although, these media can be formally treated as solutions (especially colloids with turbulent motion when gravitational separation does not occur and relative motion is related to turbulent diffusion), such an approach can be applied only in individual cases. In general, motion of suspension is described by trajectories of particular particles together with analysis of their course and structure (structural method - Sawicki, 2007).

The shape of the trajectory of an individual particle is described by a simple differential relation of the particle radius vector $\mathbf{r_p}$ and its velocity vector $\mathbf{v_p}$:

$$\frac{d\mathbf{r_p}}{dt} = \mathbf{v_p} \tag{2.1}$$

where particle velocity vector $\mathbf{v_p}$ is determined from Newton's second law of motion.

Taking into account the characteristics of suspensions, particles occurring in systems related to environmental engineering are considered as material points with translational motion, that do not affect each other. Thus, equation of particle motion acquires the simple form (Gronowska, 2012a; Sawicki, 2007; Soo, 1969):

$$m_p \frac{d\mathbf{v_p}}{dt} = \mathbf{F_M} + \mathbf{F_P} + \mathbf{F_{AM}} + \mathbf{F_N} \tag{2.2}$$

where: m_p - mass of the particle which trajectory is determined; $\mathbf{F_M}$ - resultant mass force (including centrifugal force in the considered case of curvilinear motion); $\mathbf{F_P}$ - resultant force related to changes in pressure across the particle trajectory (including transverse drift); $\mathbf{F_{AM}}$ - associated mass force; $\mathbf{F_N}$ - drag force.

As there is no practical possibility and justification to determine trajectories of each individual particle forming the suspension, only characteristic particles are taken into account. Such particles are chosen basing on two aspects:

– dynamic properties of the particle (defined by physical quantities included in equations of motion) - usually particles are divided into different fractions and each group is represented by a characteristic particle typical of the fraction;
– initial position of the particle chosen so that trajectory of particle motion sufficiently defines behaviour of the whole fraction.

While dealing with practical problems a set of characteristic trajectories is matched with geometry of the object. Two general categories of such problems include:

– operation problem: characteristic trajectories are determined for a known or an existing object to evaluate its efficiency of operation; principle of such a problem referred to devices for suspension removal is presented in Fig. 2.1.

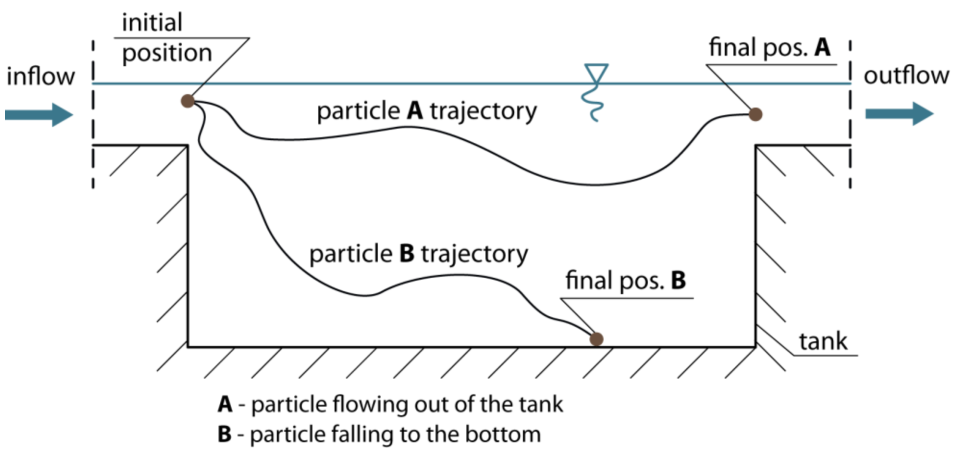

Fig. 2.1. Schematic diagram of an operation problem

– design problem: geometry of an object being designed is chosen so that characteristic trajectories fulfil certain requirements - Fig. 2.2.

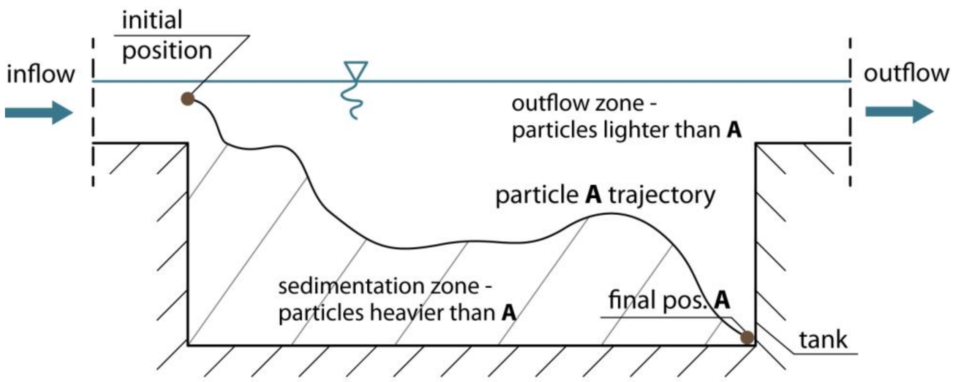

Fig. 2.2. Schematic diagram of a design problem

In general case, relations (2.1) and (2.2) are mathematically complex, thus they can only be solved by numerical methods. However, such a set of equations proves to be a useful tool in hands of both a researcher and an engineer. Solution of these equations results in detailed course of particle trajectories presented on graphs, e.g., in Fig. 2.3.

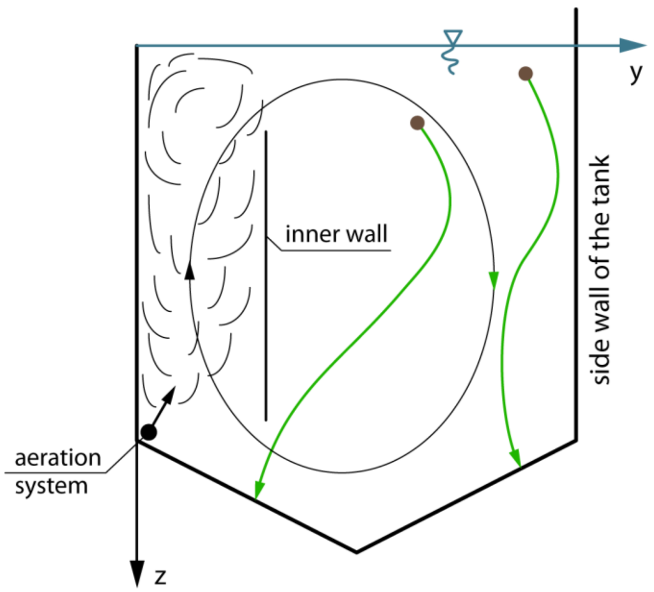

Fig. 2.3. Sample course of a particle trajectory in an aerated grit chamber determined by numerical means

Fortunately, technical objects frequently have simple shapes and can be described by simplified models yielding approximate relations that are very convenient in everyday work of an engineer. For instance, a settling tank in the shape of a rectangular cuboid (Fig. 2.4) is technically approved to be described by a mean velocity model. In such a case, equation (2.1) can be replaced by:

$$\frac{dx}{dt} = u_{av} = \frac{Q}{WH} \tag{2.3}$$

$$\frac{dz}{dt} = v_{fs} \tag{2.4}$$

where: u_{av} - mean liquid velocity; Q - discharge; W - tank width; H - liquid depth; v_{fs} - particle free sedimentation velocity.

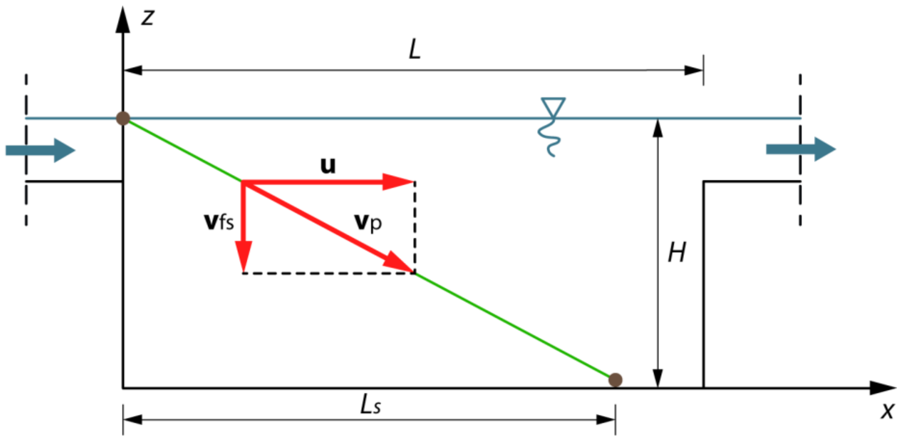

Fig. 2.4. Simple computational scheme for a rectangular settling tank

Division of relations (2.3) and (2.4) by sides provides an equation that describes linear trajectory of a particle:

$$\frac{dz}{dx} = \frac{v_{fs}\, WH}{Q} = \frac{H}{L_s} \tag{2.5}$$

where: L_s - settling tank minimum length which guarantees that every particle moving with free sedimentation velocity v_{fs} is removed from the liquid stream. In practice, this value becomes a limiting factor that is most commonly regulated by requirements of the technological process taking place inside the tank. The object designed in such a way ensures that all particles bigger than the limit particle will be removed from the liquid and all particles smaller than the limit size will remain in the flowing stream.

Acceptance of such a method to describe operation of devices for suspension removal makes the ideal (theoretical) efficiency ε of the object to appear as a discrete line in Fig. 2.5. By referring to the requirements of grit chamber operation stated in subsection 2.3.1, it can be seen that the device fundamental parameter is the limit size of the particle d_{pmax} = 0.2 m that together with bigger ones must be completely removed from the liquid stream. The second particle size d_{pmin} = 0.1 mm is only supplementary and expresses "technical caution" of the designer. Real effectiveness of such an object is expressed by a specific continuous line. As it is impossible to mathematically determine the real effectiveness of a grit chamber (this would require description of numerous trajectories in a detailed velocity field), it is determined empirically (chapter 10).

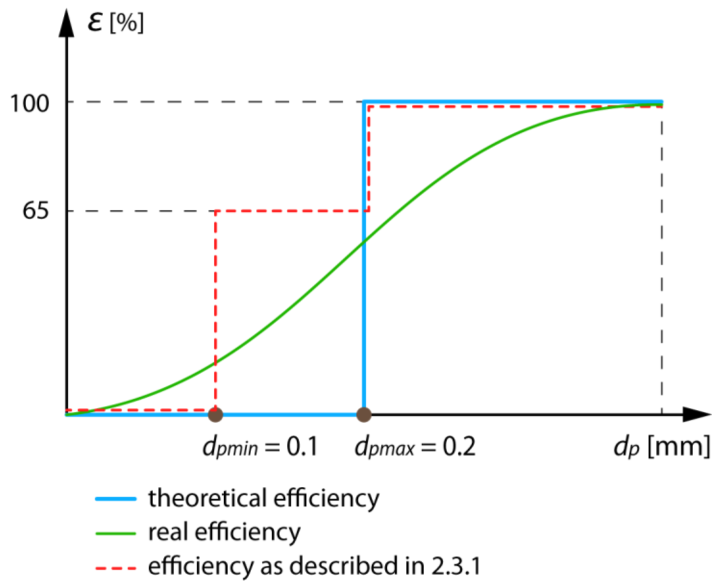

Fig. 2.5. Typical course of efficiency curves of devices for suspension removal

The described method to design objects for suspension removal is not always applied in its direct version based on the analysis of the trajectory of the characteristic particle. Sometimes it is more convenient to describe trajectories by a set of forces acting on a particle. Such an approach yields relations quantitative in character and helpful in the design process. Therefore, it will be used in further considerations.

2.3.3. The concept of vortex separator

As stated at the beginning of this section 2.3, mechanical methods comprise the first stage of wastewater treatment that should be applied to clean storm wastewater so its quality fulfils law requirements described in subsection 1.4.1, before it is discharged into the receiver. In general, devices employed for mechanical treatment are located at the beginning of the technological line comprising an important element of bigger wastewater treatment plants (local industrial sewage treatment plants, municipal wastewater treatment plants). Taking into account the technical scale, these devices have considerable dimensions and operate in complex systems that require constant supervision of the servicing personnel. On the other hand, when the degree of wastewater treatment is sufficient, these devices may exist as individual units or as a part of simple systems. This fact is of highest importance in case of sewerage systems adapted for storm wastewater collection. Such devices are small and operate in harsh conditions. Applied to treat storm wastewater on a local scale, they usually lack constant supervision. Therefore, objects of this type should be efficient, tiny fitting, fracture proof and durable. Furthermore, they should be automatic and operate without the need of 24 hours a day maintenance and control. Taking the listed aspects into account, separators are the most commonly chosen devices for storm wastewater treatment. They are installed in wastewater sewerage systems collecting storm wastewater from catchments that are exposed to contamination by oil derivatives: roads, highways and expressways, parking lots, car washes, transportation vehicles terminals, industrial plants, etc. In order to be highly efficient, separators are equipped with auxiliary components that enhance the process of separation (Ecol-Unicon Sp. z o.o., 2014a, b):

– lamella sections composed of a pack of parallel plates that trap suspensions and oils by flotation and sedimentation - contaminants are separated during multilayer flow of wastewater through the lamella section inside the separator;
– coalescence inserts in the form of a cylinder made of metal chips or a sponge that separates oils from wastewater by gravitational separation supported by coalescence and sorption phenomena; mineral suspension is removed from wastewater by sedimentation and filtration through the coalescence material.

Recently, producers of devices for storm wastewater treatment are becoming increasingly interested in applying centrifugal force to enhance the process of separation of suspension. In the field of water and sewage technology, first devices that made use of this force included circular (vortex) grit chambers, designed by, e.g., Geiger, Erben or Pista (Kujawa-Roeleveld *et al.*, 2011). The Geiger grit chamber with horizontal flow has the shape similar to a cone (Fig. 2.6). A specially designed inlet placed near the device perimeter forces circular motion of wastewater. Within the flow, besides vortices on a horizontal plane, secondary vertical vortices are formed that increase effectiveness of grit separation. Under the influence of centrifugal force and gravity grit settles on device bottom, whereas, organic matter is flushed out from the device with the outflowing stream near the device perimeter. Separated grit accumulates in the central part of the chamber and is usually removed by means of pumping.

In Poland, one of few objects, in which separation is enhanced by the centrifugal force, is an element of the technological line of municipal wastewater treatment plant in Tczew, belonging to Zakład Wodociągów i Kanalizacji Sp. z o.o. w Tczewie. The considered object consists of two independent sets of circular grit chambers (one working, one on standby) put into operation in 1997. These devices (Fig. 2.7) were designed to remove from wastewater and collect mineral matter composed of particles of diameter $d_p \geq 0.2$ mm with settling velocity greater than 0.02 m/s.

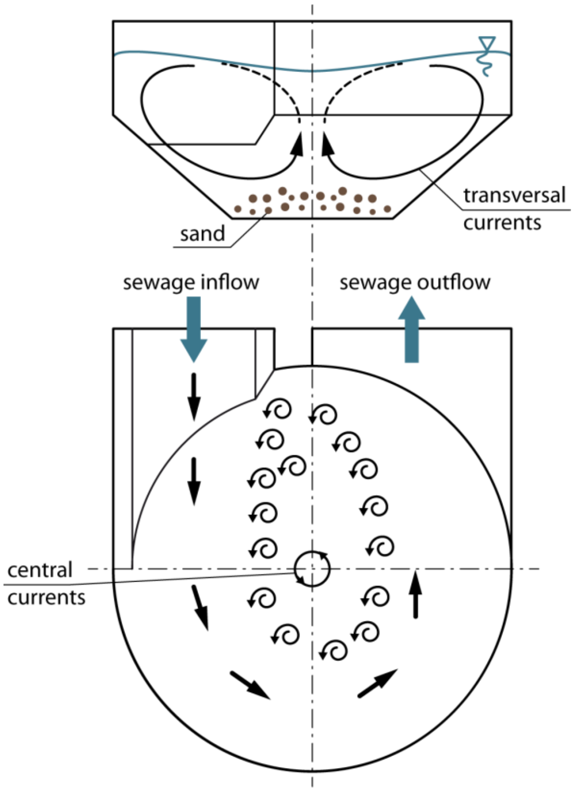

Fig. 2.6. Wastewater flow in the Geiger grit chamber (based on: Kujawa-Roeleveld *et al.*, 2011)

Wetted grit is stopped in the sedimentation cone and collected in wells of diameter 1.0 m and depth 1.2 m located centrally beneath the conical section of the device. The sediment is then pumped into the grit separator. The design flow velocity of both grit chambers is Q_{hmax} = 2260 m^3/h, diameter of a single chamber is equal to 6.11 m and diameter of the sedimentation cone - 1.0 m. Wastewater flows out of each device in a separate channel and is directed for further treatment. Both channels are equipped with Venturi tubes to measure the volume of flowing wastewater and control its level inside the grit chambers. Discharge measurements are conducted continuously, results registered and summed up.

On 5-6 July 2007 an efficiency test of suspension removal from wastewater on the currently operating grit chamber was conducted. Wastewater samples were collected at the inlet and at the outlet of the device. According to the results the amount of total suspended solids before the device was 562 g/m^3 and after the device - 402 g/m^3, what means that efficiency of the grit chamber on the date of measurement was equal to 40%.

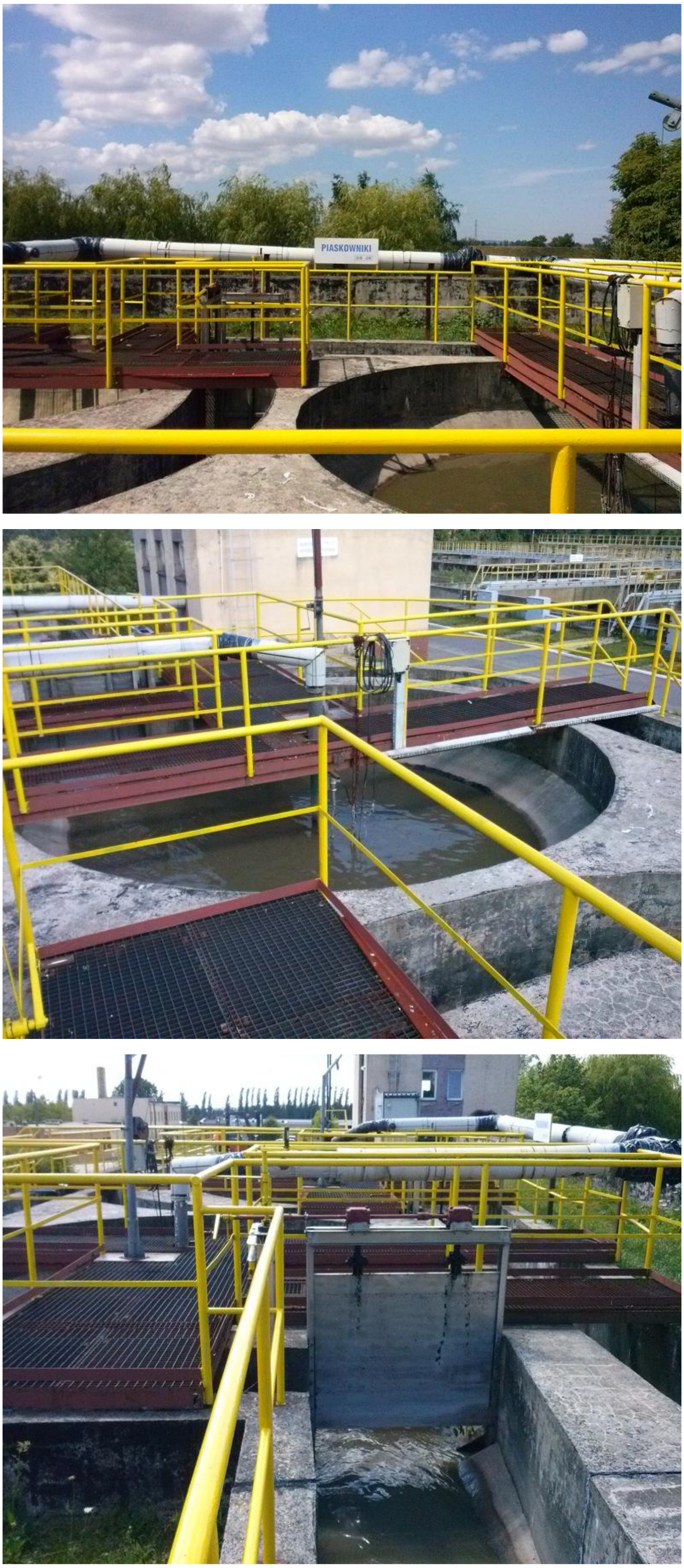

Fig. 2.7. Circular grit chambers as a part of municipal wastewater treatment plant in Tczew, Poland

3. Centrifugal force as a factor enhancing separation

3.1. General remarks

Induction of circulative motion in a fluid-flow object is an intended action that, in many cases, enhances the effectiveness of devices for water and wastewater treatment. Two general effects resulting from circulation include:

– regulation of the effective velocity field (resulting in better use of cubic capacity);
– generation of the centrifugal force (the main focus of the dissertation).

The first effect can be described by a simple relation:

$$\mathbf{u} = \mathbf{u_m} + \mathbf{u_c} \tag{3.1}$$

where: $\mathbf{u}$ - real velocity field; $\mathbf{u_m}$ - velocity component resulting from forces that induce flow through the object (e.g., water conduit or water reservoir); $\mathbf{u_c}$ - velocity component resulting from circulative motion (circulation). Practical application of this effect can be presented on an example of aerated grit chambers (e.g., Albrecht, 1967). When flow velocity decreases and wastewater discharge rate is low, undesirable sedimentation of suspended particles may occur. In such a case introduction of transverse circulation (most frequently induced by an aeration system) expands the transport capacity of the stream. On the other hand, when an increase of discharge is followed by an increase of conduit flow velocity, transverse circulation may be reduced. In this type of objects axis of rotation is usually horizontal.

In case of the second effect, liquid usually rotates around a vertical axis and generates centrifugal acceleration a:

$$a = u_\omega^{\ 2} r \tag{3.2}$$

where: u_ω - liquid angular velocity; r - distance from the axis of rotation. By directing the suspended particles outwards, this factor may substantially boost the separation process. There are two categories of technical objects that utilize this effect:

– centrifugal separators - liquid circulation is induced by rotary motion of the chamber;
– rotational separators: cyclones (carrier fluid - air), hydrocyclones (carrier fluid - water) and vortex separators (carrier fluid - water or wastewater) - fluid circulation is induced by position of the inlet or guide bars in a fixed chamber.

Objects that make use of the first effect (aerated grit chambers) have been already described on a sufficient level (e.g., Sawicki, 2004). Centrifugal separators and cyclones are also quite broadly discussed (e.g., Stairmand, 1951). However, this does not apply to vortex separators that are discussed further in the course of the dissertation.

3.2. *Description of vortex separator operation*

3.2.1. Fundamental equations

Vortex separators comprise a separate category of devices used for mechanical removal of suspensions from liquid (municipal wastewater, storm wastewater or industrial waste effluents). Their operation is based on gravitational separation (sedimentation or flotation) supported by the centrifugal force. The inlet pipe is installed at a tangent to the tank wall to induce circulative motion of the liquid around a vertical axis. The rotating liquid generates the centrifugal force which directs suspended particles towards the outer wall of the tank. As a result, particle residence time inside the device is elongated increasing the probability of its removal from the liquid stream (Fig. 3.1).

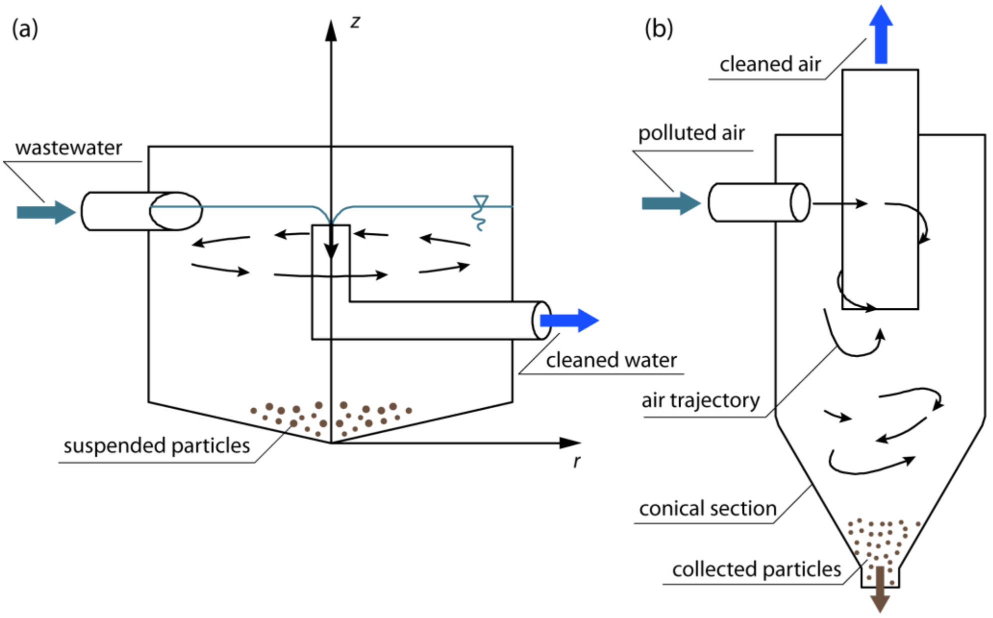

Fig. 3.1. Schematic diagrams of main types of circulative separators: a) vortex separator; b) cyclone

From physical point of view, operation of a vortex separator is described by a set of four relations (Gronowska, 2012a; Sawicki, 2012; Slattery, 1999; Soo, 1969):

– equation of carrier continuity:

$$\mathrm{div}\mathbf{u} = 0 \tag{3.3}$$

– Reynolds equation:

$$\rho \frac{D\mathbf{u}}{Dt} = \rho \mathbf{f} - \mathrm{grad} p + \mu \Delta \mathbf{u} \tag{3.4}$$

where: ρ - liquid density; $\mathbf{u}$ - liquid velocity; p - pressure; μ - dynamic viscosity coefficient;

– equation of the trajectory of a suspended characteristic particle given by (2.1);

– equation of motion of a characteristic particle (Newton's second law of motion):

$$\rho_p V_p \frac{d\mathbf{v_p}}{dt} = \left(\rho_p - \rho\right) V_p \, \mathrm{g} + \mathbf{F_{AM}} + \mathbf{F_D} + \mathbf{F_C} + \mathbf{F_{TD}} \qquad (3.5)$$

where: ρ, ρ_p - carrier and suspension densities; V_p - particle volume; $\mathbf{v_p}$ - particle velocity vector; g - gravity acceleration; $\mathbf{F_{AM}}$ - associated mass force; $\mathbf{F_D}$ - drag force; $\mathbf{F_C}$ - centrifugal force; $\mathbf{F_{TD}}$ - transverse drift. Equations (2.1) and (3.3)-(3.5) are written in their simple forms, including commonly applied simplifications (suspension is dynamically passive and does not influence the carrier liquid).

3.2.2. The need for simplification

The set of equations (2.1) and (3.3)-(3.5) must be supplemented with essential initial and boundary conditions. These conditions include geometrical and kinematic (liquid discharge) characteristics of the device, as well as initial position of the computational suspended particle. Formal difficulties make the solution obtainable only by computer-aided means (CFD - Computational Fluid Dynamics). The fundamental element of this solution is the trajectory of the considered particle given by its radius vector (liquid velocity field is treated only as an additional information). Sample shape of such a trajectory is presented in Fig. 3.2 (Gronowska *et al.*, 2013).

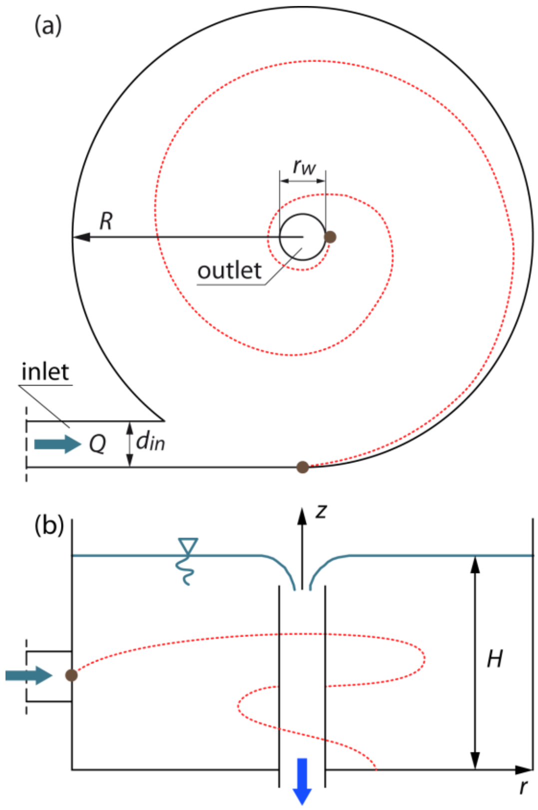

Fig. 3.2. Sample trajectory of a characteristic suspended particle: a) plan view; b) cross-section

Analysis of the course of the trajectory can be used to assess whether device geometry has been chosen properly. If the computational particle of diameter d_p (a boundary between fraction d_{ps} to be separated and fraction d_{pz} that can be suspended in the carrier) settles on separator bottom, device dimensions can be accepted. This theoretical criterion of device efficiency assessment is of “zero-one” character: when $d_{ps} \leq d_p$ all particles are removed from the carrier, and when $d_{pz} > d_p$ particles are suspended in the carrier (Fig. 2.5). This characteristic is important, as producers of devices are required to provide information on real rate of particles removal (according to particle diameter), and this rate can only be determined by empirical research on devices already in operation.

The above described procedure can be applied to simulate operation of a particular device. However, the majority of users is interested in designing a new object, not simulating an already existing one. To design a new object, an inverse problem must be solved - what system geometry to choose so that device works as planned (a solution to system of equations).

In most cases, theory of equations within mathematical physics does not specify methods to describe system geometry (and initial and boundary conditions) in such a way to acquire the assumed solution. Thus, researchers and engineers are usually forced to rely on their intuition, the trial and error method or some kind of an iteration method (provided that it exists). **That is why, it is essential to find intermediate simplified methods that can be helpful in solving inverse problems, as well as become a separate design tool.**

3.2.3. Possibilities of simplification

The source of formal difficulties in equations (2.1) and (3.3)-(3.5) describing operation of vortex separators are relations (3.3) and (3.4) that express motion of the carrier liquid. Their solution in differential version has numerical form, the fact forcing usage of an analogical method to solve equations (2.1) and (3.5). Application of an approximate model of carrier liquid velocity field gives a possibility to adapt one of the simplified versions of equations (2.1) and (3.5), even ones that can be solved by analytical means. As a result, one could obtain final algebraic relations for separators dimensioning, as well as choosing geometry on subsequent steps of CFD design procedure. Such methodology is often used in engineering, especially for flow-through objects and will be applied in formulation of the vortex separators design method within next chapters of the dissertation.

4. Existing methods for dimensioning vortex separators

4.1. General remarks

In general, principle of vortex separators operations is analogical to that of a cyclone, however, vortex separators are deprived of the conical section that is crucial for the process of air treatment in a cyclone, even though it complicates description of device operation. This conical part is not employed in sewerage devices mainly due to problems with their installation in the ground. Furthermore, separators and cyclones treat different media - water and air, as well as work in a different way - separators are characterized by water free surface, whereas, cyclones work under pressure. As differences between these two types of objects have already been discussed in detail by Gronowska and Sawicki (2011), only the main issues are presented in this chapter.

4.2. Description of the methods

Mathematical description of gravitational separators is based on the direct analysis of the trajectory of a suspended particle characteristic for the device (subsection 2.3.2). However, in most cases such a method is an inconvenient design tool as it is time-consuming. Therefore, other methods often make use of characteristic situations or states that represent the developed object and serve as design criteria. Literature concerning devices for air treatment present two such methods that may be adapted to design vortex separators.

The first method, described by, e.g., Warych (1998) is based on the following characteristic state: a particle, motionless relative to a horizontal plane, is subjected to the force $\mathbf{F_{DS}}$ of the liquid flowing radially from the outer wall to the central pipe with velocity $\mathbf{u}$. The stress is balanced by the centrifugal force $\mathbf{F_C}$. Transversal pressure effect $\mathbf{F_{TD}}$ is also included (Fig. 4.1a).

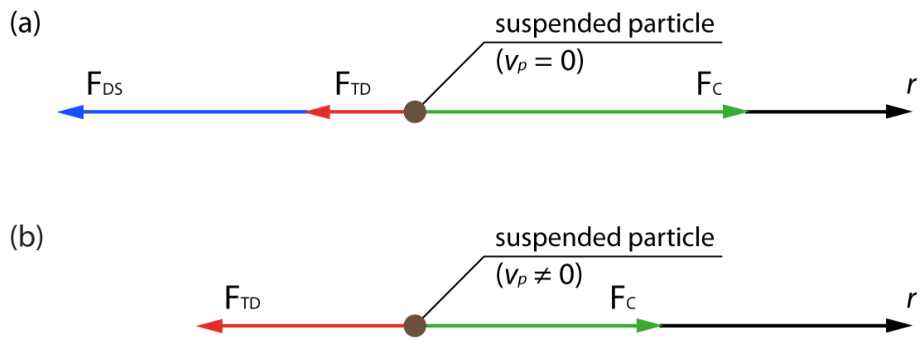

Fig. 4.1. Balance of characteristic forces: a) immovable particle; b) movable particle

It is assumed that the critical particle is the smallest one from particles that are to be removed in the process of separation. With design criterion defined by the relation:

$$\mathbf{F_C} = \mathbf{F_{DS}} + \mathbf{F_{TD}} \tag{4.1}$$

all the particles bigger and heavier that the critical one will be directed towards the outer wall simultaneously descending towards the bottom due to the gravity force. In this way particles are removed from the suspension. On the contrary, particles smaller than the critical one are carried away from the device with the outflowing liquid stream. Individual forces employed in the first method are described as follows (Wikipedia, 2010):

– centrifugal force:

$$F_C = m_p u_\omega^2 r \tag{4.2}$$

– Stokes' drag force:

$$F_{DS} = 3\pi\mu d_p u \tag{4.3}$$

– transverse drift:

$$F_{TD} = m_d u_\omega^2 r \tag{4.4}$$

where: u - liquid velocity; m_d - mass of liquid displaced by the particle.

Distribution of maximum values of these forces seems to be problematic, as the maximum value of F_{DS} occurs near the outflow pipe ($r = r_w$ - tank outlet radius), contrary to remaining two forces whose maximum values are found near the outer wall ($r = R$ - tank radius). In order to avoid description of the design criterion by a radius r function, relation (4.2) was analyzed in terms of maximum values of all the forces. Transformation of this equation yielded a formula for diameter of the critical particle (particle is immovable):

$$d_p = \sqrt{9\frac{\mu R Q}{\Delta\rho r_w \pi H u_t^2}} \tag{4.5}$$

where: R - tank radius; r_w - radius of the outlet pipe; u_t - liquid tangential velocity. It is assumed that the liquid angular velocity is constant and defined by the velocity in the inlet pipe:

$$u_\omega = \frac{u_t}{R} \tag{4.6}$$

The second method, presented by, e.g., Mitosek (1997) is derived from another characteristic state. Initially, the critical particle is located near the outlet pipe and then directed towards the outer wall by the centrifugal force $\mathbf{F_C}$ (horizontal motion of liquid is neglected). Thus, the drag force $\mathbf{F_{DS}}$ also acts on the particle and the transverse drift $\mathbf{F_{TD}}$ is omitted. As a result, the force balance looks as follows (Fig. 4.1b):

$$\mathbf{F_C} = \mathbf{F_{DS}} \tag{4.7}$$

Substitution of equations (4.2) and (4.3) into (4.7) gives the formula for liquid radial velocity:

$$u_r = \frac{dr}{dt} = \frac{{u_\omega}^2 {d_p}^2 \rho_p}{18\mu} r \tag{4.8}$$

Integration of relation (4.8) from $r = r_w$ to $r = R$ gives the time the particle requires to reach the outer wall:

$$t_r = \frac{18\mu}{{u_\omega}^2 {d_p}^2 \rho_p} \ln \frac{R}{r_w} \tag{4.9}$$

The chosen design criterion requires the time of particle displacement along the radius t_r and the time in which the particle reaches the bottom t_{fs} to be equal.

The second method in its original version developed for cyclones neglects the sedimentation process of a dust particle. In such a case, the time in which the particle reaches the bottom t_s is the time of advection of dust towards the bottom:

$$t_{fs} = \frac{H}{u_z} = \frac{\pi\left(R^2 - {r_w}^2\right)H}{Q} \tag{4.10}$$

where: u_z - fluid vertical velocity. Comparison of equations (4.9) and (4.10), as well as inclusion of (4.6), yields the formula for diameter of the suspended critical particle:

$$d_p = \sqrt{\frac{18\mu Q R^2}{\pi \rho_p {u_z}^2 H \left(R^2 - {r_w}^2\right)} \ln \frac{R}{r_w}} \tag{4.11}$$

In order to design vortex separators according to the second concept, relation (4.10) should be replaced by an expression describing the time of particle vertical displacement upon the action of the gravity force. Denoting free sedimentation velocity as v_{fs}, this time equals:

$$t_{fs} = \frac{H}{v_{fs}} \tag{4.12}$$

Taking into account the following formula for free sedimentation velocity v_{fs} (Sawicki, 2007; Soo, 1969):

$$v_{fs} = \sqrt{\frac{4\Delta\rho g d_p}{3C_D\rho}} \tag{4.13}$$

where: C_D - drag coefficient, in place of (4.11) one obtains:

$$d_p = \left[\frac{36\mu\sqrt{g}R^2}{Hu_t^{\,2}\sqrt{3C_D\rho}\,\Delta\rho}\ln\frac{R}{r_w}\right]^{2/3} \tag{4.14}$$

4.3. Verification of the methods

Possibility of application of the two methods described in the previous section 4.2 to dimension a vortex separator was verified by control calculations made for a series of devices produced by a Polish manufacturer Ecol-Unicon Sp. z o.o. These separators were designed using the classic “volumetric” method for particles with the critical diameter d_p = 0.1 mm, basing on the plug-flow model.

Circulative motion of liquid induced inside the separator is treated as a factor that boosts the process of separation. As such, this liquid flow should additionally improve the efficiency of the device (lower the critical particle diameter d_p), even without being included in the design calculus. Consequently, diameter of the critical particle calculated from relation (4.5) (“immovable particle method”) or (4.14) (“movable particle method”) should be smaller than 0.1 mm. Test calculations were made for PDOW series of separators (μ = 0.001 kg/ms; ρ = 2700 kg/m^3; C_D = 0.44) and results listed in Tab. 4.1. It can be seen that the diameter of the critical particle determined by the described methods are more than two orders of magnitude larger than the basic value d_p = 0.1 mm. This indicates that both methods should be thoroughly discussed before being applied for vortex separators design.

4.4. Physical analysis of the methods

Analysis of both methods included three aspects of calculations. Firstly, the design criteria employed were reasonable, however, adoption of extreme values of the drag force and the centrifugal force in the first method (4.1) resulted in lower computational efficiency of the device. On the other hand, in the second method (4.14), the design criterion was typical of devices for gravitational separation. Secondly, in case of the force balance, application of the Stokes' formula (4.3) to describe the drag force may be considered as improper and the chosen Reynolds number should be analyzed.

The considered case includes the process of separation of suspension occurring in flowing liquid. Generally, when the value of d_p is equal to 1.0 mm, velocity v_{fs} equals 0.2 m/s and Reynolds number *Re* for laminar flow equals 200. Thus, the Stokes' formula, that is valid up to *Re* = 1, should be replaced by the Newton's formula for turbulent flow:

$$F_{DN} = C_D F_p \frac{\rho\left(v_p - u_{av}\right)^2}{2} \tag{4.15}$$

where: F_p - particle active cross-section. However, as this correction is not fundamental in character, it cannot justify the discrepancy between calculations (Tab. 4.1) and the efficiency of actual devices.

Tab. 4.1. Data and results of verification calculations for PDOW separators

Device type	Q [m³/s]	H [m]	R [m]	r_w [m]	u_s [m/s]	d_p [mm][1]	d_p [mm][2]
DOW 25/250	0.025	1.81	0.60	0.20	0.20	1.33	4.00
PDOW 35/350	0.035	1.85	0.75	0.25	0.18	1.73	6.14
PDOW 60/600	0.060	2.19	1.00	0.30	0.21	1.85	6.78
PDOW 100/1000	0.100	2.47	1.25	0.40	0.20	2.32	8.86
PDOW 140/1400	0.140	2.75	1.50	0.50	0.18	2.85	11.88
PDOW 350/1600	0.350	4.03	2.50	0.60	0.31	2.52	10.38
PDOW 550/1600	0.550	4.03	3.00	0.60	0.49	2.20	7.85

[1] calculated according to immovable particle method
[2] calculated according to movable particle method

Thirdly, a detailed study of relations used in both methods indicated that they were developed with an assumption that angular velocity u_ω in the chamber is constant. This evokes the main uncertainty resulting from relations between velocity tangent to trajectory of the mass u_t, mass trajectory radius of curvature r and angular velocity u_ω:

$$u_\omega = \frac{u_t}{r} \tag{4.16}$$

Making such an assumption means that the tangential velocity profile along the separator radius is a linear function:

$$u_t\left(r\right) = u_\omega r \tag{4.17}$$

This situation corresponds to velocity of the Couette's flow in a rotating cylinder (Fig. 4.2a) with a vertical axis what comprises a model of flow in a centrifuge instead of a vortex separator (Fig. 4.2b).

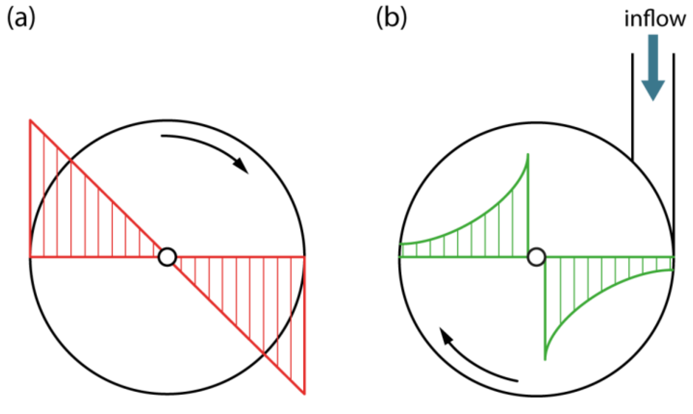

Fig. 4.2. Flow velocity distributions in: a) centrifuge; b) vortex separator

4.5. Propositions of corrections

Description of velocity field that corresponds to velocity distribution in a vortex separator was proposed by Stairmand (1951). According to the researcher, the maximum value of tangential velocity is found near the outlet pipe. Velocity decreases approximately exponentially towards the outer wall according to the quality relation (Fig. 4.2b):

$$u_t \; r = \text{constant} \tag{4.18}$$

Nonetheless, this information has not been so far used in designing vortex separators. Replacement of velocity profile according to (4.17) by (4.18), as well as inclusion of the variability of angular velocity along the radius:

$$u_\omega(r) = \text{constant} / r^2 \tag{4.19}$$

will change the character of the centrifugal force. Secondly, radial pressure distribution - value of transversal pressure drift F_{TD} would also change. Change in pressure may be estimated basing on the fact that, in case of free surface flow, radial pressure profile is portrayed by the shape of the free surface. In a rotating chamber liquid surface is bent convex down (Fig. 4.3a) in accordance with classic rules of hydromechanics (Sawicki, 2007).

In order to obtain a quality description of the shape of water free surface in a tank supplied by a tangent liquid inflow, a simple experiment was conducted. A transparent cylinder was equipped with a supply elastic hose installed on the outer wall. Liquid exited the chamber through a pipe located in tank axis. Liquid circulated around the axis and shape of liquid free surface was described by a convex up curve (Fig. 4.3b). The same effect may be observed while water flows out of a bathtub through a plug in the bottom. Comparison of the two situations illustrated in Fig. 4.3 provides interesting conclusions. One should remember that transversal pressure effect F_{TD} is a result of pressure difference between opposite sides of a body (a suspended particle). In the first case highest pressure diversification (highest value of F_{TD}) is found near the outer wall, the fact described by a known relation (4.4). On the contrary, in the second case, the highest value of F_{TD} is found near the outlet pipe. It seems that the two described factors - radial velocity and pressure profiles that influence the centrifugal force and the "buoyancy effect" - constitute the main reason for calculus divergences.

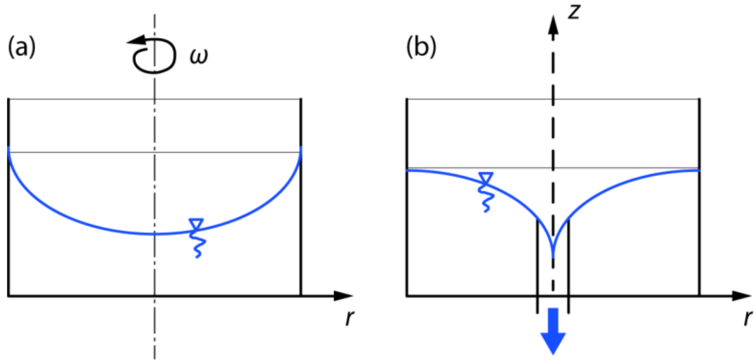

Fig. 4.3. Water free surface profiles: a) centrifuge; b) vortex separator

In order to correct the design methods described in section 4.2 according to the stated remarks, measurements of liquid velocity inside a vortex separator were performed on a laboratory test stand presented in the next chapter.

5. Empirical determination of liquid velocity field

5.1. Measurements of liquid velocity

5.1.1. Laboratory test stand

In order to determine actual velocity distribution in a vortex separator a laboratory test stand with a functional model of this device was constructed. The stand consisted of a cylindrical chamber made of stainless steel plate 0.5 mm thick, inlet tangent to the chamber wall, and hydraulic componentry used to supply and drain liquid from the chamber (Fig. 5.1, Fig. 5.2, Fig. 5.3). The inlet was installed at half height of the outlet pipe (equal distance to the outflow cross-section and chamber settling zone). Such a placement was chosen to prevent wash out of sediments from the tank (inlet too close to the bottom) and induce liquid flow in lower part of the tank (inlet just below the liquid surface). Dimensions of the chamber are shown in Fig. 5.2.

Additionally, the chamber was equipped with two inlet pipes parallel to each other, "right" inlet denoted by letter "R" and "left" inlet denoted by letter "L", so that liquid could circulate in two opposite directions. Such a construction allowed to evaluate the influence of the Coriolis force on velocity values. For each series of measurements liquid was fed using a single inlet pipe while the liquid supply to the other inlet remained closed and vice versa. Inflow of liquid to the chamber was controlled by a set of valves, discharge regulated by a flow-meter (magnetic drive LangHua Water Meter) and water depth measured by a water level gauge.

The bottom drain was situated in the centre of the separator chamber and equipped with a replaceable outlet pipe. Such a solution allowed to examine various configurations, possible from technical point of view, of the system responsible for liquid outflow from the tank. Within the course of the measurements three different versions of axial outflow through a vertical pipe were applied:

– upper orifice overflow (outlet pipe length 15 cm and 20 cm), denoted by letter "A" (Fig. 5.4a);
– perforated side surface of the outlet pipe - 9 rows of openings with diameter 5 mm in 1 cm intervals, denoted by letter "B" (Fig. 5.4b);
– three rectangular openings 29 mm x 15 mm in the outlet pipe side surface located 2 cm above the chamber bottom, denoted by letter "C" (Fig. 5.4c).

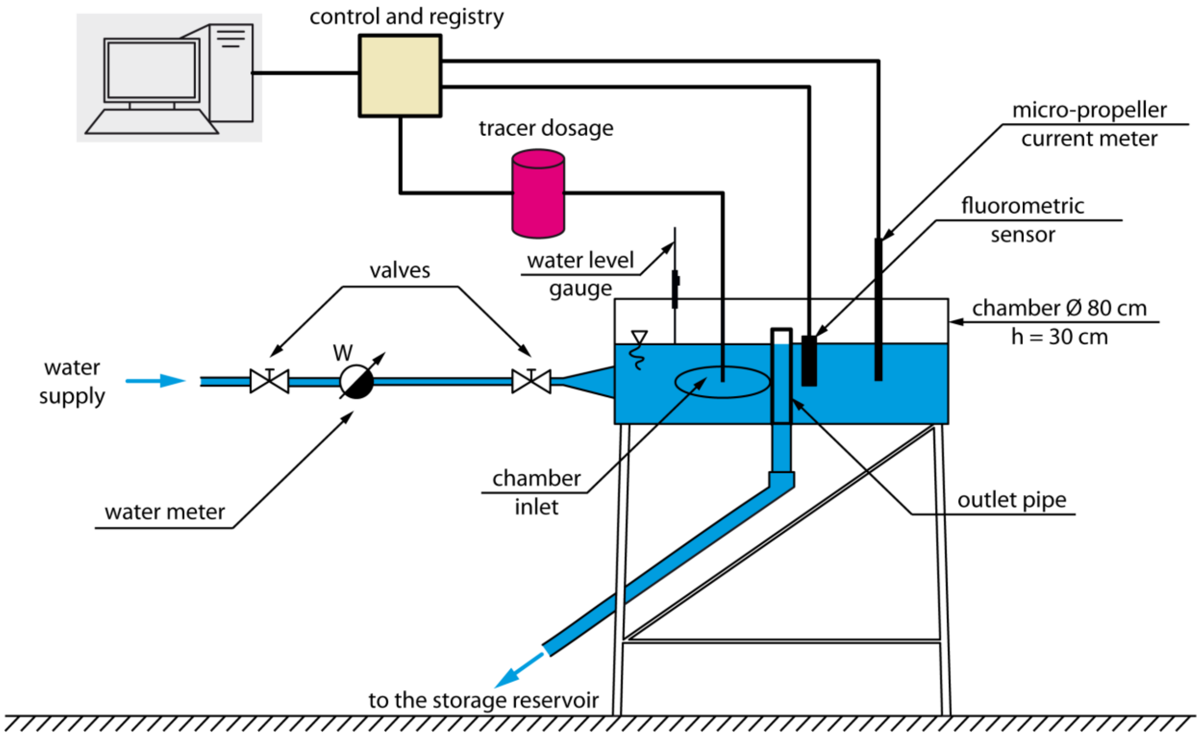

Fig. 5.1. Schematics of the laboratory test stand (includes all the equipment used for velocity and tracer measurements, described in chapter 9)

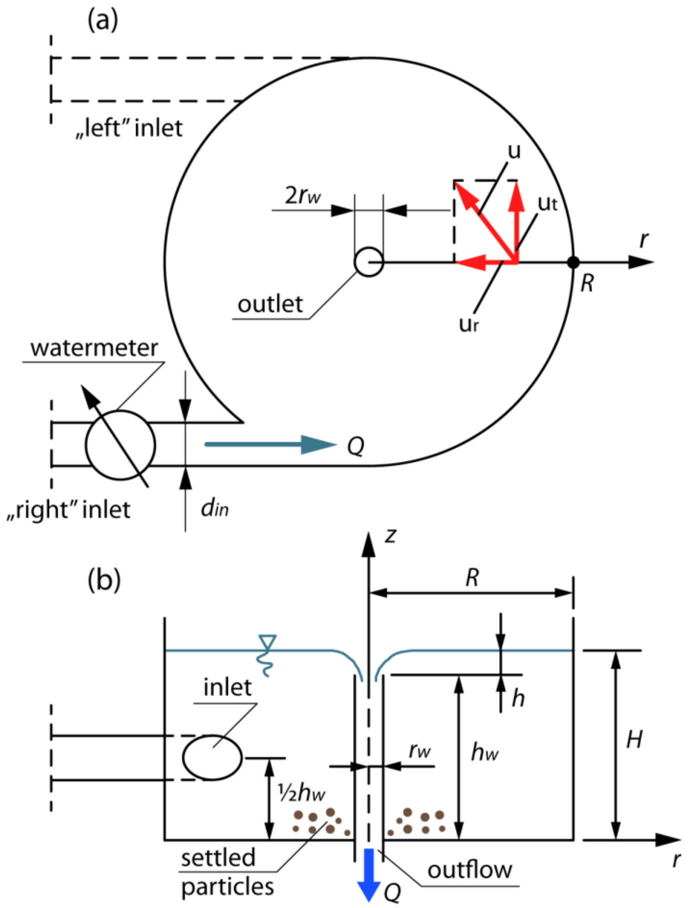

Fig. 5.2. Characteristic dimensions of the laboratory separator: a) top view; b) axial cross-section (chamber radius R = 0.40 m; inlet diameter d_{in} = 0.075 m; outlet radius r_w = 0.02 m; outlet height h_w = 0.20 m)

Fig. 5.3. Laboratory test stand (general view, water flow-meter, computer station)

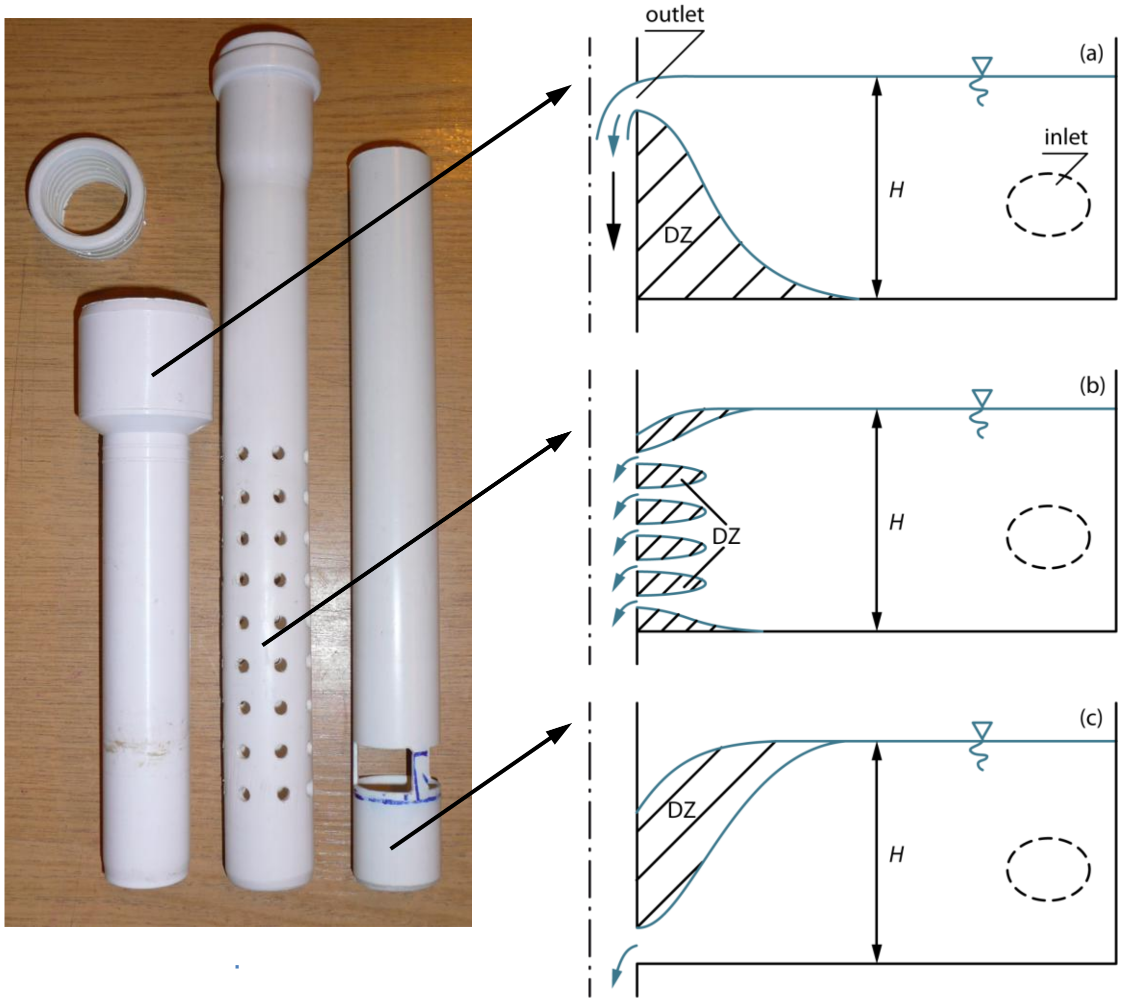

Fig. 5.4. Examined versions of the liquid outflow pipe (axial cross-section, DZ - dead zone)

However, not all three outflow variants shown in Fig. 5.4 are technically justified. The most favourable one is the “A” version that directs the outflow stream just below the liquid free surface moving it away from the bottom sedimentation zone. Moreover, in this case outflow cross-section is easily accessible for cleaning and small repairs.

The remaining two variants “B” and “C” would be troublesome in terms of maintenance and the outlet version “C” would bring the risk of sediments being washed out from the tank. Furthermore, a pipe with bottom openings would be far less durable. Nevertheless, all three configurations were included in the measurements to obtain a more complete hydraulic characteristic of the vortex separator.

5.1.2. Location of measurement points

Points for the measurement of liquid velocity were arranged in a regular pattern (Fig. 5.5). Horizontally, six radii every 60° (from I to VI) were indicated with three verticals located on each radius in specific intervals - three radial distances: r_m = R/4 = 0.1 m; r_m = R/2 = 0.2 m; r_m = 3R/4 = 0.3 m. Each vertical included three points at three levels: a level: z_m = H - 2 cm; b level: z_m = ½H; c level: z_m = 0.02 m above the chamber bottom. Altogether, velocity values were measured in 54 measurement points. Additionally, for each configuration mean velocity of the incoming liquid at the inlet u_{in} was measured.

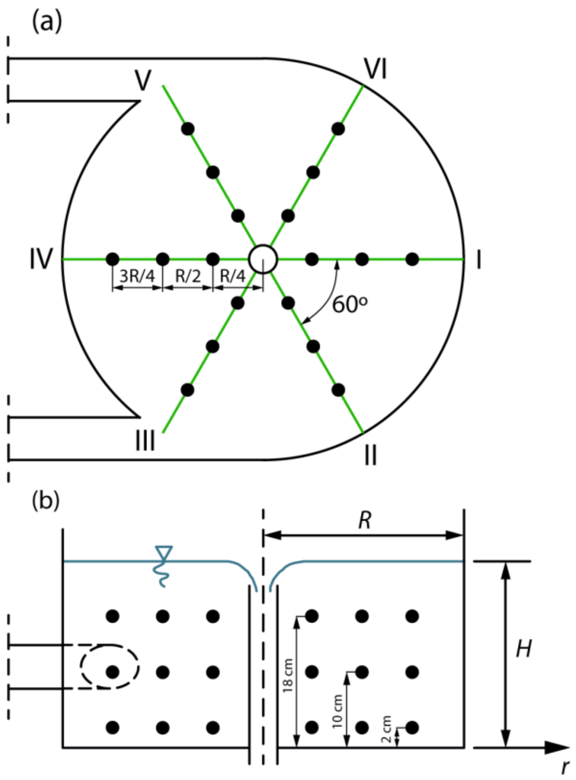

Fig. 5.5. Distribution of measurement points: a) horizontal radii; b) verticals

5.1.3. Measurements methodology

The flow model employed in this dissertation assumes a two-directional and one-dimensional velocity field in which the velocity vector is divided into two horizontal components: radial $u_r(r)$ and tangential $u_t(r)$, depending on radius r only. Taking into account technical possibilities, measurements included the absolute value of velocity vector **u**. They were performed using a micro propeller current meter (OTT Hydromet; Fig. 5.6). The device composes of a probe and a velocity meter. The probe includes a micro propeller with two electrodes and an electronic head. The four bladed micro propeller (10 mm in diameter) made of polycarbonate rotates inside a protective ring, while the meter records the number of revolutions per unit of time and displays the average velocity (mm/s). In order to measure velocity, propeller axis was aligned along the vector direction that was identified by a method commonly used in hydraulic measurements - by observations of the position of a thin thread submerged and attached to a vertical rod placed near the measurement point.

Fig. 5.6. Equipment for velocity measurements (computer station, micro propeller current meter, water level gauge, perforated outlet pipe)

5.2. Results of measurements

5.2.1. General discussion

Sample results of velocity measurements are presented in Fig. 5.7, Fig. 5.8, Fig. 5.9 (the remaining measurements are included in Appendix No. 1). First three graphs for each configuration show values measured at the three points along every radius (from I to VI) on subsequent water levels (a, b, c). The fourth graph presents mean values of velocity at each radial distance including all radii for three water levels and the final mean value of velocity at every point including all radii and all water levels. Flow and measurement parameters are gathered in Tab. 5.1.

Tab. 5.1. Flow parameters during velocity measurements

outflow variant	Q [dm³/s]	h_w [m]	H [m]	a level	b level	c level	Fig. no.
overflow orifice							
clockwise “AL”	0.37	0.15	0.20	0.18	0.09	0.02	5.7
counter-clockwise “AR”	0.37	0.15	0.20	0.18	0.09	0.02	App1.1
clockwise “AL”	0.33	0.20	0.22	0.20	0.10	0.02	App1.2
counter-clockwise “AR”	0.33	0.20	0.24	0.22	0.12	0.02	App1.3
perforated pipe							
clockwise “BL”	0.35	-	0.14	0.12	0.07	0.02	5.8
counter-clockwise “BR”	0.35	-	0.13	0.11	0.06	0.02	App.1.4
bottom openings							
clockwise “CL”	0.31	-	0.13	0.11	0.06	0.02	5.9
counter-clockwise “CR”	0.31	-	0.13	0.11	0.06	0.02	App1.5

During the measurements it was observed that whole water volume rotates around the chamber axis, as expected. Tangential velocity increases significantly near the central outlet pipe. Shape of water free surface is typically bent as of circulative motion: it lowers from the outer wall towards the chamber axis and its profile is convex up (Fig. 4.3b). Near the supply conduit a local zone of submerged inflow is present. These three-dimensional effects can be included in a comprehensive model of flow inside the vortex separator. This would require employment of general equations of fluid mechanics and computer software to solve them numerically. Taking into account the formal simplicity of the design method being developed these effects were omitted. The main reason for omission was the fact that the effects are strongly local in character. Water free surface bent is significant and readily visible as a vortex only in the direct vicinity of the outlet pipe (for r < 0.10 m) and submerged inflow stream is separated on a distance up to ¼ of the chamber perimeter.

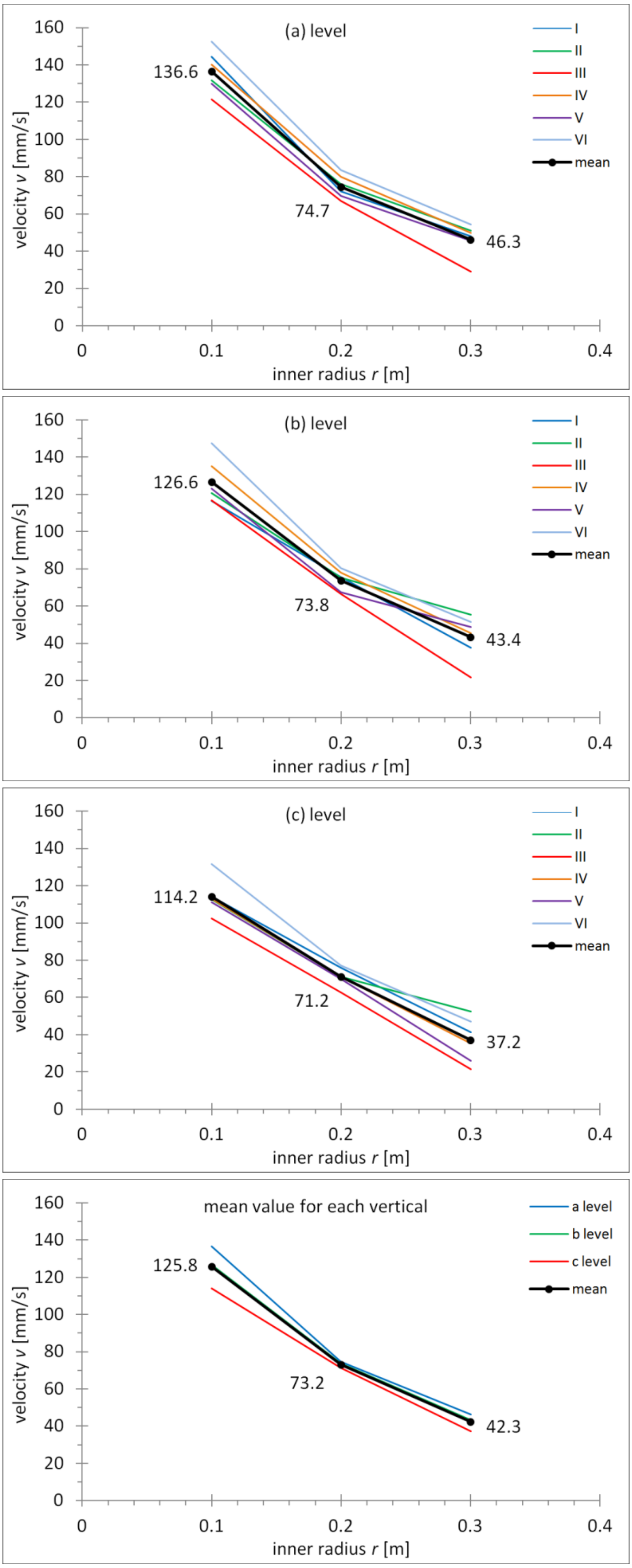

Fig. 5.7. Velocity distribution for configuration "AL" $h_w = 0.15$ m

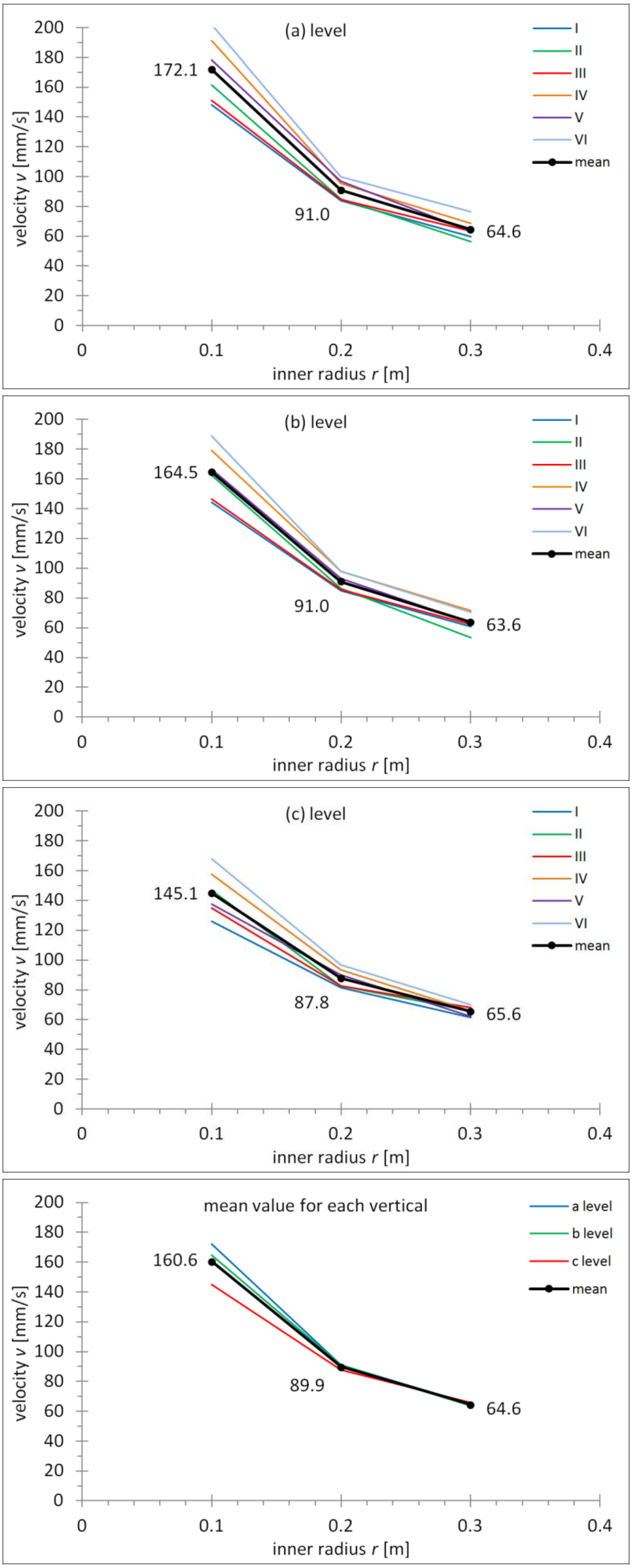

Fig. 5.8. Velocity distribution for configuration “BL”

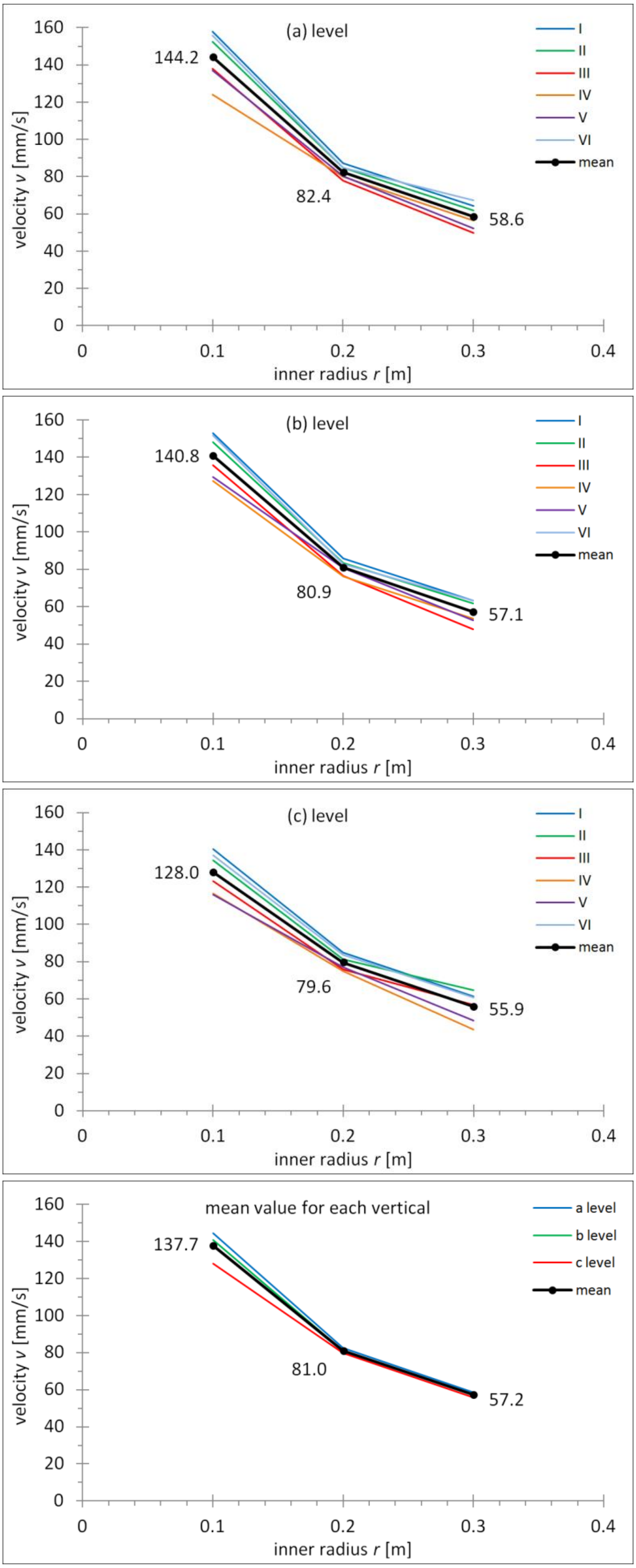

Fig. 5.9. Velocity distribution for configuration "CL"

Moreover, the proposed model of flow acquired its form thanks to constant variability of measured values of velocity modulus in relation to position of the measurement radius and water depth. Additionally, outlet pipe combination (Fig. 5.4.) had a small influence on the velocity field. Finally, results of measurements obtained for various discharges and water depths were stable and repeatable.

Due to measuring capabilities of the equipment (issue explained in subsection 5.1.3.) the object measured was the modulus of flow horizontal velocity. Tangential u_t and radial u_r velocity components, so the velocity vector, could be determined by measuring the angle α indicated by the deviation of the position of the thread floating underwater from the direction perpendicular to the chamber radius:

$$u_t = u \sin\alpha \tag{5.1}$$

$$u_r = -u \cos\alpha \tag{5.2}$$

However, in general values of these two velocity components are greatly disproportional as $u_t >> u_r$. Results of measurements (e.g., Fig. 5.7a for confoguration AL h_w = 0.15 m) for Q = 0.37 dm^3/s and H = 0.20 m, in subsequent verticals gave velocity values u equal to:

r_m = 0.10 m	u = 136.6 mm/s	u_r = 2.94 mm/s
r_m = 0.20 m	u = 74.7 mm/s	u_r = 1.47 mm/s
r_m = 0.30 m	u = 46.3 mm/s	u_r = 0.98 mm/s

where radial velocity u_r was calculated from relation (6.5). Even by assuming that the active (computational) water depth for radial direction (desribed in subsection 6.2.1) is smaller than the measured water depth H, due to flow dead zones visible in Fig. 5.4., values of u_r are no higher than few % of u_t values. This statement was confirmed by direct observations of the flow made during the measurements. Deviation of the velocity vector from the tangential direction of flow was minimal within the prevailing part of the chamber. Only near the outlet pipe the previously described three-dimensional effects were visible. Additionally, taking into account the pulsations responsible for thread velocity direction (turbulence) it was assumed that the presented velocity distributions acquired through measurements describe profiles of tangential velocity u_t of the flow. Such an approach eliminated the need to calculate values of both velocity components, only radial velocity u_r.

5.2.2. Evaluation of the influence of the Coriolis force

Every element (with mass Δm) of the liquid moving with velocity $\mathbf{u}$ in relation to the Earth rotating with angular velocity $\boldsymbol{\omega}_\mathbf{z}$ is affected by the Coriolis force that can be expressed as follows (LeMehaute, 1976):

$$\mathbf{F}_\mathbf{C} = -2\Delta m(\boldsymbol{\omega}_\mathbf{z} \times \mathbf{u}) \tag{5.3}$$

The Coriolis force may be a source of significant kinematic effects. As far as circulative systems are concerned, the Coriolis force generates circulative motion of the liquid around the outflow pipe that can be observed even in technically simple systems (e.g., outflow of water from a bathtub, removal of bulk material from a silo). Accordingly, in case of vortex separators one may expect that the intensity of liquid circulation inside the chamber will be influenced by this factor to some extent. Taking into account the fact that on the northern hemisphere the Coriolis force causes objects to deflect to the right of their intended path, the following should be observed:

– in clockwise flow intensity of circulation is increased as liquid is pushed towards the centre of the object (Fig. 5.10a);
– in counterclockwise flow intensity of liquid circulation is decreased as liquid path of motion is diverted towards the outer wall of the chamber (Fig. 5.10b).

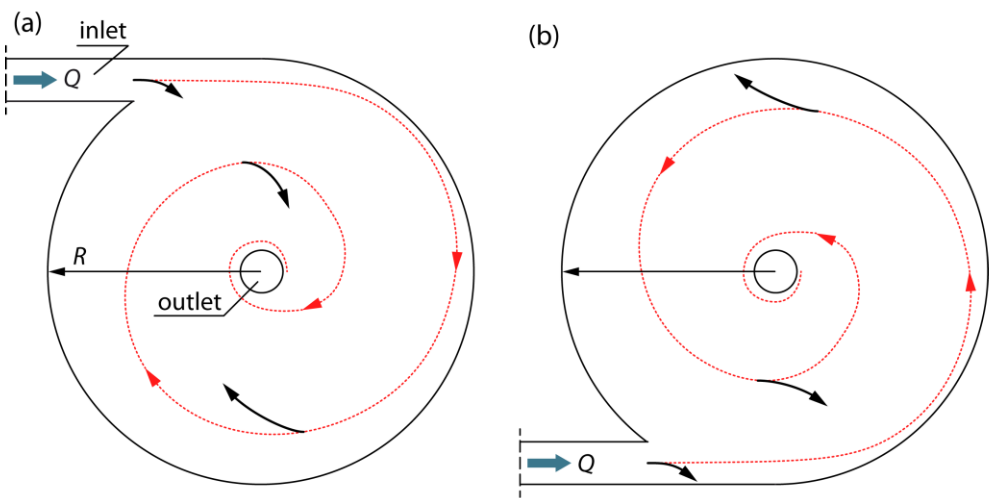

Fig. 5.10. Visualisation of the Coriolis effect in a vortex separator: a) clockwise flow; b) counterclockwise flow

In order to examine this effect velocity field in the laboratory separator was determined for both “right” and “left” inlet (Fig. 5.2) for every variant of the outlet (Fig. 5.4.). The obtained results confirm the quality evaluation stated above. The majority of examined configurations displayed a tendency of velocities being higher in case of clockwise flow (configurations “AL”, “BL”, “CL”) than in counterclockwise flow (configurations "AR", "BR", "CR"). From quantitative point of view, however, the influence of the Coriolis force is limited - the biggest difference between measured velocities was equal to 15.2% (Fig. App1.2 and Fig. App1.3), whereas, taking into account all measurement points, the mean difference was 3.6%. This means that, although the Coriolis acceleration could be included in a detailed three-dimensional model, it can be omitted in the model being developed.

5.2.3. Relation between measured and calculated inlet velocities

In some models of vortex separators it is assumed that flow velocity near the outer wall of the object is equal to the mean inlet velocity (Ciborowski, 1973) or can be determined using this value (Rhodes, 2008). In order to verify this assumption, for each examined configuration inlet velocity u_{in}^m was measured in the axis of inlet conduit. Then, mean values u_{in}^c were calculated from the following relation:

$$u_{in}{}^{c} = \frac{4Q}{\pi d_{in}{}^{2}} \tag{5.4}$$

Measured u_{in}^m and calculated u_{in}^c values of inlet velocity, together with mean values of flow velocity $v_{0.3}$ measured at r = 0.3 m from the chamber axis (results in Fig. 5.7, Fig. 5.8, Fig. 5.9) are presented in Tab. 5.2. It can be observed that in each case flow velocity inside the chamber $u_{0.3}$ is considerably smaller than both corresponding inlet velocities u_{in}^m and u_{in}^c. This fact should be taken into account in every rational method of vortex separators design - the method that should include dynamics of the inlet stream. Such a model will be proposed further in the dissertation.

Tab. 5.2. Comparison of measured values of inlet velocity u_{in}^m, calculated values of inlet velocity u_{in}^c and values of flow velocity $u_{0.3}$

outflow variant	u_{in}^m [m/s]	u_{in}^c [m/s]	$u_{0.3}$ [m/s]
overflow orifice (h_w=15cm)			
clockwise "AL"	0.093	0.084	0.042
counter-clockwise "AR"	0.080	0.084	0.040
perforated pipe			
clockwise "BL"	0.088	0.079	0.065
counter-clockwise "BR"	0.078	0.079	0.066
bottom openings			
clockwise "CL"	0.079	0.071	0.057
counter-clockwise "CR"	0.069	0.071	0.060

6. Description of velocity field and pressure distribution

6.1. Choice of the velocity model

6.1.1. Analysis of existing possibilities

From physical point of view, the general and theoretical tool used for velocity field determination is the equation of mass conservation (continuity) given by (3.3) together with the equation of momentum conservation given by (3.4) (in the form of Navier-Stokes' equation and known as the dynamic equation). These two relations form a set of four scalar equations with four scalar unknowns: three velocity vector **u** components and pressure *p*. This set can be used for the purpose of the design method being developed provided that liquid density and its temperature do not change. Otherwise, equations (3.3) and (3.4) should be supplemented with the equation of state and the equation of energy conservation (Sawicki, 2009).

In their analytical form these equations can be solved only for a limited number of very simple situations, e.g., flow in a straight circular conduit according to Hagen-Poiseuille or shear stress according to Couette. The majority of important technical problems require fast and simple methods, especially numerical ones. The highly effective family of numerical methods called Computational Fluid Dynamics (CFD) offer a wide range of possibilities. However, CFD methods have some disadvantages as they are expensive, time-consuming and involve employment of highly-trained personnel. Moreover, results of their calculations refer to individual objects. Generalization of CFD methods is a complex process that often require a significant number of numerical experiments resulting in conclusions on a generality level which does not match the results of analysis of relations in an analytical form. Additionally, one should remember that CFD is an irreplaceable tool for bigger companies and research teams, while smaller units are interested in less-demanding and simpler methods.

A formal alternative to general theoretical methods are the empirical ones. In some cases employment of empirical experiments is crucial, even though they are expensive, time-consuming and marked by measurement errors. Moreover, utilization of their results is limited to identical or fairly similar objects (Sawicki, 2009; Zierep, 1978). Therefore, empirical methods in their pure form are chosen very rarely, still experiments remain an inseparable supplementary element of every research.

In the light of two discussed groups of methods, the researcher is encouraged to turn to simplified ones which usefulness is defined by the compromise between decrease in formal (mathematical) difficulties of application and retention of the highest possible level of detail in physical and technical description of the phenomenon. The family of simplified methods is vast, thus, only one category - kinematic models, will be further discussed in the dissertation.

The fundamental characteristic of kinematic models is their fulfilment of the condition of flow continuity given by relation (3.3) with simultaneous substitution of the dynamic equation (3.4) by another quantitative condition that results from analysis of an empirically determined velocity field (in other words, from analysis of the kinematic characteristics of the flow, hence the category name). A few such models are available and applied in practice (Sawicki, 2009). The most popular one is the irrotational (potential) two-dimensional model of motion valid when there are no vortex structures in the flow. In this model relation (3.4) is replaced by a simple condition:

$$\mathrm{rot}\mathbf{u} = 0 \tag{6.1}$$

A more convenient one is the model based on Stokes' assumption (non-linear advection term in equation (3.4) is omitted) used for solving problems that inlcude flow of viscous liquid around a sphere (Sawicki, 2007; Soo, 1969). This assumption allows to replace relation (3.4) by a biharmonic equation for the stream function ψ in case of two-dimensional flow:

$$\Delta\Delta\psi = 0 \tag{6.2}$$

On the other hand, in the model of helical motion velocity vector and rotation vector are parallel to each other, and consequently:

$$\mathbf{u} = \alpha\,\mathrm{rot}\mathbf{u} \tag{6.3}$$

Within further course of the dissertation, a velocity model in a vortex separator is proposed basing on the described general principle of kinematic models construction.

6.1.2. Formulation of general relations

Liquid flow in vortex separators has the following characteristics:

– radial component of velocity u_r is directed from the outer wall ($r = R$), where its value equals zero (liquid adheres to the immovable wall):

$$u_r\left(r = R\right) = 0 \tag{6.4}$$

towards the central outlet pipe ($r = r_w$). Although, the active zone of radial flow has variable depth and as such complicates the description of flow (Fig. 6.1), it must be taken into account in the developed model. Moreover, as radial velocity is responsible for liquid transit through the device it must be included in the mass balance;

– tangential component of velocity u_t has no direct influence on the mass balance, however, it generates two other factors that are crucial for the flow: the centrifugal force and the transverse drift;
– vertical component of velocity u_z is mainly responsible for the shape of the radial flow zone (Fig. 6.1), therefore, may be neglected in the first place. On the contrary, in case of cyclones that are slimmer than vortex separators, vertical velocity must be included in the design. As a result, design methods for cyclones are not fully compatible with vortex separators.

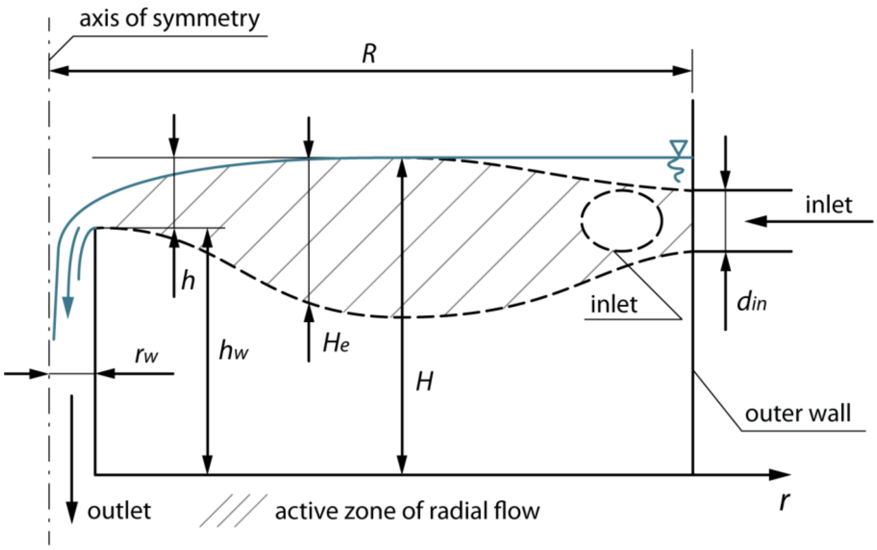

Fig. 6.1. Schematics of radial flow in a vortex separator (vertical cross-section; H - total water depth; h - liquid elevation over the outlet pipe; h_w - outlet height; H_e - active layer of flow)

Taking the above facts into account and analysing the results of velocity measurements presented in section 5.2, the following relations were accepted:
– radial component of velocity u_r can be defined by its mean value for each given distance from the separator axis:

$$u_r(r) = -\frac{Q}{2\pi H_e r} \tag{6.5}$$

where: H_e - active layer of liquid flow expressed as substitute water depth (Fig. 6.1). This relation is commonly employed for dimensioning flow-through reactors with radial flow (Piotrowski and Roman, 1974; Wodociągi i Kanalizacja. Poradnik, 1971), as well as separators (Rhodes, 2008). Additionally, equation (6.5) fulfils the condition of continuity Q = constant. This radial velocity model introduces the concept of substitute (computational) water depth H_e inside the device. Referring to characteristics of vortex flow this parameter must be determined individually (description in subsection 6.2.1);

– tangential component of velocity u_t may be described by an irrational function (basing on the analysis of laboratory experiments presented in section 5.2 and research done by Stairmand, 1951):

$$u_t(r) = \frac{B}{r^{m/n}} \tag{6.6}$$

where: B - special multiplier. After analysing research by Stairmand (1951), Rhodes (2008) assumed that exponent m/n in relation (6.6) should equal 0.50. However, quantitative assessment of the shape of the obtained velocity profiles (Fig. 5.7, Fig. 5.8, Fig. 5.9) indicated that this value should be a little higher and m/n = 0.65:

$$u_t(r) = \frac{B}{r^{0.65}} \tag{6.7}$$

According to Rhodes (2008) multiplier B can be calculated from the condition:

$$u_t(r = R) = u_R = \frac{B}{R^{0.65}} \tag{6.8}$$

where resultant tangential velocity u_R is a distinct resultant value of velocity of the inlet stream and velocity of liquid circulation inside the separator induced by this stream. As the researcher did not provide a way to determine this resultant velocity u_R, multiplier B is calculated from the method basing on the balance of kinetic energy of tangential motion (subsection 6.2.2);

– vertical component of velocity u_z is neglected:

$$u_z = 0 \tag{6.9}$$

and a model of two-dimensional flow on a horizontal plane is implemented.

6.2. Determination of velocity field model parameters

6.2.1. Radial flow

The parameter that describes radial flow in a vortex separator is the substitute water depth H_e (active layer of circulative flow) appearing in relation (6.5). Keeping in mind the aim of the research - development of a simplified model of vortex separator operation, a model that is algebraic and useful in the design process, as well as a model that can work as a supplementary tool for CFD methods - substitute depth must be described by a formally simple relation which binds together principal geometric dimensions of the device. In the simplest case active layer of flow is equal to the total depth of liquid, so H_e = H (Rhodes, 2008), although, H_e should be placed somewhere between the values of total water depth H and inlet pipe diameter d_{in} (Fig. 6.1).

In order to find the actual value of substitute water depth, time characteristics of the separator were determined in a series of measurements on the laboratory test stand. Description of the test stand can be found in subsection 5.1.1 and tracer measurements in chapter 9. The principal time characteristic - liquid residence time inside a vortex separator t_K can be calculated from the relation expressing the plug-flow time t_{PF}:

$$t_{PF} = \int_{R}^{r_w} \frac{dr}{u_r(r)} = \frac{\pi H_e \left(R^2 - r_w{}^2\right)}{Q} \tag{6.10}$$

Calculations according to equation (6.10) for flow conditions as in tracer measurements (configuration PG - overflow orifice outlet and “right inlet R” - counterclockwise flow): Q = 0.34 dm^3/s and $H_e = H$ = 0.24 m from $r = R$ to $r = r_w$ yielded the plug-flow time equal to t_{PF} = 355 s. On the contrary, the average residence time of liquid inside the separator calculated as the first moment on the residence time distribution curve $E(t)$ was t_A = 217 s (Tab. 9.4). Taking this results into account it was decided that the mean depth of active layer of flow, as a characteristic technical parameter, is located at half height between the inlet diameter d_{in} and the total liquid depth H:

$$H_e = \frac{1}{2}\left(d_{in} + H\right) = \frac{1}{2}\left(d_{in} + h + h_w\right) \tag{6.11}$$

where liquid elevation over the outlet pipe h can be determined from classic methods of hydraulics (Nalluri and Featherstone, 2001) as the outlet pipe works like a shaft overfall or the “morning glory spillway” (Camargo *et al.*, 2006). Making use of Bernoulli’s theorem one can write:

$$Q = \frac{4}{3} \mu_p \pi r_w \sqrt{2g} h^{3/2} \tag{6.12}$$

where discharge coefficient μ_p can be calculated from the empirical relation (Gronowska and Sawicki, 2014b):

$$\mu_p = \frac{0.245}{\left(h/r_w\right)^{0.87}} \tag{6.13}$$

6.2.2. Tangential flow

Analysis of the velocity field structure observed inside a vortex separator revealed that this field is a superposition of radial and tangential flow, the two being almost completely independent from each other. This fact was confirmed by the preformed measurements.

Tangential circulation is strongly related to the position of the inlet conduit - liquid stream is inflowing at a tangent to the outer chamber wall. On the contrary, radial flow is governed by the decrease in level of water free surface on the distance between the outlet and the inlet. In case of vortex separators (inlet conduit mounted in the chamber wall, outlet placed in the chamber axis) a characteristic “cone” occurs on the outlet in the centre of the device (Fig. 6.1). This “cone” is also formed when another configuration of the inlet (perpendicular to the wall and equipped with a dispersion wall) does not generate circulation, provided that the above position inlet-outlet is retained. Moreover, resistance to transit motion of flow between reactor walls (Fig. 6.2) is compensated by a decrease in liquid surface level along the direction of motion. The shape of water free surface adjusts itself automatically to flow conditions. In order to avoid the rise in water level inside the inlet conduit (“flooding of sewerage system”), designers and producers of devices lower the elevation of the outlet by a specific value h_{str}. Usually this value equals h_{str} = 20 mm, however, it can reach tens of centimetres in case of maximal flows (Bering and Sawicki, 2002).

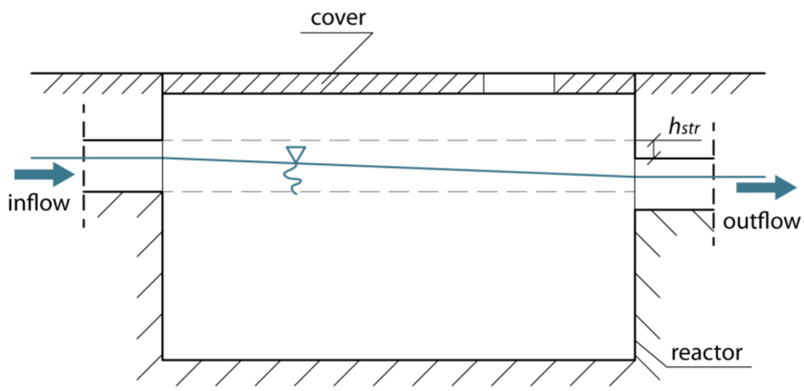

Fig. 6.2. Schematics of the amount of energy loss during transit flow

The above discussion arises a possibility to assume that both velocity components are energetically independent from each other. In terms of energy balance, tangential flow is supplied by inflowing energy stream and transit radial flow by potential energy related to the slope of water free surface. On the other hand, there are situations when some part of energy of the inflowing stream is transferred to the outflowing stream. However, such a situation is unfavourable in case of devices belonging to the category of reactors (occurrence of the “hydraulic short-circuit”).

In order to determine the actual distribution of energy, momentary kinetic energy of both velocity components was evaluated. For radial flow with velocity described by equation (6.5) momentary kinetic energy is given by:

$$EK_R = \int_r \frac{1}{2}\rho u_r{}^2 dV = \frac{\rho Q^2}{4\pi H_e}\ln\frac{R}{r_w} \tag{6.14}$$

where: V - separator volume. On the contrary, for tangential motion with mean velocity u_{tav} which can be determined from the measurements (Fig. 5.7, Fig. 5.8, Fig. 5.9) kinetic energy is equal to:

$$EK_T = \frac{1}{2}\rho V u_{tav}{}^2 = \frac{1}{2}\pi\rho\left(R^2 - r_w{}^2\right)H u_{tav}{}^2 \tag{6.15}$$

Calculations made for values corresponding to the performed measurements: R = 0.40 m; r_w = 0.02 m; $H \approx 0.20$ m; $H_e \approx 0.05$ m; $Q \approx 0.30$ dm^3/s; $u_{tav} \approx 0.10$ m/s; yielded:

$$EK_R \approx 0.5\cdot 10^{-3} J \ll EK_T \approx 0.5 J \tag{6.16}$$

According to equation (6.16) momentary energy of radial flow is definitely smaller than momentary energy of tangential flow. As a result, it was assumed that the kinetic energy flux delivered by the inlet cross-section E_{in} is equal to the energy flux dissipated during liquid flow through the device E_{dis}:

$$E_{in} = E_{dis} \tag{6.17}$$

Kinetic energy flux E_{in} of water stream flowing with inlet velocity v_{in} and discharge Q is expressed by the relation:

$$E_{in} = \frac{1}{2}\rho Q u_{in}{}^2 = \frac{8\rho Q^3}{\pi^2 d_{in}{}^4} \tag{6.18}$$

Flux of energy dissipated E_{dis} during liquid flow through the device is a combination of products of components forming the deformation velocity tensor (Puzyrewski and Sawicki, 2013; Serrin, 1959). Taking into account the fact that the employed velocity model is simple in character (tangential component of velocity depends only on the radius r and kinetic energy of radial flow is negligible compared to tangential flow) and liquid flow inside the device is turbulent (for tank radius around 0.5 m and mean tangential velocity 0.1 m/s Reynolds number is Re = 50 000), equation (6.18) acquires the form (Slattery, 1999; Sawicki, 2012):

$$E_{dis} = \frac{1}{2}\int_V \mu_T r^2 \left[\frac{\partial}{\partial r}\left(\frac{u_t}{r}\right)\right]^2 dV \tag{6.19}$$

where coefficient of turbulent viscosity μ_T can be described by an algebraic relation (Launder and Spalding, 1972):

$$\mu_T = 0.00113 \rho u_t(r) l_m(r) \tag{6.20}$$

where mixing length l_m is defined by classic Prandtl equation:

$$l_m = 0.41r \quad \text{for } r < \frac{R}{2} \tag{6.21}$$

$$l_m = 0.41(R - r) \quad \text{for } r > \frac{R}{2} \tag{6.22}$$

Substitution of equations (6.8) and (6.20) - (6.22) into relation (6.19) gives:

$$E_{dis} = 0.00387 H \rho B^3 \left(r_w^{-0.95} - 1.41 R^{-0.95} \right) \tag{6.23}$$

Comparison of (6.18) and (6.23) yields the relation to calculate multiplier B:

$$B = 4.63 Q \left[H d_{in}^{4} \left(r_w^{-0.95} - 1.41 R^{-0.95} \right) \right]^{-1/3} \tag{6.24}$$

In order to verify the chosen tangential velocity model, multiplier B was calculated for flow conditions that occurred during performed measurements of velocity. Next, values of the multiplier (Tab. 6.1) were introduced into equation (6.7) and obtained velocity profiles compared with results of measurements described in chapter 5.

Tab. 6.1. Calculated values of multiplier B and u_t (d_{in} = 0.075 m; r_w = 0.02 m; R = 0.40 m)

outflow variant	Q [dm^3/s]	H [m]	B [1/s]	u_t [m/s]		
				r = 0.1 m	r = 0.2 m	r = 0.3 m
overflow orifice						
h_w = 15 cm						
clockwise “AL”	0.37	0.20	0.0276	123.3	78.6	60.4
counter-clockwise “AR”	0.37	0.20	0.0276	123.3	78.6	60.4
h_w = 20 cm						
clockwise “AL”	0.33	0.22	0.0239	106.6	67.9	52.2
counter-clockwise “AR”	0.33	0.24	0.0232	103.5	66.0	50.7
perforated pipe						
clockwise “BL”	0.35	0.14	0.0294	131.4	83.7	64.3
counter-clockwise “BR”	0.35	0.13	0.0301	134.7	85.8	65.9
bottom openings						
clockwise “CL”	0.31	0.13	0.0267	119.3	76.0	58.4
counter-clockwise “CR”	0.31	0.13	0.0267	119.3	76.0	58.4

Analysis of data gathered in Tab. 6.1, Fig. 6.3 and Fig. 6.6 indicates that, in general, the level of agreement between results of calculations and measurements is technically satisfying. In case of outlet in the form of overflow orifice (shaft overfall) the agreement level is indeed very high in the central part of the chamber (mean relative difference between results equals 5.5%). However, this difference consecutively rises while approaching the outer wall where its value exceeds 50% (Fig. 6.3 and Fig. 6.4).

On the contrary, this situation reverses for outflow in the form of a perforated pipe (Fig. 6.5) and a pipe with bottom openings (Fig. 6.6). In this two cases calculations of tangential velocity in the central part of the chamber yield values that are on average 10% lower than measured, whereas, values calculated and measured near the outer wall display a difference of only circa 1%. From all three types of outlets that were examined, the most important one is the overflow orifice ("A" series) as this variant provides direct access to the outlet pipe while the device is working (maintenance, removal of possible floating bodies). The remaining two outlet pipe versions ("B" and "C" series) were taken into account merely from cognitive point of view. Consequently, further measurements included only the overflow orifice outlet.

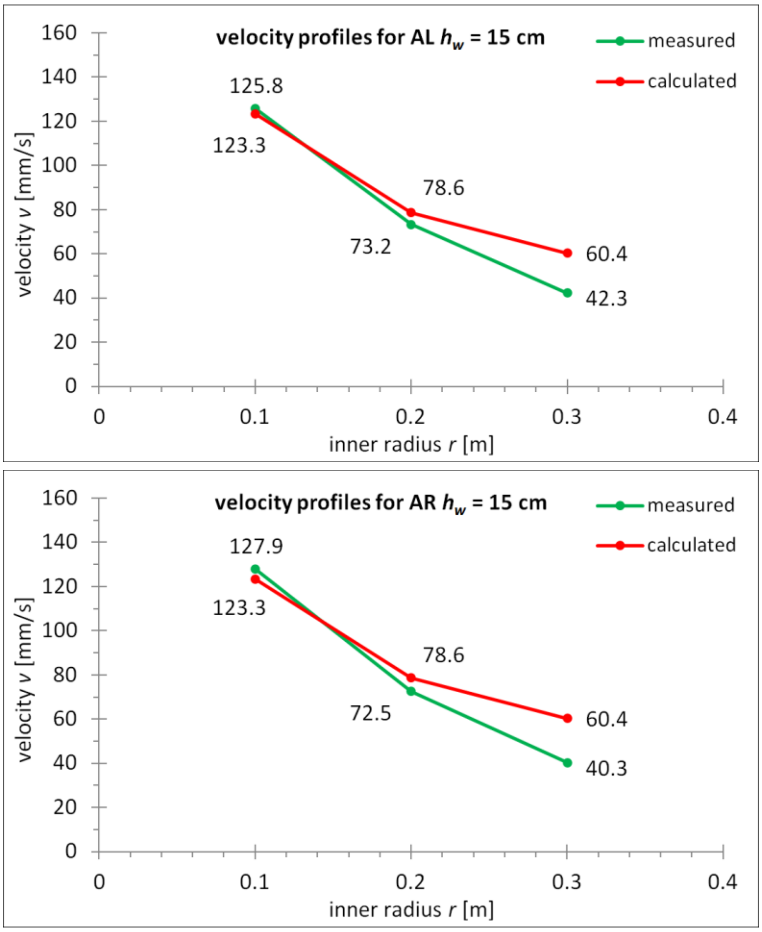

Fig. 6.3. Comparison of measured and calculated tangential velocity profiles for „A" h_w = 0.15 m

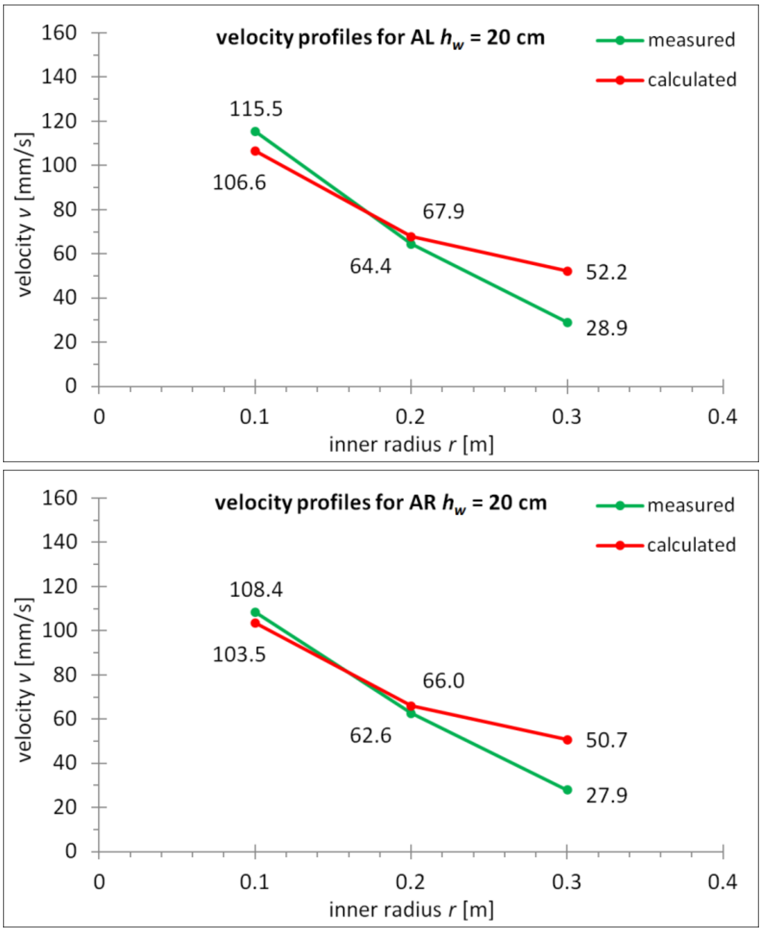

Fig. 6.4. Comparison of measured and calculated tangential velocity profiles for „A” h_w = 0.20 m

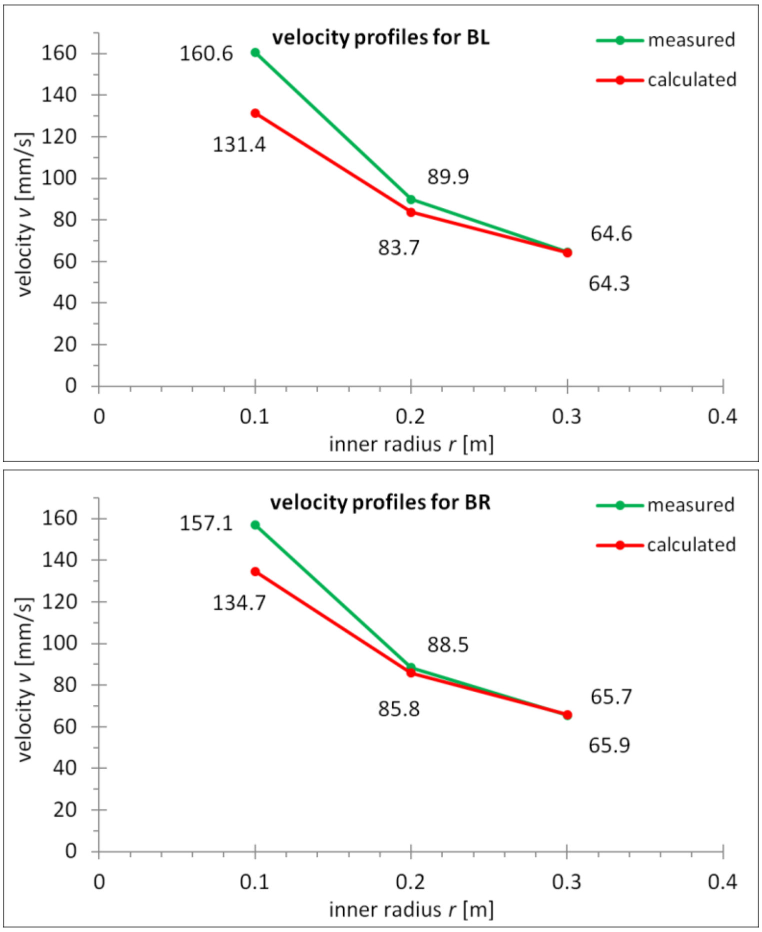

Fig. 6.5. Comparison of measured and calculated tangential velocity profiles for „B” outlet

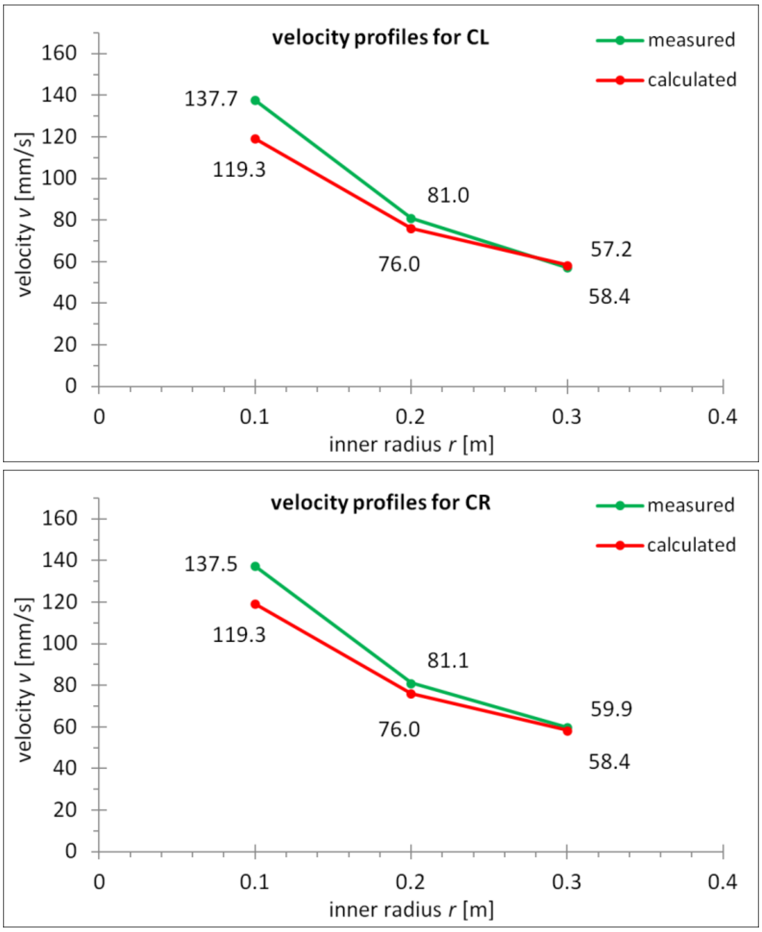

Fig. 6.6. Comparison of measured and calculated tangential velocity profiles for „C" outlet

The difference between calculations and measurements at measurement point near the outer wall at r = 0.3 m in "A" series could be diminished by correcting parameters of the model. However, a correction was not applied due to two factors:

– the developed model is utterly independent from conducted measurements what makes it advantageously objective;
– further research (development of design criteria - chapter 8) includes balance of forces in the vicinity of the outlet cross-section where agreement between calculations and measurements is high.

Taking all the discussed aspects into account, the presented tangential velocity model was accepted (relations (6.7) and (6.24)).

6.3. Pressure distribution

As already mentioned (subsection 6.1.1), in kinematic models velocity field is determined from a chosen condition that characterises the flow (e.g., relations (6.1), (6.2) or (6.3)), whereas, liquid pressure from the dynamic equation. A fine example is the classic problem of ideal liquid flow around a sphere (Sawicki, 2007; Soo, 1969).

In case of vortex separators with axial-symmetrical circulation on a horizontal plane the dynamic equation acquires the form (Łojcjanskij, 1977; Slattery, 1999):

– for pressure radial component:

$$-\rho u_r \frac{\partial u_r}{\partial r} - \frac{\rho {u_t}^2}{r} = -\frac{\partial p}{\partial r} \tag{6.25}$$

– for pressure vertical component:

$$\frac{\partial p}{\partial z} = -\rho \mathrm{g} \tag{6.26}$$

By substituting $u_r(r)$ according to (6.5) and $u_t(r)$ according to (6.7), the set of equations (6.25)-(6.26) can be solved giving (Sawicki, 2012):

$$p(r,z) = p_a + \rho g(H-z) + 0.77\rho B^2\left({r_w}^{-1.3} - r^{-1.3}\right) + \frac{\rho Q^2}{8\pi^2 H^2}\left({r_w}^{-2} - r^{-2}\right) \tag{6.27}$$

where: p_a - atmospheric pressure. The obtained pressure values are needed to calculate the force that is exerted on suspended particles by pressure variability.

On the other hand, this force can be determined basing on general relations found in literature (e.g., Soo, 1969). The term that expresses pressure dependence on the liquid depth in equation (6.27) is responsible for occurrence of the Archimedes force:

$$F_A = \rho \mathrm{g} V \tag{6.28}$$

whereas, the remaining terms generate the force that is characteristic for curvilinear motion and named "the transverse drift" F_{TD} (subsection 3.2.1) and described by a general relation (Soo, 1969):

$$F_{TD} = -V\frac{\partial p}{\partial r} \tag{6.29}$$

The radial derivative of pressure is expressed by equation (6.25), however, the influence of radial flow is generally neglected in this equation (Rhodes, 2008). Comparison of the two last terms on the right side of relation (6.27) confirms this fact. The last but one term related to tangential motion is significantly higher than the last term connected with radial motion. Finally, omission of the radial term yields the formula describing the transverse drift:

$$F_{TD} = \rho V \frac{{u_t}^2}{r} \tag{6.30}$$

where tangential component of velocity u_t is calculated from relation (6.7).

7. Solution of the general equation of particle motion

7.1. Calculation of the time of particle motion

As stated at the beginning, the aim of the dissertation is to determine a design method for vortex separators that is as formally simple as possible and physically justified at the same time. Such an approach requires mathematical relations to be expressed in an algebraic form at the cost of lower accuracy of the solution. That is why, it is always wise to have more precise, but complicated, methods at ones disposal. Usually, they come as a set of differential equations and are solved by numerical means. Such methods can be used to perform simulations of considered systems for various external conditions and states, as well as yield full sets of information needed to solve the considered problem.

Determination of particle trajectory by means of the structural method (subsection 2.3.2) is the basic tool for description of vortex separators operation. Particle trajectory is expressed by radius vector $\mathbf{r_p}$ related to particle velocity $\mathbf{v_p}$ as in equation (2.1). Description of particle velocity by Newton's second law of motion yields a set of three equations (Gronowska *et al.*, 2013; Soo, 1969):

– radial direction:

$$\left(\rho_p+\alpha_s\rho\right)V_p\frac{dv_r}{dt}=\left(\rho_p-\rho\right)V_p\frac{u_t^{\,2}}{r}-C_DF_p\frac{\rho\left(v_r-u_r\right)^2}{2} \tag{7.1}$$

– tangential direction:

$$\left(\rho_p+\alpha_s\rho\right)V_p\frac{dv_t}{dt}=C_DF_p\frac{\rho\left(v_t-u_t\right)^2}{2} \tag{7.2}$$

– vertical direction:

$$\left(\rho_p+\alpha_s\rho\right)V_p\frac{dv_z}{dt}=\left(\rho_p-\rho\right)V_p\mathrm{g}-C_DF_p\frac{\rho v_z^{\,2}}{2} \tag{7.3}$$

where: α_s - associated mass coefficient; v_r, v_t, v_z - particle radial, tangential and vertical velocity component.

The presented set of relations (7.1)-(7.3) together with equations (6.5) and (6.7) expressing radial and tangential velocity components can be used to describe operation of the vortex separator. Low acceleration of suspended particles allows to exclude the inertial force from relations (7.1) and (7.2). As a result, equation (7.1) acquires the form:

$$v_r(r) = \frac{dr_p}{dt} = u_r + \frac{v_{fs}B}{\sqrt{g}r^{1.15}} \tag{7.4}$$

where free sedimentation velocity v_{fs} of a particle of diameter d_p is calculated from relation (4.13). After transforming equation (7.2) one obtains:

$$v_\omega(r) = r_p \frac{d\omega_p}{dt} = u_\omega(r) \tag{7.5}$$

where: v_ω - particle angular velocity; ω_p - particle angular coordinate; u_ω - liquid angular velocity. Division of equations (4.13) and (7.5) by sides yields the equation describing the shape of particle trajectory:

$$\frac{dr_p}{d\omega_p} = -\frac{Q}{2\pi H_e B} r_p^{\ 0.65} + \frac{v_{fs}}{\sqrt{g}} r_p^{\ 0.5} \tag{7.6}$$

Computational time of particle motion needs to be correlated with the time of particle sedimentation t_{fs} given by equation (4.12). The time of particle motion on a horizontal plane t_p (between the inlet and the outlet) can be easily calculated from equation (7.5) using (6.7). Single integration with initial condition $t_p = 0$ when $r_p = R$ results in the equation:

$$t_p = \frac{\omega_p r_p^{\ 1.65}}{B} \tag{7.7}$$

The calculations are done in a number of steps:

– particle coordinates and the actual time of particle motion t_p are determined from relation (7.6) for subsequent time intervals (beginning from the particle initial position);
– if $t_p < t_{fs}$ and $r_p > r_w$ calculations are continued;
– if $t_p = t_{fs}$ and $r_p > r_w$ calculations are stopped - the particle settled on the tank bottom;
– if $t_p < t_{fs}$ and $r_p = r_w$ calculations are stopped - the particle left the separator with the liquid stream.

7.2. Determination of the suspended particle trajectory

Sample calculations of the particle sedimentation time t_{fs} according to equation (4.12) and the time of particle horizontal displacement t_p according to relations (7.6) and (7.7) were performed for the following data set: R = 0.50 m; H = 1.00 m; r_w = 0.05 m; d_{in} = 0.10 m; v_{fs} = 0.02 m/s and for three values of discharge. Results of calculus are presented in Tab. 7.1.

Tab. 7.1. Times of particle horizontal motion and sedimentation for different discharges

Q [m³/s]	t_p [s]	t_{fs} [s]
0.050	8.6	50.0
0.010	43.0	50.0
0.005	86.0	50.0

The highest discharge Q = 0.05 m³/s resulted in the time of particle motion shorter than the time of particle sedimentation ($t_p < t_{fs}$) what means that this characteristic suspended particle was removed from the device (particle trajectory marked by a solid line in Fig. 7.1). For the smaller discharge Q = 0.01 m³/s the particle motion time was still shorter than the particle sedimentation time ($t_p < t_{fs}$). Even though, the horizontal motion time was distinctively longer than in case of the first discharge Q = 0.05 m³/s, the particle was again removed from the separator (dashed line). Finally, the lowest discharge Q = 0.005 m³/s yielded the particle horizontal motion time longer than the particle sedimentation time ($t_p > t_{fs}$). In this case the particle settled on the separator bottom (dotted line, sedimentation point SP).

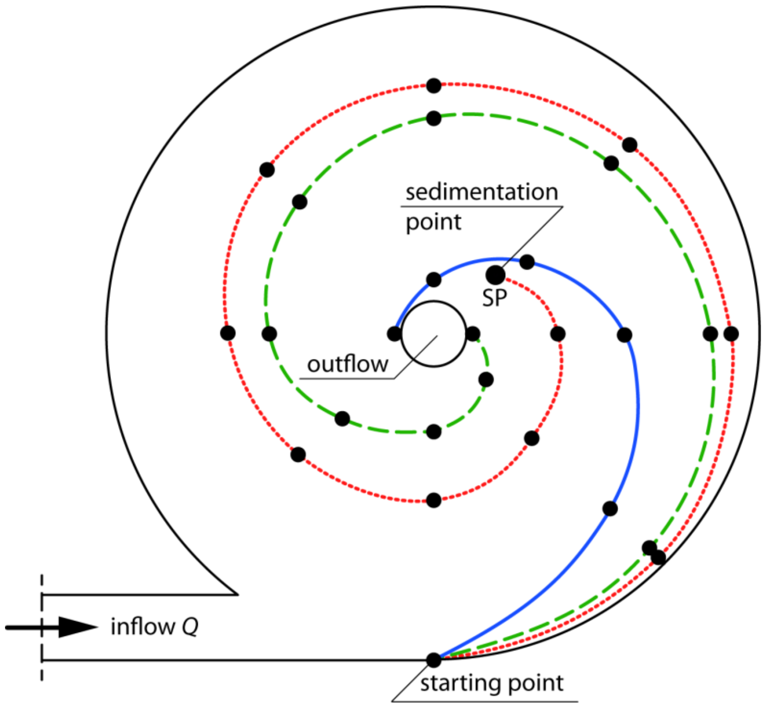

Fig. 7.1. Sample trajectories of the characteristic suspended particle

While describing motion of a suspended particle inside the separator, the sign of the derivative in relation (7.6) needs to be taken into account. The right side of this equation includes a sum of two terms. The first term (the negative one) describes the stress force $\mathbf{F_{DN}}$ that directs the particle towards the outlet, while the second term (the positive one) - the centrifugal force $\mathbf{F_C}$, reduced by the transverse drift $\mathbf{F_{TD}}$, directs the particle towards the outer wall. When the stress force is bigger than the centrifugal force the particle is directed towards the separator axis (the derivative has a negative sign). When the modulus of the derivative decreases, influence of the centrifugal force increases. When derivative equals zero, the particle reaches a balance point - its horizontal motion ceases and the particle falls to the bottom. On the other hand, a positive derivative means that the centrifugal force is stronger than the stress force and directs the particle towards the outer wall (the separator acts like a cyclone).

7.3. Practical remarks

The presented description of the computer simulation of the suspended particle motion belongs to the category of CFD methods. As explained in subsection 6.1.1 results of such a simulation can be used in the design process. However, when the course of the simulated phenomenon (in this case: sedimentation of suspension) does not meet the expectations, the result obtained needs to be corrected. In order to choose a proper correction method it is convenient to have draft relations (that combine characteristic dimensions of the object) at ones disposal. Such relations constitute simplified design criteria, that will be presented in chapter 8 of the dissertation, that may be used by engineers as a separate design tool.

8. Practical design criteria for vortex separators

8.1. General remarks

As already explained in subsection 6.1.1, detailed description of phenomena that important from technical point of view, generally requires solutions of complex sets of differential equations (taking into account the existing theories of physics). In case of devices designed for removal of particles suspended in liquids, especially vortex separators, the set of equations includes relations given by (7.1)-(7.3). However, the process of finding a solution to such equations cannot be acknowledged as a fundamental tool for everyday work of both engineers and researchers. Due to mathematical difficulties, computer methods (including CFD) need to be employed what results in higher expenses and longer worktime (gathering of data and preparation of information about the given object, formulation of boundary and sometimes initial conditions). Moreover, employment of computer aided methods usually yields comprehensive results, while, in majority of practical cases synthetic variables characteristic of the object are sufficient.

That is why, development of simplified methods that could be successfully used to design vortex separators is well justified, especially that they would be most convenient for small companies as well as individual users. These methods should be in the form of cohesive synthetic design criteria that may comprise a separate tool for an individual work of an engineer and a supplementary element for computation using CFD methods at the same time. Two such criteria will be presented further in this chapter.

8.2. General classification of conditions

Analysis of quantitative conditions, both cognitive and technical in character, used for simplified description of devices for suspension removal, allows to divide these conditions into two general categories (Ciborowski, 1973; K. Imhoff and K.R. Imhoff, 1979; Mitosek, 1997; Piotrowski and Roman, 1974; Wodociągi i kanalizacja. Poradnik, 1971):

- conditions expressing the balance of “boundary” forces;
- conditions based on the comparison of the time of horizontal motion of a representative particle in the system (movement from the outer wall to the central outlet pipe) and the time required for gravitational separation of this particle.

8.3. The criterion of force balance

8.3.1. Description of force balance in vortex separators

In general, this criterion is formed by comparing two forces:

– the resultant force responsible for removal of particles, representative of the suspended matter, with the carrier fluid from the object (wastewater, water, air or other substance in case of reactors applied in industry);

– the resultant force that keeps the representative particles inside the device.

These forces should be analysed at the cross-section that is "boundary" in character - when the particle crosses a certain point inside the device it is washed out from the object (negative outcome), whereas, when the particle is unable to reach that point, it remains inside the device and is removed from the liquid undergoing treatment (positive outcome). Moreover, the force balance should include forces that are described by algebraic relations and refer to steady flow. Otherwise, the resulting criterion would be functional or differential in character making it impractical for application. This requirement, however, does not significantly limit the accuracy of the method as devices for wastewater treatment are characterised by small flow accelerations.

Application of the criterion of force balance is limited to devices that utilize an additional factor which keeps the particles inside the object. Such devices include circulative separators (centrifugal force; Fig. 8.1b), as well as reactors with a fluidization bed that maintains a layer of immovable suspended sediment in a fluid moving upwards. Such an effect is obtained when the drag force $\mathbf{F_{DN}}$ of the incoming liquid holding the particles in place is balanced by a difference between the gravity force $\mathbf{F_G}$ and the buoyancy force $\mathbf{F_B}$. For particles susceptible to sedimentation this situation is shown in Fig. 8.1a. In case of water or wastewater treatment such a force balance is present in clarifying tanks (Piotrowski and Roman, 1974).

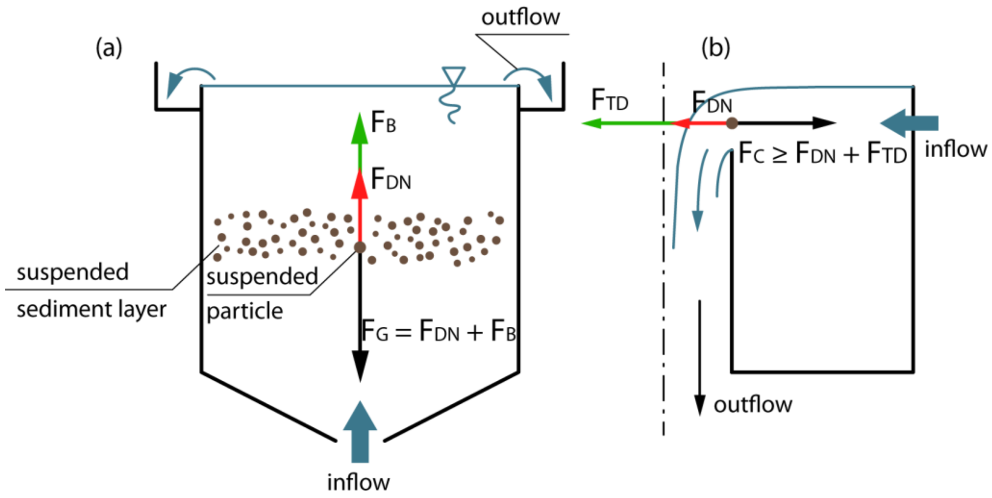

Fig. 8.1. The force balance criterion: a) fluidization bed; b) circulative separator

In case of vortex separators the forces that are crucial for the design criterion include (section 7.1): the drag force $\mathbf{F_{DN}}$, the transverse pressure drift $\mathbf{F_{TD}}$ responsible for washout of the particles from the device and the centrifugal force $\mathbf{F_C}$ that keeps the particles inside the chamber. As these three forces reach their highest values at the outlet cross-section, the "boundary" condition (it is impossible for the particles to leave the tank with the outflowing liquid) acquires the form:

$$\mathbf{F_C}(r=r_w) \geq \mathbf{F_{DN}}(r=r_w) + \mathbf{F_{TD}}(r=r_w) \tag{8.1}$$

8.3.2. Determination of the first design criterion

Substitution of relations describing particular forces listed above and given by equations (4.2), (4.4) and (6.30) transformed according to the accepted velocity model described in chapter 6, into the condition (8.1) gives:

$$\rho_p V_p \frac{u_t^2}{r_w} \geq C_D F_p \frac{\rho u_r^2}{2} + \rho V \frac{u_t^2}{r_w} \tag{8.2}$$

To sort relation (8.2) both its sides were divided by the equation for $\mathbf{F_{TD}}$ (6.30):

$$1 + \frac{C_D F_C r_w}{2V_p}\left(\frac{u_r}{u_t}\right)^2 \leq \frac{\rho_p}{\rho} \tag{8.3}$$

Employment of additional calculations:

$$\frac{F_p}{V_p} = \frac{3}{2} d_p \tag{8.4}$$

$$\frac{u_r}{u_t} = \frac{Q}{2\pi r_w^{0.35} H_e B} \tag{8.5}$$

and substitution of an approximate relation for multiplier B (valid for $R >> r_w$; the basic equation for B is given by (6.24)):

$$B = \frac{4.63 Q r_w^{0.32}}{\left(H d_{in}^{4}\right)^{1/3}} \tag{8.6}$$

yields the following formula:

$$\frac{u_r}{u_t} = 0.034 \frac{H^{1/3} d_{in}^{4/3}}{r_w^{2/3} H_e} \tag{8.7}$$

Relation (8.3) includes the drag coefficient C_D of the particles forming the suspension. In a comprehensive approach its value is determined individually taking into account the shape of the particle. As suspended matter is formed by compacted particles that are not spherical, the drag coefficient can be calculated from the formula given by Orzechowski (1990) for a non-spherical particle:

$$C_D = 5.31 - 4.88\phi \tag{8.8}$$

where particle sphericity ϕ is defined as the ratio of the substitute area of a spherical particle (having the same volume as the real particle) and the area of the real particle. For cubic particles $\phi \cong 0.8$. As real particles have a definitely less regular shape than cubic particles it was assumed that $\phi = 0.7$. For such a value of particle sphericity ϕ the drag coefficient equals:

$$C_D = 1.89 \tag{8.9}$$

Substitution of equations (8.4), (8.7), (8.9) and transformation of equation (8.3) gives:

$$1 + \frac{0.0016 d_{in}^{8/3} H^{2/3}}{H_e^{2} r_w^{1/3} d_p} \leq \frac{\rho_p}{\rho} \tag{8.10}$$

The active layer of liquid flow (substitute water depth) H_e for $r = r_w$ is equal to the thickness of water layer at the outlet pipe h determined from relation (6.12) (for shaft overfall, as in case of vortex separators, length of the overflow orifice is equal to the perimeter of the outlet conduit with radius r_w). Determination of the H_e value from relations (6.12), (6.13), and its substitution into relation (8.10) gives the first design criterion which looks as follows (Gronowska and Sawicki, 2014a):

$$\frac{0.0052 d_{in}^{2.7} H^{0.7} r_w^{5.6} g^{1.6}}{d_p Q^{3.2}} + 1 \leq \frac{\rho_p}{\rho} \tag{8.11}$$

This criterion given by (8.11) - the criterion based on the balance of forces in the vortex separator - relates liquid discharge Q to three characteristic geometric dimensions of the separator (liquid depth H, inlet diameter d_{in}, outlet radius r_w), parameters of the computational particle (diameter d_p and density ρ_p), as well as density of the carrier liquid ρ. This criterion does not include the fourth of the most important geometrical dimensions of the device - separator radius R. This results from the fact that this technical criterion refers to the outlet cross-section where $r = r_w$.

Relation (8.11) can be used to determine one of the values included in the criterion. There are numerous variants, however, it is convenient to firstly simplify this equation to perform preliminary calculations. Simplification can be based on a technical statement that dimensions of the inlet and the outlet are significantly smaller than the separator depth. Assuming inlet and outlet diameters equal to $0.1H$ and particle diameter d_p = 0.0002 m, as well as the remaining values equal to g = 9.81 m/s^2; ρ_p = 2700 kg/m^3; ρ = 1000 kg/m^3, the following relation is obtained:

$$H \le H_{max} = 5.86 Q^{0.36} \tag{8.12}$$

where: [H] = m; [Q] = m^3/s.

8.4. The criterion of the particle time of advection and sedimentation

8.4.1. Exact calculation of the time of advection

In order to calculate the exact value of the residence time of the representative suspended particle inside the separator (as well as in other devices for suspension removal), general equations of particle motion given by (7.1)-(7.3) must be solved. The solution should include both horizontal motion (from outer wall r_p = R towards the outlet cross-section r_p = r_w) and vertical motion (initial position of the particle on liquid free surface z_p = H is the least favourable; final position of the particle is the bottom of the chamber z_p = 0; Fig. 2.2). In engineering practice such a solution is obtainable only by numerical means with calculus starting at the initial position:

$$t_p = 0; \quad r_p\left(t_p = 0\right) = R; \quad z_p\left(t_p = 0\right) = H \tag{8.13}$$

Subsequent particle positions after subsequent time intervals are compared with coordinates of the chamber wall. When the particle reaches the bottom before nearing to the central outlet:

$$t = t_s; \quad r_p\left(t = t_s\right) = r_s; \quad z_p\left(t = t_s\right) = 0 \tag{8.14}$$

it is assumed that the particle was removed from the liquid stream and its time t_s is equal to the particle residence time inside the separator. Such a situation applies to particles with favourable settling velocity that can easily be removed from the liquid stream inside the separator.

On the contrary, particles of less favourable sedimentation properties do not settle directly on the bottom, however, are still removed from the liquid stream. Such particles reach the lower part of the central outlet conduit at such height h_{min} that the particle is not flushed out with the treated liquid and falls along the outlet pipe to the bottom. This situation is described by:

$$t = t_b; \quad r_p\left(t = t_b\right) = r_b; \quad z_p\left(t = t_b\right) \le h_{min} \tag{8.15}$$

where time t_b is the particle residence time inside the separator. Determination of the limit value of h_{min} requires a comprehensive description of the vertical structure of the velocity field. In an extremely cautious approach this value is assumed as:

$$h_{min} = 0 \tag{8.16}$$

whereas, from technical point of view:

$$h_{min} = 0.5H \tag{8.17}$$

The third category of particles concerns particles that flow out of the device with the treated liquid:

$$t = t_w; \quad r_p\left(t = t_w\right) = r_w; \quad z_p\left(t = t_w\right) \geq h_{min} \tag{8.18}$$

The calculated value of t_w is the residence time of these particles.

Such detailed calculations are justified in case of important problems when sufficient financial support and time span are available. In practice, however, these two factors are limited, therefore, it is most convenient to develop simplified methods.

8.4.2. Approximate calculation of the time of sedimentation

Many simplified methods applied for designing devices for gravitational removal of suspensions from water or wastewater are based on separate calculations of the time of particle advection and the time of particle sedimentation. The two-dimensional velocity model determined in chapter 6 assumes that radial u_r and tangential u_t velocity components are independent from vertical coordinate "z". Therefore, both directions of particle motion: horizontal and vertical (in z axis direction) can be analyzed individually. In case of vertical direction equation (7.3) acquires the form:

$$\frac{dv_z}{dt} = -\frac{\left(\rho_p - \rho\right)\mathrm{g}}{\left(\rho_p + \alpha_s \rho\right)} + \frac{\rho C_D F_p}{2V_p\left(\rho_p + \alpha_s \rho\right)} {v_z}^2 \tag{8.19}$$

Relation (8.19) is analytically integrated yielding (Sawicki, 2007):

$$v_z\left(t\right) = -\, v_{fs} tgh\left(\sqrt{\frac{3\rho \mathrm{g}\left(\rho_p - \rho\right)C_D}{4d_p\left(\rho_p + \alpha_s \rho\right)^2}}\; t\right) \tag{8.20}$$

where particle free sedimentation velocity v_{fs} (subsection 2.3.2) is given by:

$$v_{fs} = \sqrt{\frac{2\left(\rho_p - \rho\right)\mathrm{g}V_p}{\rho F_p C_D}} \tag{8.21}$$

Taking into account the fact that the hyperbolic tangent of an increase in the argument tends to unity, vertical component of suspended particle velocity tends to the value of free sedimentation velocity. Relation (8.20) allows to estimate how fast particle velocity v_z tends to v_{fs}. Assuming typical values: g = 9.81 m/s^2; d_p = 0.0002 m; ρ_p = 2700kg/m^3; ρ = 1000 kg/m^3; $C_D \approx 1$; α_s = 0.5; relation (8.20) gives:

$$v_z(t) = -v_{fs} tgh(87.2t) \tag{8.22}$$

Just after t = 0.02 s instantaneous particle velocity $v_z(t)$ differs from the final value of v_{fs} only by less than 5%. This confirms the common approach, employed in theory of sedimentation, that a particle falling straight downwards (vertical component of particle motion is not present) almost at ones reaches the value of free sedimentation velocity:

$$v_z = v_{fs} \tag{8.23}$$

Besides this approach, equality (8.23) can also be determined from an estimation that particle acceleration is negligibly small. Omission of the derivative with respect to time in equation (8.19) directly leads to relation (8.23), resulting in a simple way to calculate the particle sedimentation time t_{fs}:

$$t_{fs} = \frac{H}{v_{fs}} \tag{8.24}$$

8.4.3. Approximate calculation of the time of advection

The simplified approach of calculating the time of particle advection (particle floating on a horizontal plane in wastewater) is based on the estimation made in the previous subsection 8.4.2 that particle acceleration is negligibly small (Sawicki, 2007). As a result equation (7.1) obtains the form:

$$C_D F_p \frac{\rho(u_r - v_r)^2}{2} = (\rho_p - \rho) V_p \frac{B^2}{r^{2.3}} \tag{8.25}$$

After adequate transformations, equation (8.25) gives a relation describing radial component of particle velocity:

$$v_r = u_r - \frac{v_{fs} B}{\sqrt{g} r^{1.15}} \tag{8.26}$$

Expression (8.26) indicates that radial velocity of the particle is smaller than radial velocity of the carrier liquid (water or wastewater) due to influence of the centrifugal force. Moreover, this relation can be also used to quantify the difference between these two velocities (subsection 8.4.4).

By substituting relation (6.5) describing radial velocity into (8.26) one obtains:

$$v_r\left(r_p\right)=\frac{dr_p}{dt}=\frac{Q}{2\pi H_e r_p}-\frac{v_{fs}B}{\sqrt{g}r_p^{\ 1.15}} \tag{8.27}$$

Such a form of relation (8.26) cannot be solved in an analytical way. However, keeping in mind the aim of the analysis - approximate evaluation of the time of advection by means of a relation that can be used in technical applications - equation (8.27) can be simplified basing on the small value of the index of variable *r* on the right side of (8.27):

$$r_p^{\ 1.15}=R^{1.15}\left(\frac{r_p}{R}\right)^{1.15}\approx R^{1.15}\left(\frac{r_p}{R}\right)=R^{0.15}r_p \tag{8.28}$$

The calculated error ΔB resulting from this simplification is shown in Fig. 8.2:

$$\Delta B=\frac{R^{0.15}r_p-r_p^{\ 1.15}}{R^{0.15}r_p}=1-\left(\frac{r_p}{R}\right)^{0.15} \tag{8.29}$$

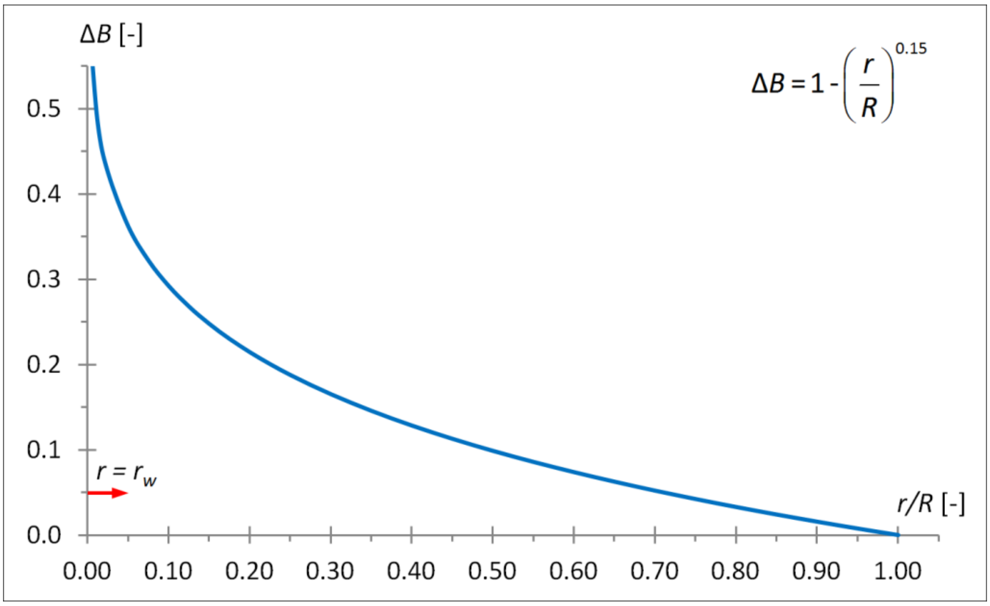

Fig. 8.2. Error resulting from simplification of index of *r*

Fig. 8.2 indicates that the error ΔB resulting from the chosen simplification reaches tens of percents for small values of r_p, however, it significantly decreases further from the outflow zone ($r > 0.2R$). The use of relation (8.28) allows to rewrite equation (8.27) in the following form:

$$\frac{dr_p}{dt}=\left(\frac{Q}{2\pi H_e}-\frac{v_{fs}B}{\sqrt{g}R^{0.15}}\right)\frac{1}{r_p}=\left(X_L-X_p\right)\frac{1}{r_p} \tag{8.30}$$

where parameter X_L refers to the liquid carrier and X_p to the particle.

Single integration of equation (8.30) with initial condition:

$$r_p = R \text{ for } t_p = 0 \tag{8.31}$$

yields a relation combining the time of particle motion with the particle position along the separator radius:

$$t\left(r_p\right) = \frac{R^2 - r_p^{\ 2}}{2\left(X_L - X_p\right)} \tag{8.32}$$

Consequently, the time of advection of the suspended particle from the outer wall ($r_p = R$) to the outlet pipe ($r_p = r_w$) can be determined from:

$$t_p = \frac{R^2 - r_w^{\ 2}}{2\left(X_L - X_p\right)} \tag{8.33}$$

Additionally, relation (8.32) can be also used to calculate the time of advection of the carrier liquid along the same distance, provided that $X_p = 0$:

$$t_L = \frac{R^2 - r_w^{\ 2}}{2X_L} \tag{8.34}$$

8.4.4. Determination of the influence of the centrifugal force on the suspended particle time of advection

Relations (8.33) and (8.34) show that the time of advection of the suspended particle t_p is longer than the time of advection of the carrier liquid t_L. By denoting the difference between this two times of advection as:

$$\Delta t = t_p - t_L \tag{8.35}$$

a relation which refers this difference to the time of particle motion is obtained:

$$\frac{t_L}{t_p} = \frac{t_p - \Delta t}{t_p} = 1 - \frac{\Delta t}{t_p} = 1 - e_p = \frac{X_L - X_p}{X_L} = 1 - \frac{X_p}{X_L} \tag{8.36}$$

Substitution of parameters X_p and X_L according to equation (8.30) into (8.36) gives:

$$e_p = \frac{\Delta t}{t_p} = \frac{2\pi v_{fs} B H_e}{Q\sqrt{g} R^{0.15}} \tag{8.37}$$

and substitution of relation (6.24) describing multiplier B into (8.37) yields:

$$e_p = \frac{29.1 v_{fs} r_w^{\ 0.31} H_e}{H^{0.33} d_{in}^{\ 1.33} \sqrt{g} R^{0.15}} \tag{8.38}$$

Relation (8.38) combines six variables that characterize vortex separator. However, these variables have indices given by fractions resulting in complicated calculations. Therefore, the following evaluation was introduced:

$$\begin{aligned} &2r_w \approx H_e \approx d_{in} \\ &d_{in} \approx 0.2R \\ &H \approx 0.5R \end{aligned} \qquad (8.39)$$

and equation (8.38) rewritten giving:

$$e_p = \frac{30.6 v_{fs}}{\sqrt{gR}} = 30.6 Fr_s \qquad (8.40)$$

Equation (8.40) indicates that the relative elongation of the time of particle advection given by equation (8.33) referred to the time of carrier liquid advection given by equation (8.34) is described by "settling" Froude number Fr_S (calculated for free sedimentation velocity v_{fs}). Finally, relation (8.40) can be used to evaluate the influence of the centrifugal force on the time of advection of the suspended particle. For sand particles with v_{fs} = 0.0067 m/s (K. Imhoff and K.R. Imhoff, 1996) the time of particle advection will be elongated by 20% provided that:

$$e_p \geq 0.2 \text{ and } R \leq 0.11\text{m} \qquad (8.41)$$

On the other hand, for the relative elongation to reach at least 10%, the following must be fulfilled:

$$e_p \geq 0.1 \text{ and } R \leq 0.44\text{m} \qquad (8.42)$$

Such results mean that the influence of the centrifugal force on the time of advection of the suspended particle (the time of particle advection is over a dozen longer than the time of liquid advection) is observed for small dimensions of the tank chamber (diameter of the order of tens of centimetres). This applies to such devices as hydrocyclones or centrifuges, whereas, separators employed in sewerage systems require larger dimensions.

8.4.5. Determination of the second design criterion

The conclusion drawn from mathematical analysis in the previous subsection 8.4.4 means that the influence of the centrifugal force on the time of suspended particle advection can be omitted. Consequently, it can be assumed that the time of advection of the suspended particle is equal to the time of advection of the carrier liquid which can be conveniently expressed by a commonly employed indicator - the plug-flow time t_{PF}

(Sawicki, 2007). Making use of the proportion $R >> r_w$ the expression for the plug flow-time looks as follows:

$$t_{PF} = \frac{V}{Q} = \frac{\pi R^2 H}{Q} \tag{8.43}$$

For the device to operate properly, the residence time must be no shorter than the time required for particle sedimentation given by equation (8.24):

$$t_{PF} = \frac{\pi R^2 H}{Q} \geq t_{fs} = \frac{H}{v_{fs}} \tag{8.44}$$

thus:

$$R \geq \sqrt{\frac{Q}{\pi v_{fs}}} \tag{8.45}$$

Equation (8.45) is the draft version of the developed criterion of the time of suspended particle advection and sedimentation. Analogically to the first criterion expressed by (8.12), this criterion can be written as (for v_{fs} = 0.0067 m/s):

$$R \geq 6.84 Q^{0.5} \tag{8.46}$$

where: [R] = m; [Q] = m^3/s.

8.5. Comparison of the developed design criteria

Within this chapter two technical criteria were developed that are a result of discussion, analysis and simplification of general relations given by equations by (7.1)-(7.3). These criteria should be fulfilled by properly operating vortex separators. As such, the two relations (8.12) and (8.46) are practical in character and can be used to design new objects. The design process can be conducted in two ways:

- approximate dimensioning - the criteria comprise the basis for calculations;
- comprehensive simulation by CFD methods - the criteria comprise additional relations that can be used to correct subsequent approximations of values characterizing the designed object.

The first criterion - the criterion of force balance described by the draft relation (8.11) results from a requirement for the centrifugal force, that keeps the particles inside the separator, to be no weaker than the forces responsible for washing the particle out of the separator. Balance of these forces is referred to the outlet cross-section where they reach their highest values.

The second criterion - the criterion of the suspended particle time of advection and sedimentation given by the draft equation (8.45) describes a requirement that the characteristic (simplified) time of the particle advection must not be shorter than the time of particle sedimentation.

Furthermore, equations (8.11) and (8.45) were simplified giving preliminary relations that are easily understandable. In order to obtain the criteria in the form of relations (8.12) and (8.46), estimations stated in (8.39) were introduced. The criteria given by (8.12) and (8.46) may also be used in engineering practice, moreover, they allow to find the range of design values for vortex separators. Practical applications of these relations are presented in section 10.4.

8.6. The influence of the centrifugal force on the difference between suspended particle and carrier liquid velocities

The difference between velocities of the suspended particle and the carrier liquid is expressed by relation (8.26). The difference reaches its maximum value when $r = r_w$ and its relative value can be described by:

$$s = 1 - \frac{v_r}{u_r} = \frac{v_{fs} B}{u_r \sqrt{g} r_w^{\ 1.15}} \tag{8.47}$$

Substitution of the developed relations for multiplier B (6.24) and liquid radial velocity u_r (6.5), assumption that v_{fs} = 0.0067 m/s and employment of equation (8.39) gives:

$$s = 584 \frac{Q^{1.6}}{H^{4.5}} \tag{8.48}$$

where: [Q] = m^3/s; [H] = m. For a given minimum value of s_{min} equation (8.48) can be transformed into:

$$H \le 4.06 s_{min}^{-0.22} Q^{0.36} \tag{8.49}$$

Equation (8.49) is analogical to the first criterion (8.12) and for s_{min} = 0.2 these two become identical. This results from the fact that both relations describe the same condition. The difference between this two lies in criterion (8.12) being developed basing on the force balance (forces acting on a particle at the ending cross-section as given by equation (8.1)), whereas, relation (8.49) was based on the difference between final velocities established by the forces included in the balance (including the centrifugal force).

9. Determination of liquid residence time

9.1. General remarks

Within the previous chapters of the dissertation (subsection 5.2.2, 8.4.4 and section 8.6) it was mentioned that the influence of the centrifugal force on the process of suspension removal in vortex separators is very specific. The range of values characterizing the device (geometrical dimensions and wastewater discharge) to choose from indicate that the centrifugal force is not a crucial factor. Results of measurements clearly show that producers interested in investing in such devices cannot be fully satisfied, because vortex separators are unable to work so efficiently as centrifuges or cyclones.

Nevertheless, vortex separators are characterized by an increase in favourable proportions between the forces acting on a suspended particle near the outlet conduit and the device axis of symmetry. **In the central part of the separator a local "dynamic buffer zone" is formed which prevents the particles from flowing out of the object, so they can undergo sedimentation.** However, comparison of the two design criteria proposed in chapter 8 (the force balance criterion given by equation (8.12), and the criterion related to the time of particle sedimentation given by equation (8.46)), confirm the fact that such a situation is relatively hard to obtain. Fig. 10.6 shows that the range of device parameters shared by both criteria is rather narrow, moreover, there are some cases when there is no common range whatsoever. Regardless, the centrifugal force proves to be a positive factor and research results presented in this dissertation explain how to quantify its influence, both for scientific and technical reasons.

The second characteristic of separators with circulative flow is the better use of the tank cubic capacity by the active liquid flow than in case of systems with translational motion. In vortex separators dead zones of flow occupy far less volume than in other objects. This fact was confirmed by the research presented so far in this dissertation, as well as literature sources (e.g., Veerapen *et al*., 2005).

Therefore, a series of measurements were conducted to evaluate the influence of circulation on the length of liquid residence time within the considered devices.

9.2. Measurements methodology

In order to determine time characteristics of vortex separators, a series of measurements on the laboratory test stand (description in subsection 5.1.1) were performed. The measurements of liquid residence time in the separator were based on a fluorometric technique which employs tracer monitoring. The equipment used included the Rhodamine WT tracer (the concentration specified by the manufacturer was 21.33% ± 2.5%, and the value taken for recalculations - 20%) and CYCLOPS-7 Submersible Fluorometer from Turner Designs USA, of the Fluorescent Dye Tracing sensor type (Fig. 9.1). Rhodamine WT is a highly fluorescent material with the ability to absorb green light and emit red light what makes it a very specific tracer. The applied fluorometer is configured to shine green light on the liquid and detect the red light emitted. The amount of red light emitted is directly proportional to the concentration of the dye, up to 100 μg/dm^3.

Firstly, a known volume of tracer (5 cm^3 of the prepared standard solution 1.5 cm^3/5 dm^3) was injected at the inlet by means of a specially constructed automatic feeder. From this point, the sensor installed at the outlet and coupled with the computer station started to register concentration $c(t)$ of the dye at the outlet cross-section. The results in the form of a curve were instantly displayed on the computer screen thanks to a specially prepared software. They were saved in a computer file and then viewed in a numerical way. Each time the sensor was placed over or near the outlet conduit depending on its variant. The general rule was to position the sensor so no influence of the bottom and the outlet pipe itself was observed. Position of the sensor was defined by three variables: horizontal distance to the outlet pipe, elevation over the outlet pipe and elevation over the chamber bottom.

Secondly, values of chosen synthetic indicators were determined:

– average residence time t_A equal to the first moment on the residence time distribution curve $E(t)$:

$$t_A = \int_0^\infty tE(t)dt \tag{9.1}$$

where function $E(t)$ was calculated for a known value of discharge Q and mass of the tracer dose M:

$$E(t) = \frac{c(t)Q}{M} \tag{9.2}$$

– modal time t_M calculated as the time of the maximum concentration of the tracer at the outlet averaged over five (or three) consecutive measurements;

– plug-flow time t_{PF} according to the formula:

$$t_{PF} = \frac{V}{Q} \tag{9.3}$$

calculated for a known value of discharge Q and height of water surface H in each configuration and for diameter of the chamber $D = 2R = 0.80$ m.

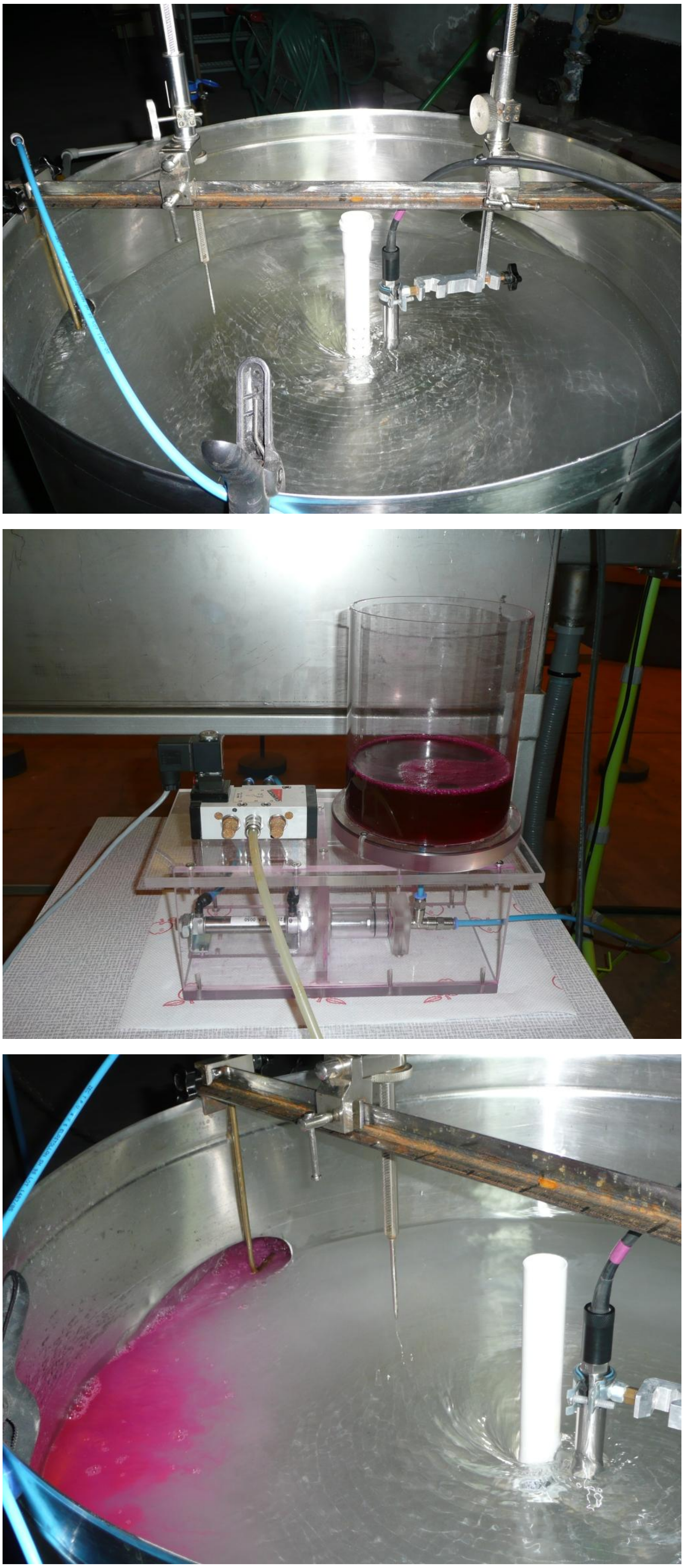

Fig. 9.1. Equipment used for residence time measurements (general view, tracer feeder, tracer injection)

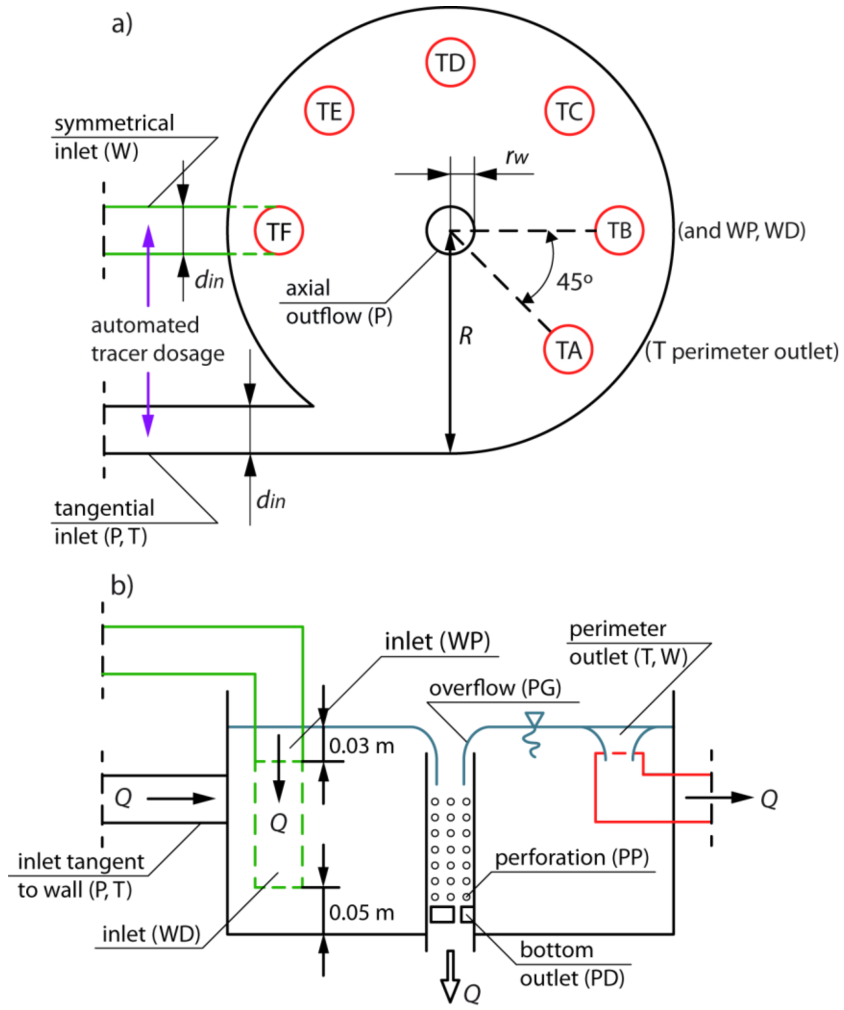

Fig. 9.2. Schematics of the analyzed configurations of the inlet-outlet: a) plan view; b) cross-section

Schematics and dimensions of the test flow-through chamber, as well as configurations of inlet and outlet pipes are shown in Fig. 9.2. Altogether, three groups of inlet and outlet combinations were investigated (Fig. 9.3):

(1) Inlet pipe tangent to the chamber wall and axial outflow through a vertical pipe (description of outlet pipe types in subsection 5.1.1):
   – upper orifice overflow, denoted by letters "PG";
   – perforated side surface of the outlet pipe, denoted by letters "PP";
   – three rectangular openings 29 mm x 15 mm, denoted by letters "PD".

(2) Inlet pipe tangent to the chamber wall (as in "P" series) and outlet pipe located at various points along the perimeter inside the chamber (configurations denoted by letters "TA", "TB", "TC", "TD", "TE" and "TF").

(3) Inlet pipe symmetrical to the chamber wall with vertical liquid inflow and outlet pipe near the opposite wall (as in "T" series):
   – inlet submerged 3 cm below the water surface, denoted by letters "WP";
   – inlet located 5 cm above the chamber bottom, denoted by letters "WD".

Fig. 9.3. Inlet-outlet combinations used in tracer measurements ("P" series, "T" series, "W" series)

The third group of combinations ("W" series) cannot be accepted as rational from hydraulic point of view. Nevertheless, such solutions can be found in catalogues offered by producers of separators. That is why, they were included in the measurements clearly for cognitive reasons. Summing up, three combinations of flow were investigated:

(1) Liquid circulation (tangent inlet) and forced flow in the central part of the chamber (effect of outlet pipe location, "P" series).

(2) Liquid circulation (tangent inlet) and no flow in the central part of the chamber (outlet pipe along the chamber perimeter, "T" series).

(3) Non-circulative flow and forced flow in the central part of the chamber (location of inlet and outlet pipes, "W" series).

The first series of tracer measurements ("P" series) were conducted using the same three outlet pipes, as well as flow parameters, as in velocity measurements. The remaining two series ("T" and "W") were done for three chosen values of discharge Q: Q_1 = 0.4 dm³/s; Q_2 = 0.5 dm³/s and Q_3 = 0.6 dm³/s. Taking into account the quantity evaluation of the influence of the Coriolis force on velocity values (it may be neglected; subsection 5.2.2) tracer measurements were performed using only one inlet conduit - "right" inlet "R" (easier access and shorter distance to the computer station). Flow parameters during measurements are gathered in Tab. 9.1, Tab. 9.2 and Tab. 9.3.

Tab. 9.1 Flow parameters for tracer measurements, "P" series

Config.	Q [dm³/s]	h_w [m]	H [m]
"PG"	0.34	0.20	0.240
"PP"	0.35	-	0.133
"PD"	0.31	-	0.132

Tab. 9.2. Flow parameters for tracer measurements, "W" series

Config.	Q [dm³/s]	h_w [m]	H [m]
"WP"	0.60	0.11	0.266
	0.50		0.206
	0.40		0.143
"WD"	0.60	0.11	0.270
	0.50		0.203
	0.40		0.142

Tab. 9.3. Flow parameters for tracer measurements, "T" series

Config.	Q [dm³/s]	h_w [m]	H [m]
"TA"	0.60	0.11	0.262
	0.50		0.190
	0.40		0.153
"TB"	0.60	0.11	0.255
	0.50		0.205
	0.40		0.151
"TC"	0.60	0.11	0.260
	0.50		0.195
	0.40		0.156
"TD"	0.60	0.11	0.269
	0.50		0.201
	0.40		0.168
"TE"	0.60	0.11	0.261
	0.50		0.188
	0.40		0.157
"TF"	0.60	0.11	0.253
	0.50		0.196
	0.40		0.151

9.3. *Results of measurements*

Sample residence time distribution curves $E(t)$ in the form of tracer concentration as a function of time $c(t)$ for each group of configurations obtained within the course of the measurements are presented in Fig. 9.4, Fig. 9.5 and Fig. 9.6. The remaining inlet-outlet variants are included in Appendix No. 2.

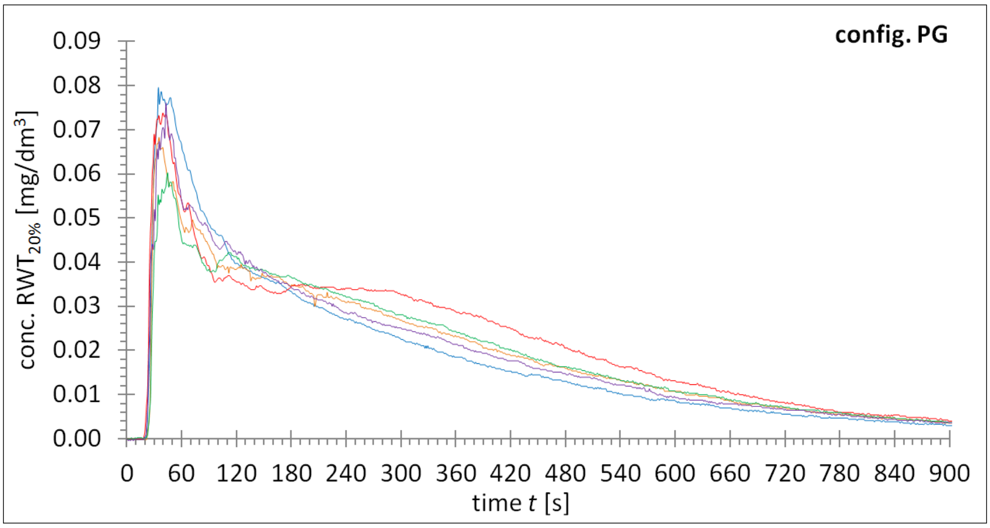

Fig. 9.4. Residence time distribution curves $E(t)$ for "PG" configuration

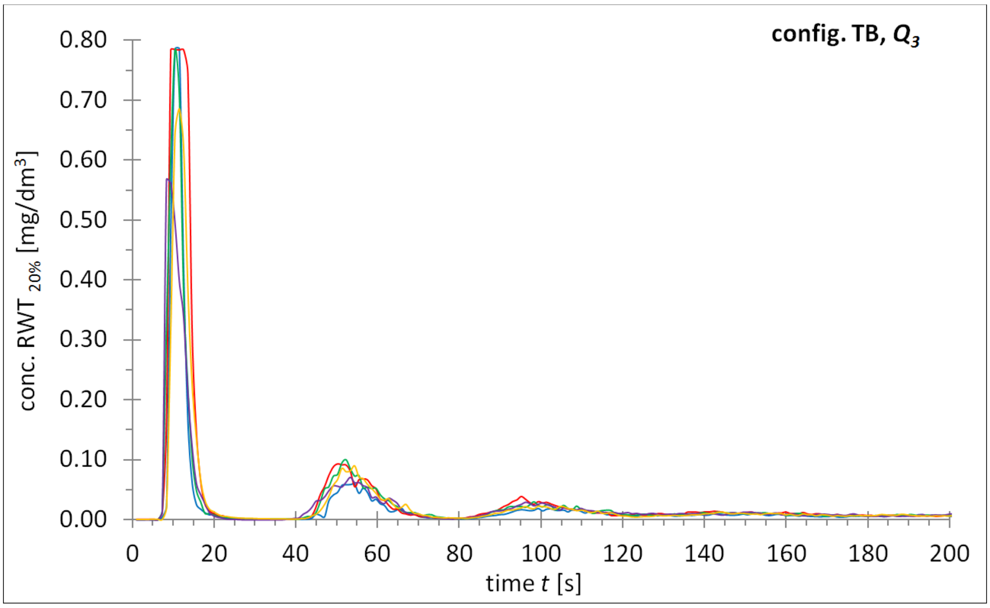

Fig. 9.5. Residence time distribution curves $E(t)$ for configuration "TB", Q_3 = 0.60 dm³/s

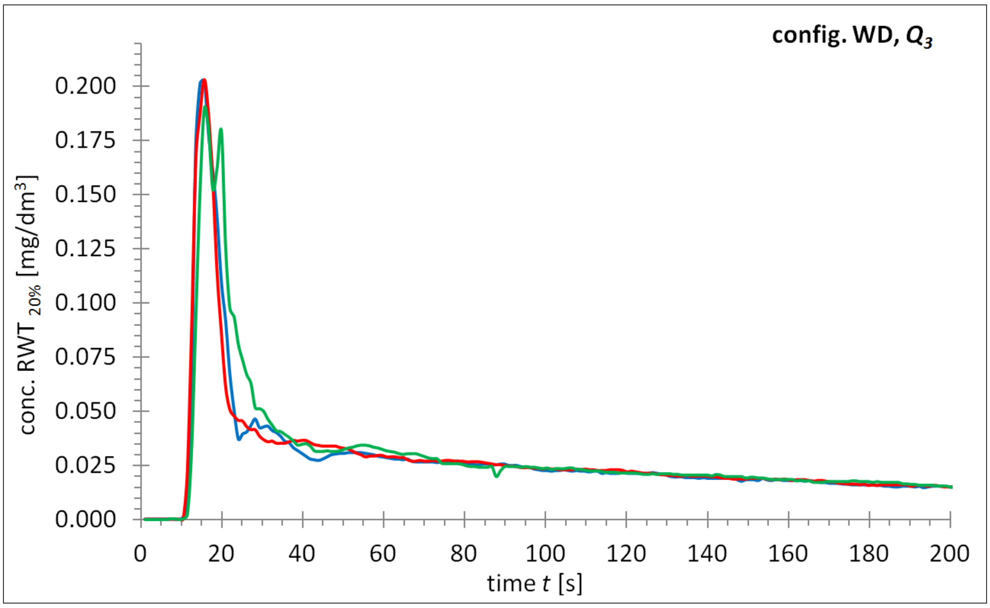

Fig. 9.6. Residence time distribution curves $E(t)$ for configuration "WD", Q_3 = 0.60 dm³/s

Analysis of the obtained residence time distribution curves $E(t)$ confirm the statement made by Veerapen *et al.* (2005) that the character of a vortex separator is very close to the specifics of a well-mixed reactor - first portions of the tracer appear at the outlet after a short period of time, then tracer concentration visibly increases to a maximum value, and finally exponentially decreases. The characteristic times (t_A, t_M and t_{PF}) determined for the investigated object are presented in Tab. 9.4. Additionally, this table includes relative values of average time t_A and modal time t_M related to the plug-flow model time t_{PF} calculated according to relation (9.3). In subsection 6.2.1 results of measurements and calculations of average time t_A were analysed and used to determine the formula (6.11) for the thickness of active layer of flow H_e.

Tab. 9.4. Time characteristics of the liquid flow in the laboratory separator

Config.	Q [dm³/s]	t_{PF} (s)	t_A (s)	t_A/t_{PF} (-)	t_M (s)	t_M/t_{PF} (-)
"PG"	0.34	355	217	61	42	12
"PP"	0.35	199	116	55	32	16
"PD"	0.31	210	118	56	29	14
"TA"	0.60	220	21	10	8	4
"TB"	0.60	213	23	11	10	5
"TC"	0.60	218	24	11	15	7
"TD"	0.60	225	30	13	19	8
"TE"	0.60	219	36	16	24	11
"TF"	0.60	212	40	19	27	13
"WP"	0.60	223	57	26	16	7
"WD"	0.60	226	66	29	15	7

9.4. Comparison of the average residence time and the plug-flow time

Results of tracer measurements confirm the qualitative statement made by Andoh and Saul (2003) that vortex separators work better than analogical objects without fluid circulation. This results from the fact that the interior of the separator is used more efficiently than in case of non-circulative devices. In order to achieve such an effect, liquid must be forced to flow in the central part of the chamber. When liquid circulation is accompanied by radial flow, the average residence time t_A reaches almost 60% of the plug-flow time t_{PF}. This means that dead and stagnant zones occupy less volume than the active layer of liquid flow. Even though the centrifugal force generated by circulation is not a key factor in the process of separation of suspension (as in centrifuges), the threefold longer average residence time t_A than in case of flow without circulation (configurations "W") is very advantageous. Moreover, the modal residence time t_M is also elongated (becomes circa two times longer). After this time period, the main portion of the tracer mass M introduced into the system leaves the chamber. This means that, according to the reaction rate curve, effective level of reduction in concentration (suspension in vortex separators) is higher for systems with fluid circulation. Finally, the research conducted indicate that "T" configurations, where location of the inlet pipe generates circulation and the outlet pipe is situated near the chamber wall, are definitely less beneficial.

10. Determination of vortex separator efficiency

10.1. Laboratory test stand

In order to verify the two design criteria developed and proposed in chapter 8, a new test stand consisting of a laboratory prototype of vortex separator made of acrylic glass and PVC was constructed. According to the first design criterion given by equation (8.11) description of vortex separator includes determination of five parameters: inlet diameter d_{in}, outlet radius r_w, liquid depth H, particle diameter d_p and liquid discharge Q. A single parameter may be calculated provided that the remaining four are known. For suspended sand particles: ρ_p = 2700 kg/m^3, ρ = 1000 kg/m^3 and g = 9.81 m/s^2. Critical size of the particle is the substitute diameter d_p = 0.10 mm (K. Imhoff and K.R. Imhoff, 1996). Taking into account the technical conditions, it was assumed that H = 0.3 m, d_{in} = 0.03 m and r_w = 0.015 m. For such dimensions equation (8.11) gave the lower limit of liquid discharge inside the separator:

$$Q \geq 0.23 \cdot 10^{-3}\, m^3/s \tag{10.1}$$

Referring to the second design criterion given by relation (8.45) and assuming this value of the lower limit of discharge, the centrifugal force should be strong enough (according to the theoretical considerations) to keep the suspended particles inside the device. As free sedimentation velocity for sand particles d_{in} = 0.10 mm equals v_{fs} = 0.0067 m/s (K. Imhoff and K.R. Imhoff, 1996), the separator radius determined from condition (8.45) is R = 0.15 m. To generate the circular motion of liquid inside the separator, the inlet stream must be directed parallel to the outer wall. Thus, the laboratory stand was equipped with an inlet conduit perpendicular to the outer wall with an elbow fitting at the ending to direct liquid towards the outer wall.

The laboratory prototype of vortex separator consisted of three basic parts (Fig. 10.1): an upper cylinder comprising the main separator chamber, a sedimentation cone 0.15 m high to accumulate suspended matter and a bottom cylinder with four legs as a physical support. The hydraulic elements included: an inlet conduit (tangent to the chamber wall) to feed the main cylinder with liquid together with a water-meter to control liquid discharge and an outlet conduit (installed inside the bottom cylinder and attached to the sedimentation cone) to drain liquid from the chamber, as well as an outlet orifice (inside the main chamber) and a valve to remove the sand accumulated on the sedimentation cone. Additionally, the device was equipped with sand dispenser in the form of a vertical pipe 300 mm in diameter, fixed on the inlet conduit. Dimensions of the prototype are shown in Fig. 10.2.

Fig. 10.1. Laboratory prototype of vortex separator

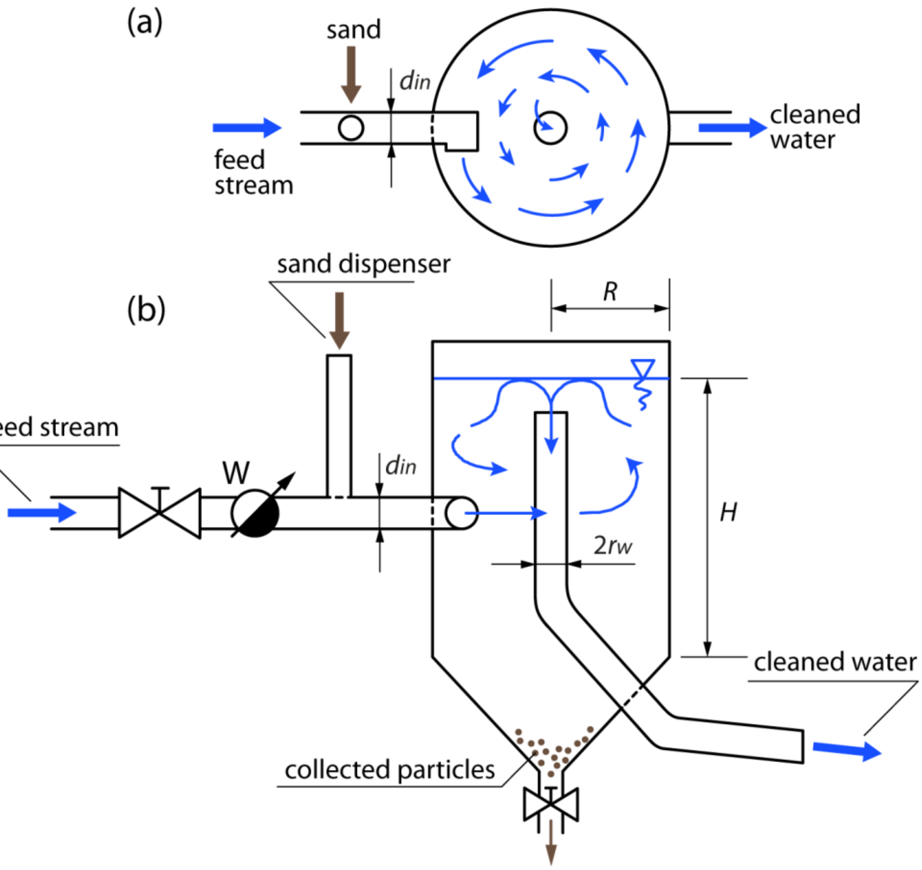

Fig. 10.2. Characteristic dimensions of the laboratory prototype: a) plan view; b) axial cross-section (chamber radius R = 0.15 m; inlet diameter d_{in} = 0.03 m; outlet radius r_w = 0.015 m)

10.2. Course of the measurements

Measurements of vortex separator efficiency were based on determination of the mass balance of sand introduced and removed from the device. A single test consisted of three steps (Fig. 10.3, Fig. 10.4):

– a dried and weighted portion of sand was mixed with water and then introduced into the water stream by the dispenser pipe;
– once the sedimentation process inside the chamber finished, the sand accumulated on the sedimentation cone was removed, dried and weighed;
– separator efficiency ε_s was calculated from the relation:

$$\varepsilon_s = \frac{M_R}{M_S} \tag{10.2}$$

where: M_S - mass of introduced sand portion; M_R - mass of sand removed from the liquid stream (accumulated on the sedimentation cone). Tests were performed altogether for four sand fractions defined by five sieve sizes: 0.063, 0.1, 0.125, 0.2 and 0.25 mm. Dried sand was partitioned into fractions by means of standard sieve analysis. Each portion of sand weighted M_S = 100 g. The liquid discharge was the same for all measurements and equal to Q = 0.30 dm^3/s. For such a discharge water depth inside the main chamber reached H = 0.335 m.

Fig. 10.3. Preparation of sand material for efficiency tests (sieve analysis, single sand portion)

Fig. 10.4. Efficiency tests (introduction of sand, sedimentation inside the chamber)

10.3. Results of the measurements

Results of measurements and calculations of separator efficiency are gathered in Tab. 10.1 and presented in the form of a histogram $\varepsilon_S(d_p)$ (Fig. 10.5).

Tab. 10.1. Results of the prototype efficiency tests

sand fraction d_p [mm]	sand removed [g]				mean % reduction	efficiency ε_S [-]
	1	2	3	4		
0.063 - 0.1	7.5	17.6	35.3	35.2	23.9	0.24
0.1 - 0.125	90.2	70.2	69.6	63.5	73.4	0.73
0.125 - 0.2	81.5	74.9	86.4	89.5	83.1	0.83
0.2 - 0.25	82.2	91.3	90.3	92.6	89.1	0.89

Similarly to other devices for removal of suspension, design of vortex separators is based on binary systems. All particles larger than the particle of the chosen limit size should be removed from the feed stream, whereas, smaller ones may remain in the stream. The theoretical efficiency curve of such a model is discrete in character. Comparison of the obtained results and the theoretical curve (Fig. 10.5 and Fig. 2.5) indicates that the real course of the process is compatible with the binary model (for particle size d_p < 0.1 mm only a small portion of particles is separated from the feed stream, and for d_p > 0.1 mm device efficiency significantly increases). Moreover, the test results show that the efficiency of the laboratory prototype is high. The rate of reduction of sand fraction 0.1-0.2 mm exceeds 78% and for fractions bigger than 0.2 mm reaches 89%. Taking into account the fact that the laboratory stand was designed using a simplified method, the results are satisfactory (K. Imhoff and K.R. Imhoff, 1996). Although, the laboratory prototype has small dimensions, it was designed as a self-contained object using the method developed in this dissertation (design criteria - chapter 8) and not as a scaled-down laboratory version of an existing technical device. This fact ensures that a device of a technical scale designed by the proposed method will operate satisfactorily.

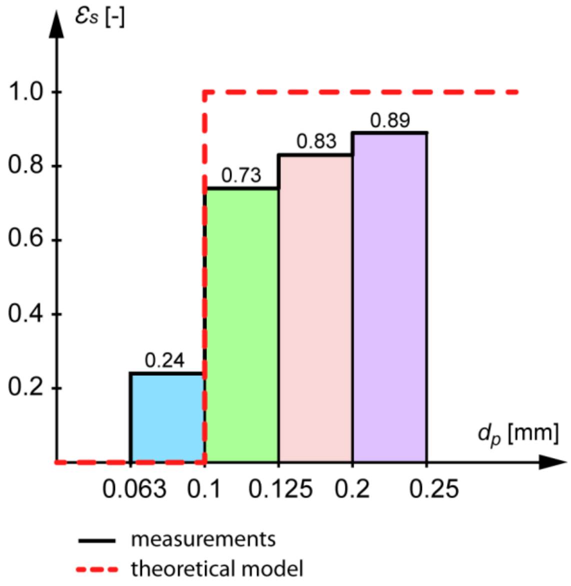

Fig. 10.5. Efficiency of the laboratory prototype of vortex separator

10.4. Design of practical objects

In the light of the positive results from research on the laboratory test stand, the developed design criteria were employed to determine dimensions of devices applied in engineering practice.

Firstly, as inlet and outlet diameters of the device are dimensions of the order of $0.1H$ the reduced version of the first design criterion given by equation (8.12) can be used (relation of the maximum allowable device height H and discharge Q). Furthermore, for the assumed free sedimentation velocity v_{fs} = 0.0067 m/s the second criterion has the simpler form given by relation (8.46). The curves expressing both design criteria are presented in Fig. 10.6. The available range of values of parameters H and R that fulfil the proposed design criteria is contained between the two curves. This range indicates the rational dimensions of the device. For a designer every value of R and H within the range may be treated as a correction for the CFD methods.

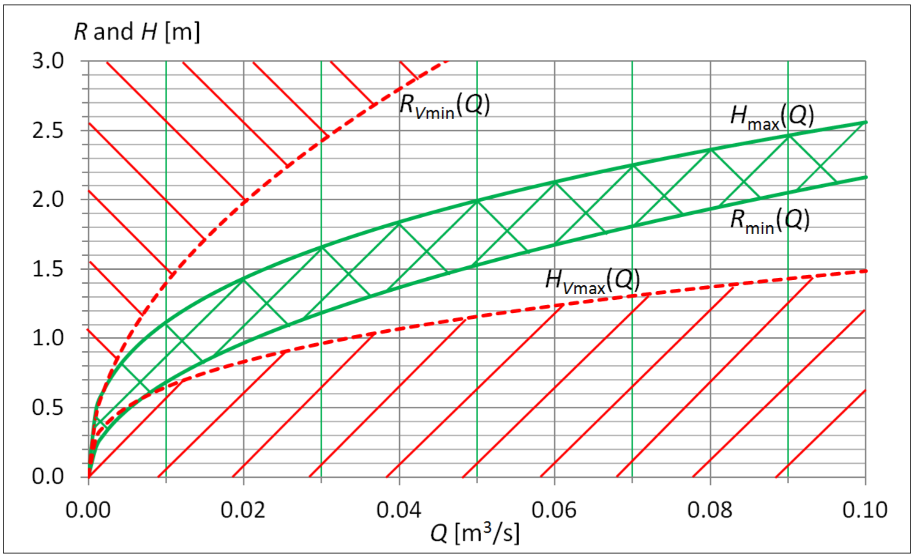

Fig. 10.6. Geometrical interpretation of the simplified design criteria

These technical criteria work as a design set and as such are inseparable. This means that values of the design variables must always be chosen from the common range determined using equations (8.11) and (8.45) or (8.12) and (8.46). For example, application of these criteria to design a vortex separator working in a closed system to remove suspension from wastewater used in fish ponds (suspension composed mainly of feed remains and fish excreta; ρ_p = 1100 kg/m^3; v_{fs} = 0.0016 m/s) yields the following design relations:

$$H_V \le H_{V\max} = 0.34 Q^{0.36} \tag{10.3}$$

$$R_V \ge R_{V\min} = 14 Q^{0.5} \tag{10.4}$$

Plots of these functions are also presented in Fig. 10.6.

As seen in Fig. 10.6 there is no common range of H_V and R_V values; thus, both design criteria cannot be met simultaneously. Consequently, one should not expect to successfully apply vortex separators to remove suspension from fish ponds. This fact was also confirmed by research conducted by Veerapen *et al.* (2005).

Conclusions

The aim of the dissertation was to propose a complete method for designing vortex separators. These devices comprise a separate category of systems used for gravitational removal of particles suspended in liquids. They prove to be relatively similar to cyclones, however, they lack cyclone's elongated conical base. Vortex separators are locally applied for waste water treatment in different systems – from storm waste water sewerage to water circulation in fish ponds, and still draw attention from specialists and engineers interested in convenient methods of removing suspended particles from various liquids. The scientific literature regarding vortex separators is extensive; however, it lacks verified methods for such separators' design. This results from the fact that there is no reasonable description of liquid velocity field and pressure distribution readily available. That is why, the author of the dissertation decided to look into this problem and propose a rational method (formally simple, and theoretically and empirically justified) that could be conveniently used to design such type of devices. The conducted research included measurements of liquid velocity on a specially constructed laboratory test stand. The obtained results led to formulation of a relatively simple two-dimensional algebraic model of liquid flow in a vortex separator of a high technical advantage (mathematical simplicity). The model for radial velocity component resulted directly from the equation of continuity, whereas for tangential velocity component it was kinematic in character. The model is physically well-grounded as it satisfies the strong condition of balance between delivered and dissipated energy flux. The mathematical model of velocity allowed the determination of forces acting on a characteristic suspended particle and formulation of equations of its trajectory. Reduction of these equations yielded practical relations that can be used to calculate particle velocity and time of particle motion on a horizontal plane. Next, a technical method composed of two quantitative technical criteria – balance of forces acting in the outflow cross-section and comparison of the time of particle advection with the required sedimentation time, was proposed. Correctness of the design relations developed was then empirically verified by measuring efficiency of a physical model of a vortex separator (the second test stand) that was designed based on the proposed criteria – computational discharge and separator diameter, and resulting technical conditions. Performed measurements showed that the laboratory model had relatively high effectiveness. Furthermore, taking into account technically justified proportions between particular dimensions of the object, two relations were obtained demonstrating that the design criteria applied for removal of mineral suspension provide an available range of device parameters to choose from. Conversely, both criteria cannot be fulfilled simultaneously for particles of small sedimentation velocity. Finally, taking into account the fact that the narrow range of device parameters indicate that the centrifugal force is not a crucial factor in the process of separation, a series of tracer measurements on the first laboratory test stand were performed to evaluate the influence of circulation on the length of liquid residence time in vortex separator. Results of tracer measurements showed that vortex separators work better than analogical objects without liquid circulation as the interior of the separator is used more efficiently than in case of non-circulative devices.

Concluding, the conducted research together with the obtained results allowed the author to formulate the following qualitative and quantitative statements:

1. With the current progress of urbanization followed by an increase in areas covered by tight surfaces and the valid law requirements highlights the need for new systems for storm run-off treatment. Vortex separators prove to be a fine alternative to other devices for suspension removal, which can be applied both in urban areas , as well as locally along express roads, etc.
2. In order to design a vortex separator, a series of characteristic quantities must be properly integrated. These quantities describe system geometry (separator diameter and depth, diameters of inlet and outlet piping, etc.), flow kinematics (liquid discharge and characteristic residence times), as well as technological factors (especially sedimentation velocity of suspended particles).
3. Influence of the centrifugal force on the process of separation in the vortex separator is very specific. The narrow range of values characterizing the device to choose from (separator radius and liquid discharge) indicate that the centrifugal force is not a crucial factor and vortex separators are unable to work so efficiently as centrifuges or cyclones.
4. Vortex separators are characterized by an increase in favourable proportions between the forces acting on a suspended particle near the outlet conduit in the device axis of symmetry. In the central part of the separator a local “dynamic buffer zone” is formed which prevents the particles from flowing out of the object, so they can undergo sedimentation.
5. The character of a vortex separator is very close to the specifics of a well-mixed reactor - first portions of the tracer appear at the outlet after a short period of time, then tracer concentration visibly increases to a maximum value, and finally exponentially decreases.

6. Vortex separators work better than analogical objects without fluid circulation thanks to better use of the tank cubic capacity by the active liquid flow than in case of systems with translational motion. In vortex separators dead and stagnant zones occupy less volume than the active layer of liquid flow.
7. Liquid circulation results in a threefold longer average residence time and a higher effective level of reduction of suspension than in case of flow without circulation.

Operation of vortex separators can be described by solving a set of specific differential equations (CFD). This method is difficult and time consuming, however, it allows for a detailed simulation of the considered process. In case of designing new objects one needs to solve a typical inverse problem. Currently, there are no methods for correcting subsequent approximations of system geometry so that assumed requirements are reached. The physical criteria developed and presented in the dissertation in the form of simple algebraic relations including basic dimensions of the vortex separator can be used both as an additional tool with CFD methods (for approximation), as well as a separate design method. The rational design process of a vortex separator can be conducted on three levels of precision:

– simplified level - preliminary calculations of device characteristics;
– technical level - calculations of device dimensions;
– comprehensive level - optional numerical simulations of suspension separation.

ACKNOWLEDGEMENTS

Scientific research has been carried out as a part of the Scientific Project N N523 554738, financed by the Polish National Centre of Science, as well as the Project "Innovative resources and effective methods of safety improvement and durability of buildings and transport infrastructure in sustainable development" financed by the European Union from the European Fund of Regional Development based on the Operational Programme of the Innovative Economy.

Notation and symbols

Notation:

a - centrifugal acceleration
B - special multiplier
c - tracer concentration
C_D - drag coefficient
d_{in} - separator inlet diameter
d_p - particle diameter
E - energy flux
E_{in} - delivered energy flux
E_{dis} - dissipated energy flux
EK - kinetic energy
EK_R - kinetic energy of radial flow
EK_T - kinetic energy of tangential flow
F_A - Archimedes force
F_p - particle active cross-section
$\mathbf{F}$ - force
$\mathbf{F_{AM}}$ - associated mass force
$\mathbf{F_B}$ - buoyancy force
$\mathbf{F_C}$ - centrifugal force
$\mathbf{F_{DN}}$ - Newton's drag force
$\mathbf{F_{DS}}$ - Stokes' drag force
$\mathbf{F_G}$ - gravity force
$\mathbf{F_{TD}}$ - transverse drift
g - gravity acceleration
h - liquid elevation over the outlet pipe
h_{min} - particle limit height over the separator bottom
h_w - separator outlet height
H - liquid depth
H_e - active layer of flow
l_m - mixing length
L - settling separator length
L_s - settling separator minimum length
m_d - mass of liquid displaced by the particle
m_p - particle mass
Δm - mass of a liquid element
M - mass of the tracer dose
M_R - mass of removed sand
M_s - mass of introduced sand portion
p - pressure
p_a - atmospheric pressure
Q - discharge
r - distance from the axis of rotation
r_p - particle distance from the axis of rotation
r_w - separator outlet radius
$\mathbf{r_p}$ - particle radius vector
R - separator radius
Re - Reynolds Number
t - time
t_{fs} - particle settling time
t_p - time of particle horizontal displacement

t_r - time of particle radial displacement
t_s, t_b, t_w - particle residence time in vortex separator
t_A - liquid average residence time in vortex separator
t_K - liquid residence time in vortex separator
t_L - time of liquid advective motion
t_M - liquid modal residence time in vortex separator
t_{PF} - plug-flow time
u - liquid velocity
u_{av} - mean liquid velocity
u_{in} - liquid inlet velocity
u_r - liquid radial velocity
u_R - resultant liquid tangential velocity
u_t - liquid tangential velocity
u_{tav} - mean liquid tangential velocity
u_z - liquid vertical velocity
u_ω - liquid angular velocity
$\mathbf{u}$ - liquid velocity vector
v_{fs} - particle free sedimentation velocity
v_p - particle velocity
v_r - particle radial velocity
v_t - particle tangential velocity
v_z - particle vertical velocity
v_ω - particle angular velocity
$\mathbf{v_p}$ - particle velocity vector
V - separator volume
V_p - particle volume
W - settling separator width
x, y, z - Cartesian coordinates
X - special parameter
z_p - particle elevation over the separator bottom

Symbols:

α_s - associated mass coefficient
ε - settling separator efficiency
ε_s - efficiency of vortex separator prototype
μ - dynamic viscosity coefficient
μ_p - discharge coefficient
μ_T - turbulent viscosity coefficient
ρ - liquid density
ρ_p - particle density
ϕ - particle sphericity
ψ - stream function
ω_p - particle angular coordinate
$\boldsymbol{\omega}_\mathbf{z}$ - Earth angular velocity

References

Literature:

1. Albrecht, A.E. (1967), "Aerated grit chamber operation and design", *Water Sewage Works*, Vol. 114, No. 9, pp. 331-335.
2. Babelski, Z. (1999), „Ocena zanieczyszczenia ścieków deszczowych z rożnych zlewni miejskich" [Evaluation of storm wastewater pollution in different urban catchments], *Gaz, woda i technika sanitarna*, Vol. 11, pp. 414-418.
3. Bering, S. and Sawicki, J.M. (2002), „Przybliżone obliczanie strat energii w zbiornikach" [Approximate calculations of energy loss in reservoirs], paper presented at the *XXII Ogólnopolska Szkoła Hydrauliki* [XXII Polish School of Hydraulics], IBW PAN, Lubniewice.
4. Camargo, S.A., Doelling, O.R. and Varas, E.A. (2006), "Mathematical model of morning glory spillways using artificial neural networks", *Proceedings of the International Symposium on Hydraulic Structures,* IAHR, Ciudad Guyana, October 2006.
5. Cho, H. and Sansalone, J. (2013), "Physical modeling of particulate matter washout from a hydrodynamic separator", *J. Environ. Eng.*, Vol. 139, No. 1, pp. 11–22.
6. Ciborowski, J. (1973), *Inżynieria Procesowa* [Process Engineering], WNT, Warszawa.
7. Cywiński, B., Gdula, S., Kempa, E., Kurbiel, J. and Płoszański, H. (1983), *Oczyszczanie Ścieków Tom 1: Oczyszczanie mechaniczne i chemiczne* [Wastewater Treatment Vol. 1: Mechanical and chemical treatment], 2nd ed., Arkady, Warszawa.
8. Dąbrowski, W. (2001), „Parametry fizyczne zawiesin wód deszczowych jako podstawa do projektowania systemów podczyszczania" [Physical parameters of rainwater suspensions as a basis for designing pretreatment systems], *Gaz, Woda i Technika Sanitarna*, Vol. 6, pp. 221-224.
9. Dyakowski, T., Kraipech, W., Nowakowski, A.F. and Williams, R. (1999), "A three dimensional simulation of hydrocyclone behaviour", in *Proceedings of the 2nd International Conference on CFD*, CSIRO, Melbourne, pp. 205–210.
10. Ecol-Unicon Sp. z o.o. (2014a), "Coalescence separators", available at: www.ecol-unicon.com/en/urzadzenia/separatory/seapartatory-koalescencyjne/ (accessed 24 November 2014).
11. Ecol-Unicon Sp. z o.o. (2014b), "Lamella separators", available at: www.ecol-unicon.com/en/urzadzenia/separatory/separatory-lamelowe/ (accessed 24 November 2014).
12. Fidala-Szope, M. (1980), „Zanieczyszczenie odpływów z kanalizacji deszczowej" [Pollution of storm sewerages outflow], in Błaszczyk, P. (Ed.), *Wybrane zagadnienia kształtowania systemów kanalizacyjnych* [Chosen problems in the design of sewerage systems], PWN, Warszawa.
13. Garbarczyk, K. (1997), „Zanieczyszczenia w spływach roztopowych odprowadzanych systemem kanalizacji deszczowej do wód powierzchniowych" [Pollutants in snowmelt run-off discharged into surface waters by stormwater

sewerage systems], *Proceedings of the IX Ogólnopolska Konferencja Naukowo-Techniczna Problemy gospodarki wodno-ściekowej w rejonach rolniczo-przemysłowych,* Rajgród 1997.

14. Gronowska, M.A. (2012a), "Specification of forces in rotational separator", *AHEEM*, Vol. 1-2, No. 59, pp. 49-62.
15. Gronowska, M.A. (2012b) *Zanieczyszczenie spływów opadowych ze zlewni zurbanizowanej* [Pollution of storm run-off from urban catchments], diploma thesis, Politechnika Gdańska, Wydział Chemiczny.
16. Gronowska, M.A. and Sawicki, J.M. (2011), "Analysis of methods of designing rotational separators", in Sawicki, J.M. and Weinerowska-Bords, K. (Eds.), *Technical progress in sanitary engineering*, Gdansk University of Technology Publishers, Gdansk, pp. 40-48.
17. Gronowska, M.A. and Sawicki, J.M. (2014a), "Simple design criteria and efficiency of hydrodynamic vortex separators", *Water Science & Technology*, Vol. 70, No. 3, pp. 457-463.
18. Gronowska, M.A. and Sawicki, J.M. (2014b), "Współczynnik wydatku przelewu szybowego w separatorze wirowym" [Discharge coefficient of shaft overfall for rotational separators], *Inżynieria Morska i Geotechnika*, Vol. 35, No. 1, pp. 11-13.
19. Gronowska, M.A., Sawicki, J.M. and Zima, P. (2013) "Motion of suspended particles in vortex separator", *Proceedings of the 13th International Symposium on Water Management and Hydraulic Engineering,* Bratislava, September 9-12, 2013.
20. Imhoff, K. and Imhoff, K.R. (1996), *Kanalizacja miast i oczyszczanie ścieków. Poradnik* [Urban drainage and wastewater treatment. A handbook], translated by Brzeski, J., Oficyna Wydawnicza Projprzem-EKO, Bydgoszcz.
21. Królikowska, J. (2011), Urządzenia inżynierskie z ruchem wirowym stosowane na sieci kanalizacyjnej do zmniejszenia ładunku zawiesiny w ściekach deszczowych [Swirl chamber equipment applied in sewage networks for decreasing suspended particle load in stormwater sewage], *Inżynieria Ekologiczna*, Vol. 26, pp. 156-170.
22. Kujawa-Roeleveld, K., Dymaczewski, Z. and Komorowska-Kaufman, M. (2011), "Rozdział 3. Oczyszczanie wstępne" [Chapter 3. Pretreatment], in Dymaczewski, Z. (Ed.), *Poradnik eksploatatora oczyszczalni ścieków* [A handbook for wastewater treatment plant operator], Polskie Zrzeszenie Inżynierów i Techników Sanitarnych Oddział Wielkopolski, Poznań, pp. 147-203.
23. Launder, B.E. and Spalding, D.B. (1972), *Lectures in mathematical models of turbulence*, Academic Press, London.
24. LeMehaute, B. (1976), *An introduction to hydrodynamics and water waves*, Springer-Verlag, New York-Heidelberg-Berlin.
25. Łojcjanskij, L.G. (1977), Mechanika żidkosti i gaza [Mechanics of liquids and gases], Izdatielstwo Nauka, Moskwa.
26. Manecki, A. and Muszyński, M. (2008), *Przewodnik do petrografii* [A guide to petrography], Uczelniane Wydawnictwo Naukowo-Dydaktyczne AGH, Kraków.

27. Martignoni, W.P., Bernardo, S. and Quintani, C.L. (2007), ”Evaluation of cyclone geometry and its influence on performance parameters by computational fluid dynamics (CFD)”, *Braz. Jour. Chem. Eng.*, Vol. 24, No. 1, pp. 83–94.
28. Mitosek, M. (1997), *Mechanika płynów w inżynierii środowiska* [Fluid mechanics in environmental engineering], Oficyna Wydawnicza Politechniki Warszawskiej, Warszawa.
29. Nalluri, C. and Featherstone, R.F. (2001), *Civil engineering hydraulics*, Wiley-Blackwell, New Delhi.
30. Orzechowski, Z. (1990), *Przepływy dwufazowe* [Two-phase flow systems], PWN, Warszawa.
31. Osmulska-Mróz, B. (1996), *Ochrona wód w otoczeniu dróg - Dział 7: Zasady ochrony środowiska w projektowaniu, budowie i utrzymaniu dróg* [Protection of waters near roads - Chapter 7: Principles of environmental protection in design, construction and maintenance of roads], Instytut Dróg i Mostów, Warszawa.
32. Osmulska-Mróz, B. and Sadkowski, K. (1991), „Zanieczyszczenie spływów opadowych z dróg szybkiego ruchu w Polsce” [Pollution of storm run-off from expressways in Poland], *Ochrona Środowiska*, Vol. 2, pp. 73-85.
33. Piotrowski, I. and Roman, M. (1974), *Urządzenia do oczyszczania wody i ścieków* (Water and wastewater treatment devices), PWN, Warszawa.
34. Puzyrewski, R. and Sawicki, J.M. (2013), *Podstawy mechaniki płynów i hydraulik*i (Principles of fluids mechanics and hydraulics], PWN, Warszawa.
35. Rhodes, M. (2008), *Introduction to particle technology.* 2nd ed., John Wiley & Sons, Ltd, New Zealand.
36. Rogers, P. (1994), “Hydrology and water quality”, in *Changes in land use and land cover. A global perspective*, Meyer, W.B. and Turner, B.L. (Eds.), 2nd ed., Cambridge University Press, Cambridge, pp. 231-257.
37. Roman, M. (1986), *Kanalizacja. Oczyszczanie ścieków. Tom 2* [Sewerages. Wastewater treatment. Vol. 2], Arkady, Warszawa.
38. Rybicki, S.A. and Rybicki, S.M. (2001), „Odprowadzanie i oczyszczanie wód deszczowych w strefach ochronnych ujęć wody” [Discharge and treatment of rainwater within protection zones of water intakes], *Ochrona Środowiska*, Vol. 1, pp. 3-8.
39. Sawicka-Siarkiewicz, H. (1999), “Zanieczyszczenia ścieków opadowych odprowadzanych z tras szybkiego ruchu i terenów obiektów towarzyszących oraz metody ograniczania ich wpływu na odbiorniki”, *Proceedings of the Seminar of Instytut Ochrony Środowiska w Warszawie, Zakład Systemów Ochrony Wód: Odprowadzanie wód opadowych z terenów zurbanizowanych - problemy prawne, techniczne i ekologiczne,* Jachranka 1999.
40. Sawicki, J.M. (2004), “Aerated grit chambers hydraulic design equation”, *J. Env. Eng.*, Vol. 9, No. 130, pp. 1050-1058.

41. Sawicki, J.M. (2007), *Migracja zanieczyszczen* [Migration of pollutants], Wydawnictwo Politechniki Gdańskiej, Gdańsk.
42. Sawicki, J.M. (2009), *Mechanika przepływów* [Flow mechanics], Wydawnictwo Politechniki Gdańskiej, Gdańsk.
43. Sawicki, J.M. (2012), "Transversal pressure effect in circulative separator", *AHEEM*, Vol. 1-2, No. 59, pp. 3-12.
44. Serrin, J. (1959), *Mathematical principles of classic fluid mechanics*, Berlin-Goettingen-Heidelberg.
45. Slattery, J.C. (1999), *Advanced transport phenomena*, Cambridge University Press, Cambridge.
46. Smith, J.L. (1959), *Experimental and analytical study of the vortex in the cyclone separator*, MIT, Cambridge, Massachusetts.
47. Soo, L. (1969), *Fluid dynamics of multiphase systems*, Blaisdell Publ. Comp., London.
48. Stairmand, C.J. (1951), "The design and performance of cyclone separators", *Trans. Inst. Chem. Eng.*, Vol. 29, pp. 356-373.
49. Szydłowski, M. (2007), „Modelowanie fal powodziowych na terenach zurbanizowanych" [Modelling of flood waves in urban areas], *Seria Monografie*, No. 86, Wydawnictwo Politechniki Gdańskiej, Gdańsk.
50. Szymańska, H. (1986), *Skład chemiczny wód opadowych* [Chemical composition of rainwater], *Gospodarka Wodna*, Vol. 1, pp. 25-26.
51. Szymkiewicz, R. (1990), *Hydrologia* [Hydrology], Wydawnictwo Politechniki Gdańskiej, Gdańsk.
52. Tarnowski, K. and Wira, J. (2000), „Charakterystyka ścieków opadowych i sanitarnych na przykładzie zlewni „Górny Brzeg" w Szczecinie" [Characteristics of storm and domestic wastewater from catchment „Górny Brzeg" in Szczecin], in *Proceedings of the IV Międzynarodowa Konferencja Zaopatrzenie w wodę, jakość i ochrona wód,* Kraków, pp. 281-288.
53. Trawinski, H. (1969), "Practical aspects of the design and industrial applications of the hydrocyclones", *Filtr. Sep.*, Vol. 6, pp. 361-369.
54. Veerapen, J. P., Lowry, B. J. and Couturier, M. F. (2005), „Design methodology for the swirl separator", *Aqua. Eng.*, Vol. 33, pp. 21 - 45.
55. Warych, J. (1998), *Oczyszczanie gazów. Procesy i aparatura* [Gas purification. Processes and apparatus], WNT, Warszawa.
56. Weinerowska-Bords, K. (2010), *Wpływ uproszczeń na obliczanie spływu deszczowego w zlewni zurbanizowanej* [Influence of simplification on calculations of storm run-off in an urban catchment], Wydawnictwo Politechniki Gdańskiej, Gdańsk.
57. White, L.C. (1932), "Results of research on cyclone dust collectors", *Power*, Vol. 75, pp. 344–346.
58. Wikipedia. The Free Encyclopedia (2010) "Cyclonic separation", available at: http://en.wikipedia.org/wiki/Cyclonic separation (accessed 22 April 2010).

59. *Wodociągi i kanalizacja. Poradnik* [Waterworks and sewerages. A handbook] (1971), Arkady, Warszawa.
60. Zakrzewski, J. and Żabowski, J. (1963), *Gospodarcze wykorzystanie ścieków miejskich* [Industrial usage of municipal wastewater], Arkady, Warszawa.
61. Zarzycki, R., Imbierowicz, M. and Stelmachowski, M. (2007), *Wprowadzenie do inżynierii i ochrony środowiska. Tom 1: Ochrona środowiska naturalnego* [An introduction to environmental engineering. Vol. 1: Environmental protection], WNT, Warszawa.
62. Zierep, J. (1978), *Kryteria podobieństwa i zasady modelowania w mechanice płynów*. [Similarity criteria and modelling principles in fluid mechanics], PWN, Warszawa.

Standards:

1. PN-EN ISO 14688-1:2006 Badania geotechniczne - Oznaczanie i klasyfikowanie gruntów - Część 1: Oznaczanie i opis [Geotechnical investigation and testing-- Identification and classification of soil - Part 1: Identification and description], Polski Komitet Normalizacyjny.

Legal acts:

1. Directive 2000/60/EC of The European Parliament And of The Council of 23 October 2000 establishing a framework for Community action in the field of water policy (Official Journal of the European Communities L 327/1).
2. Prawo Ochrony Środowiska [Environmental Protection Law] of 27 April 2001 (consolidated text: Dziennik Ustaw [Journal of Laws] of 2013, item 1232 as amended).
3. Prawo Wodne [Water Resources Law] of 18 July 2001 (consolidated text: Dziennik Ustaw [Journal of Laws] of 2012, item 145 as amended).
4. Ordinance of the Minister of the Environment of 24 July 2006 (consolidated text: Dziennik Ustaw [Journal of Laws] of 2006 No 137, item 984 as amended).

Appendix No. 1

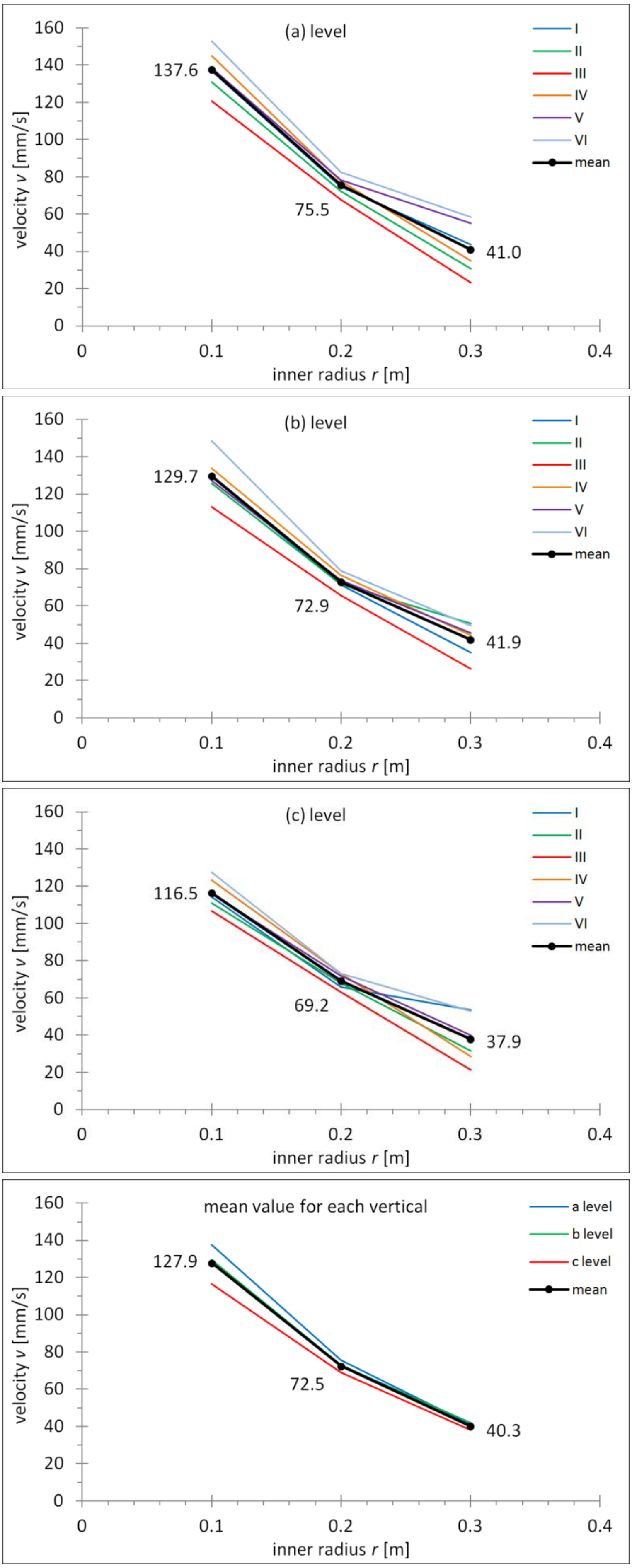

Fig. App1.1 Velocity distribution for configuration “AR” h_w = 0.15 m (description in the text)

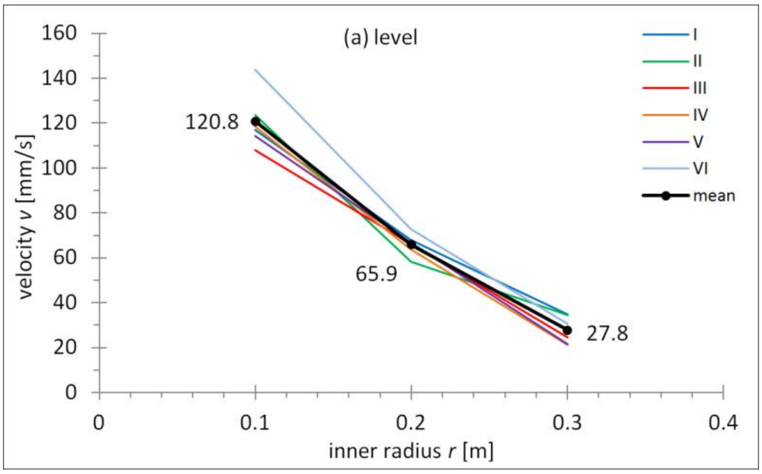

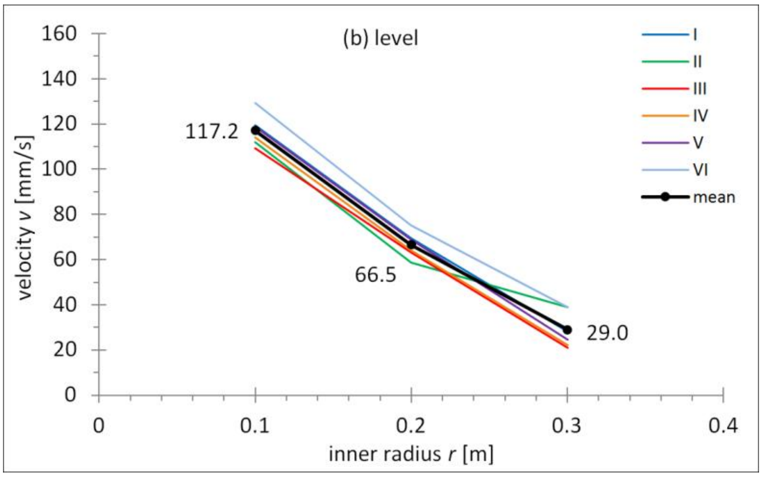

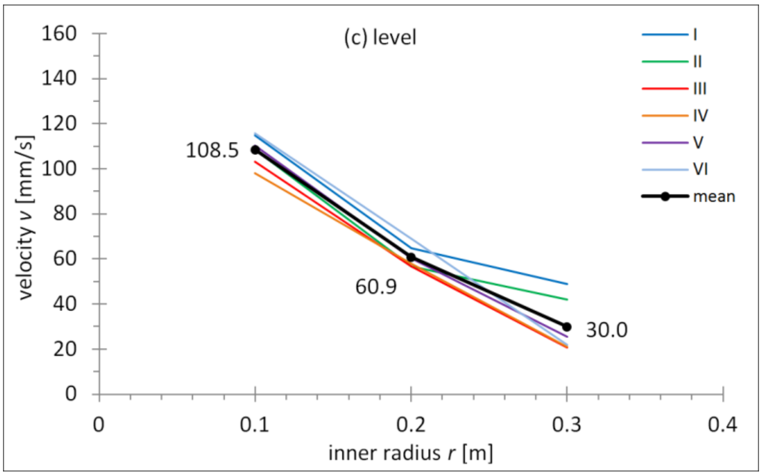

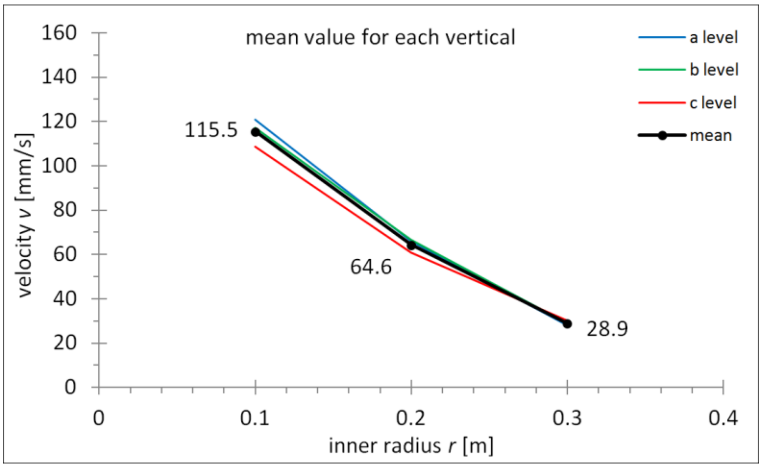

Fig. App1.2 Velocity distribution for configuration “AL” h_w = 0.20 m (description in the text)

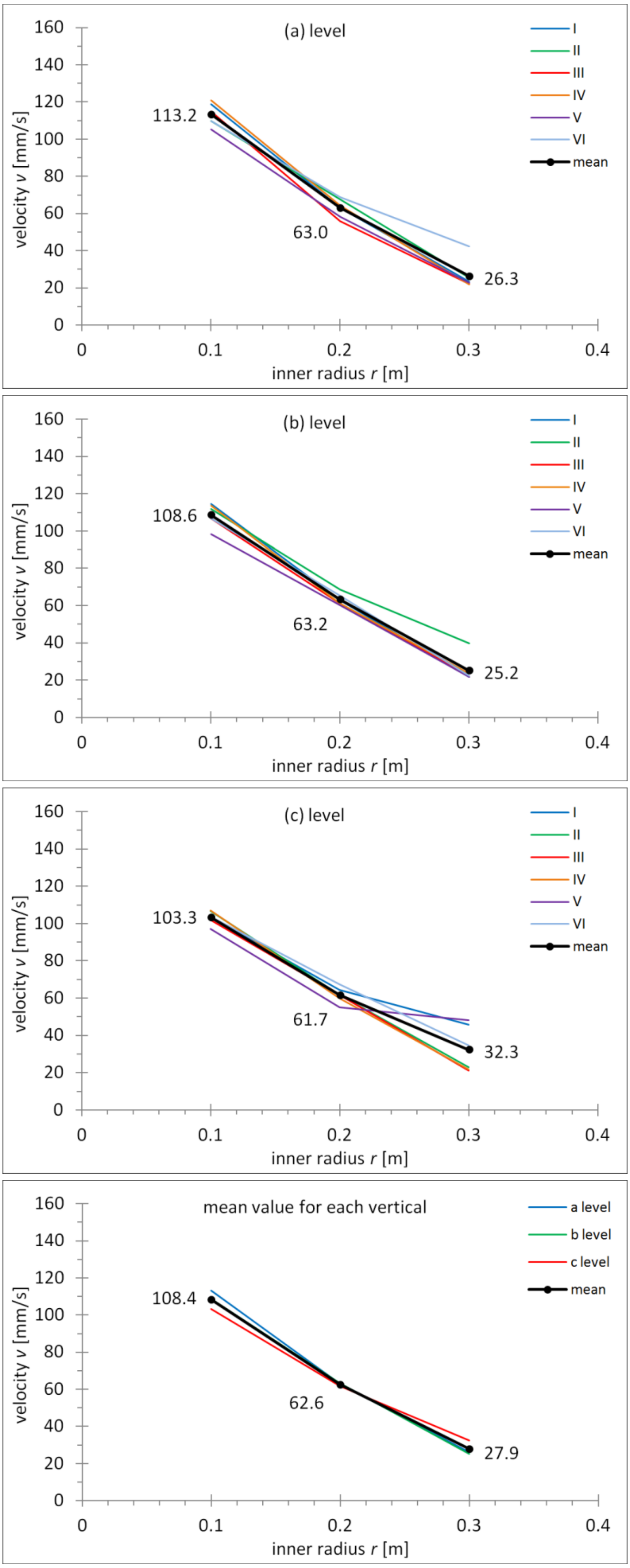

Fig. App1.3 Velocity distribution for configuration “AR” h_w = 0.20 m (description in the text)

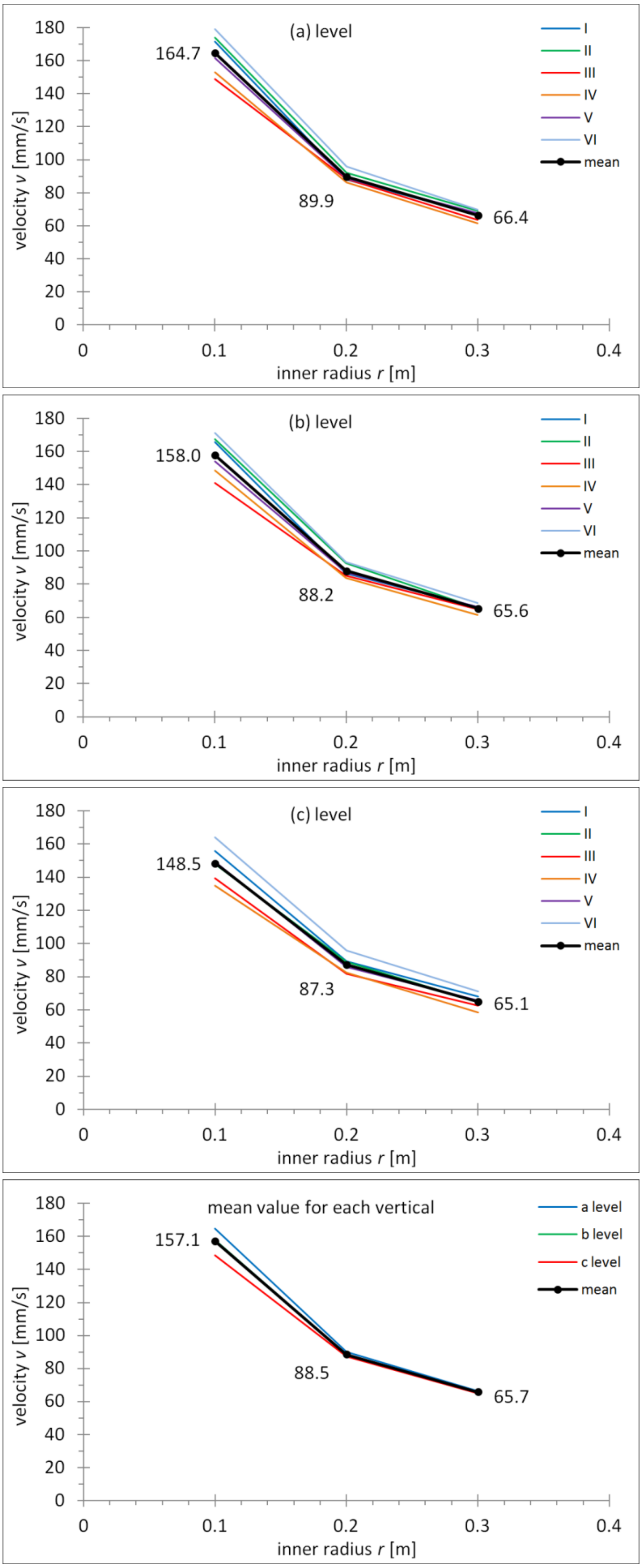

Fig. App1.4 Velocity distribution for configuration “BR” (description in the text)

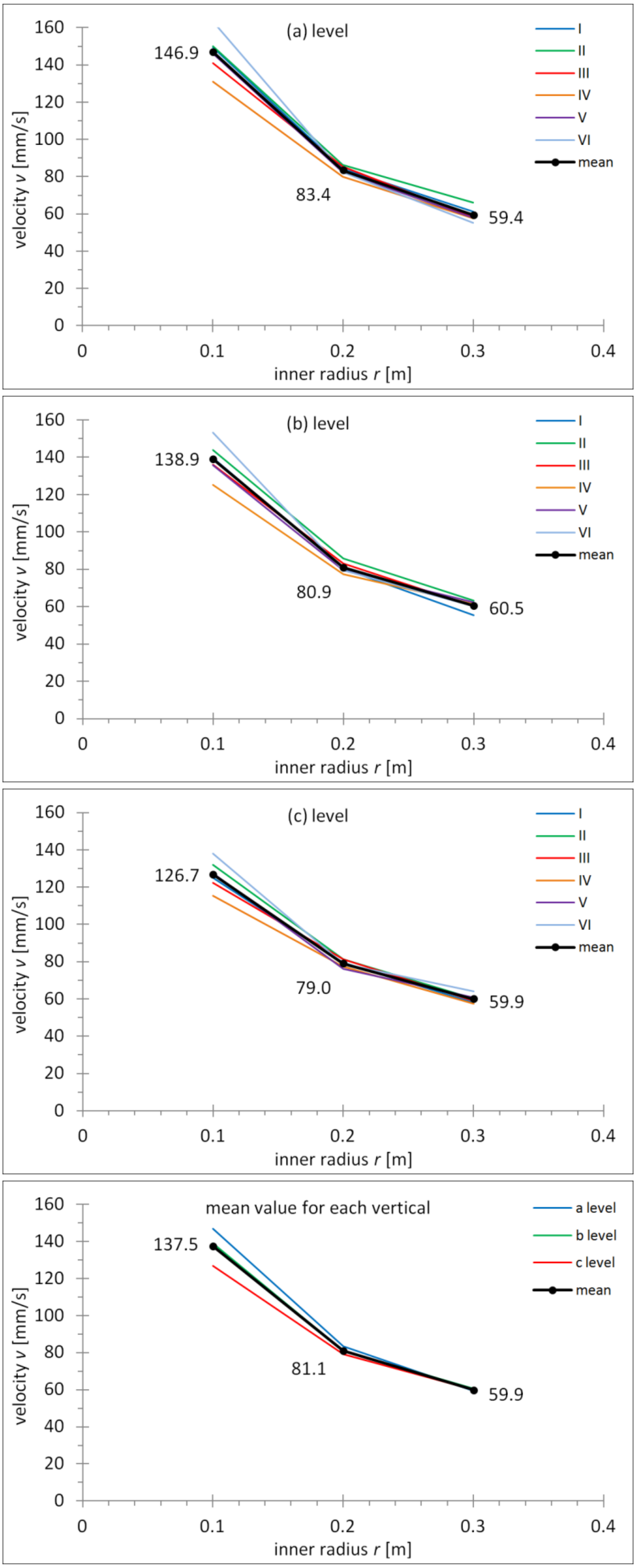

Fig. App1.5 Velocity distribution for configuration "CR" (description in the text)

Appendix No. 2

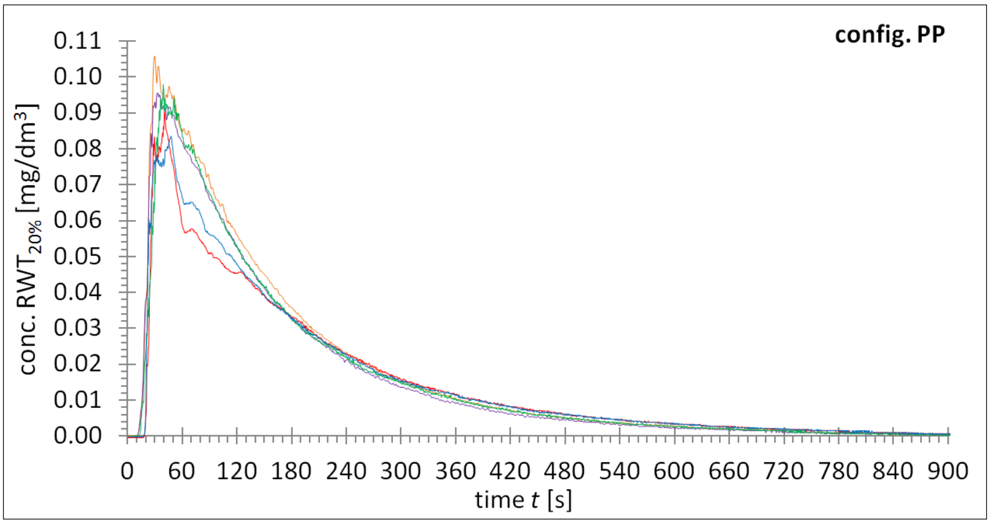

Fig. App2.1. Residence time distribution curves $E(t)$ for configuration “PP”

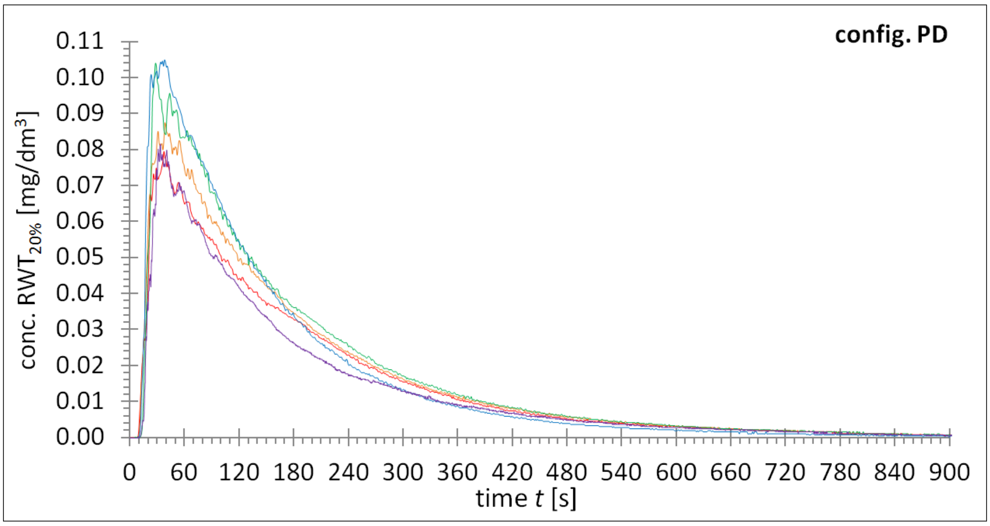

Fig. App2.2 Residence time distribution curves $E(t)$ for configuration “PD”

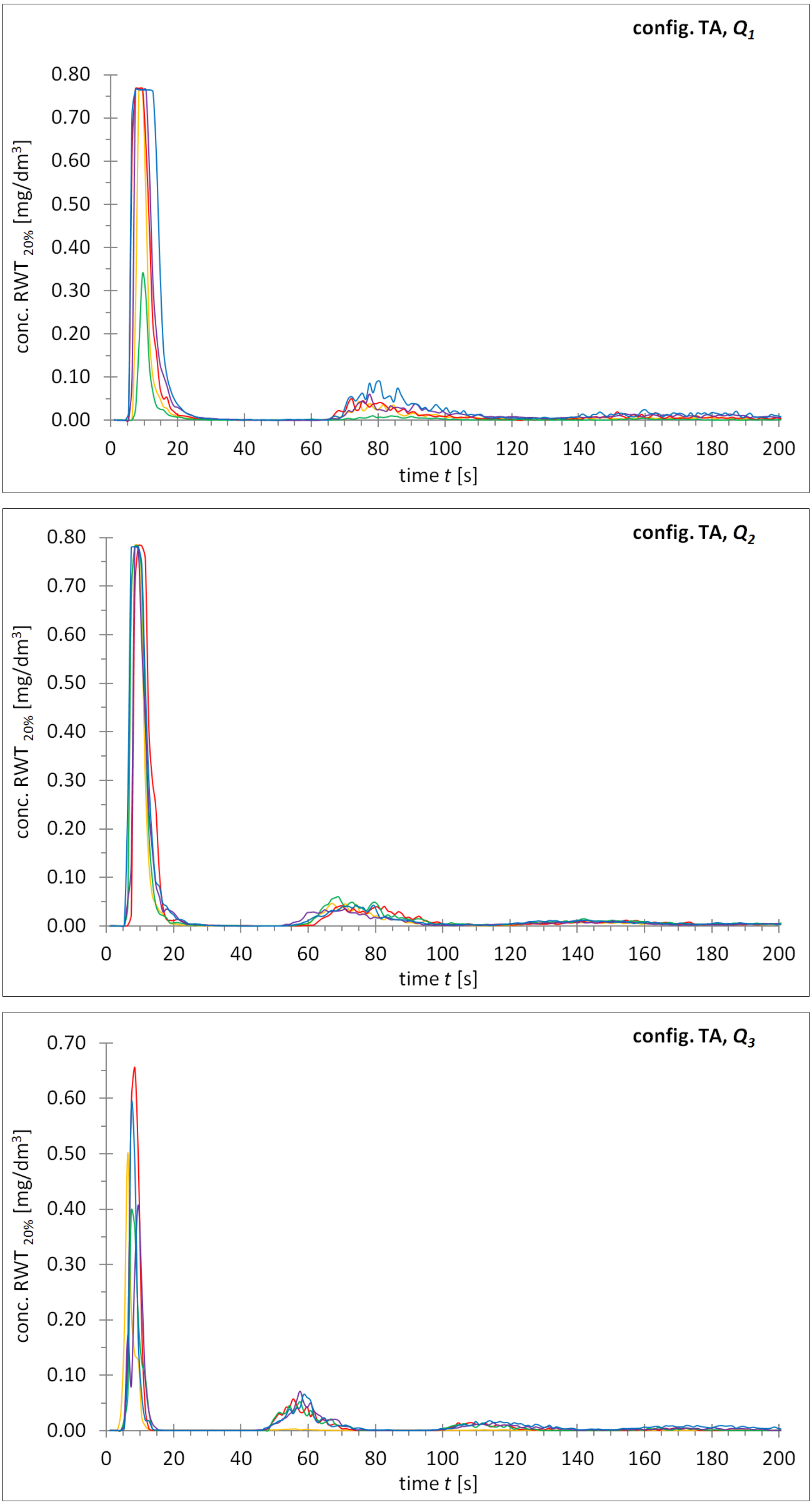

Fig. App2.3. Residence time distribution curves $E(t)$ for configuration "TA"

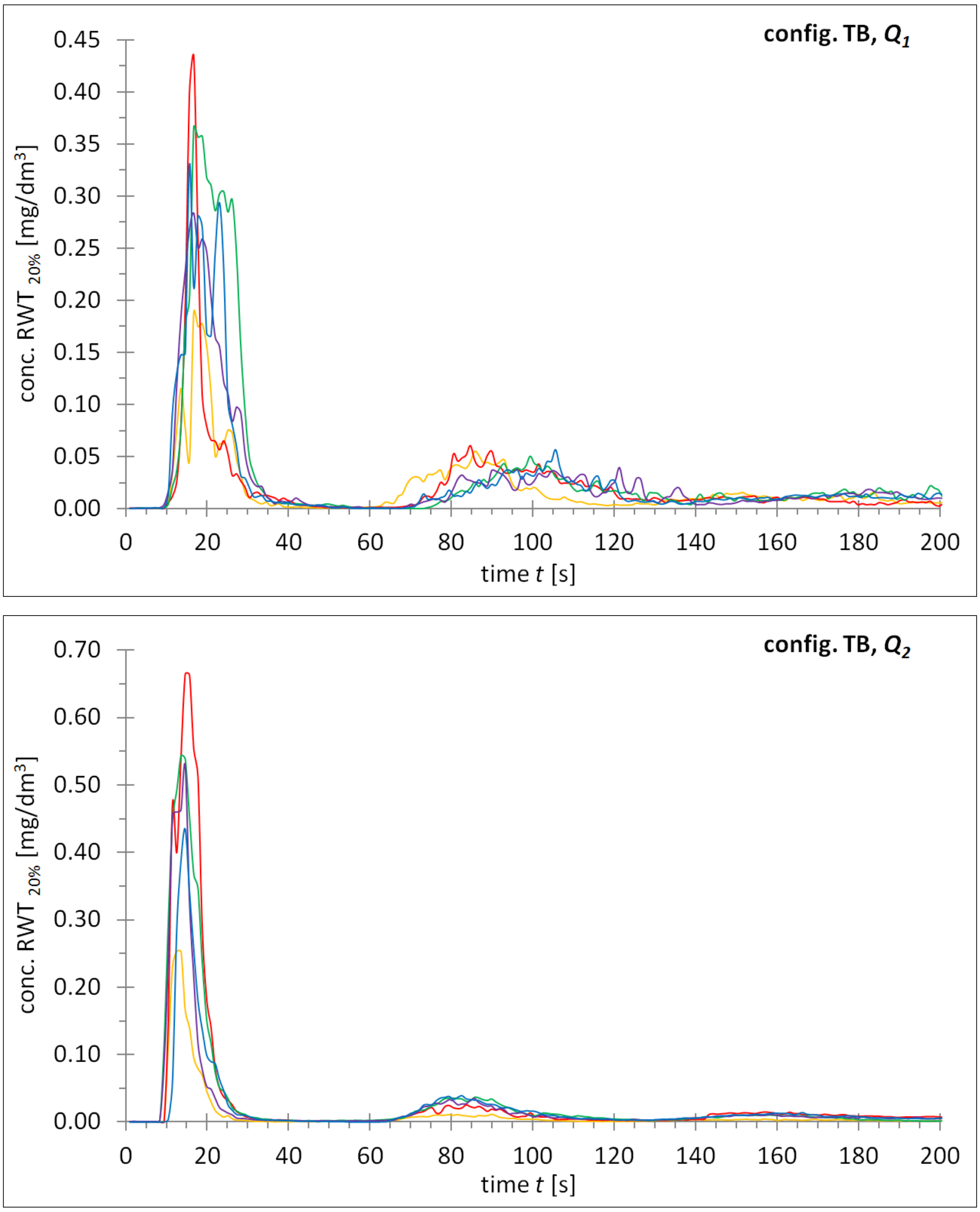

Fig. App2.4. Residence time distribution curves $E(t)$ for configuration “TB”

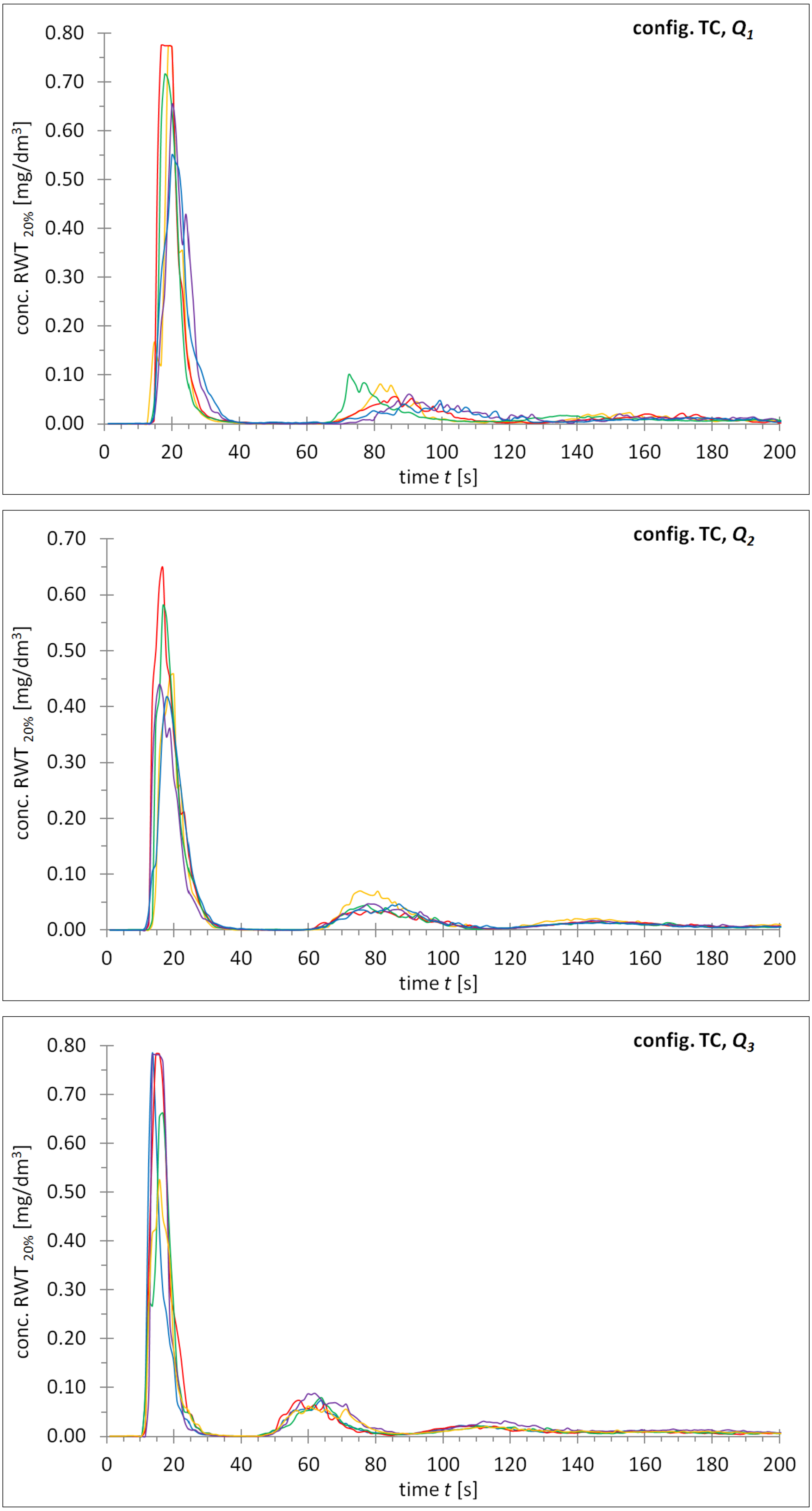

Fig. App2.5. Residence time distribution curves $E(t)$ for configuration "TC"

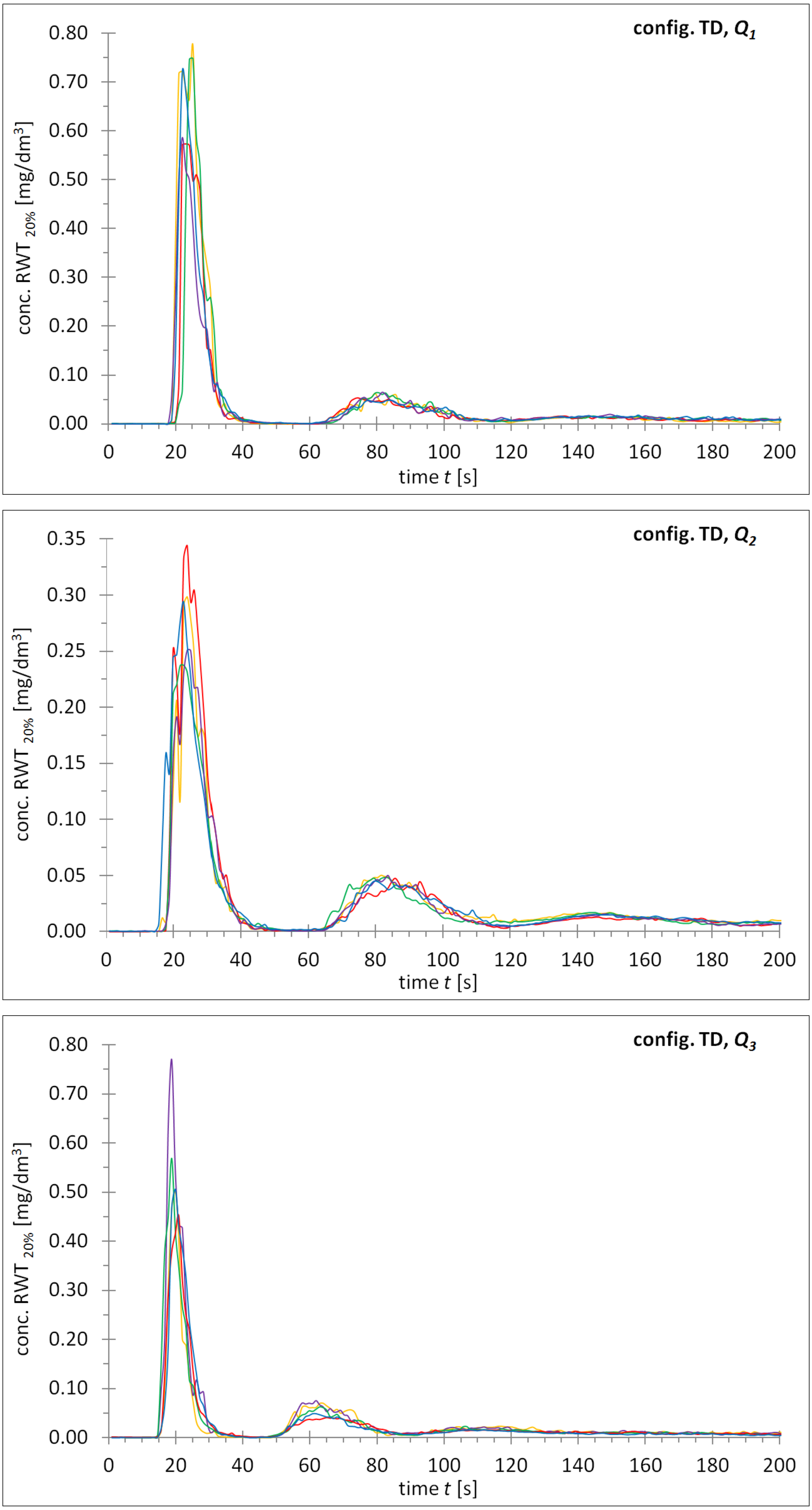

Fig. App2.6. Residence time distribution curves $E(t)$ for configuration "TD"

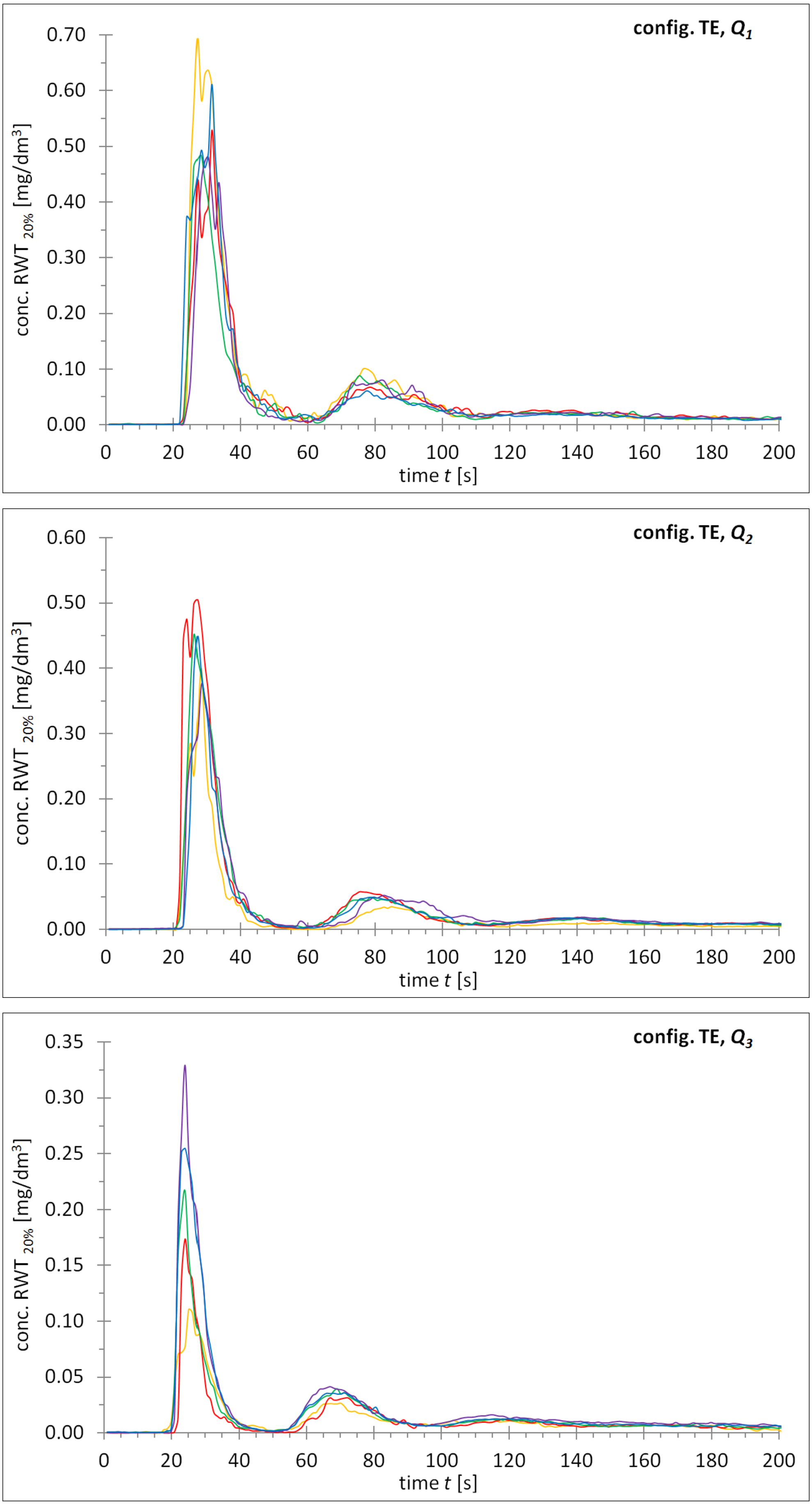

Fig. App2.7. Residence time distribution curves $E(t)$ for configuration "TE"

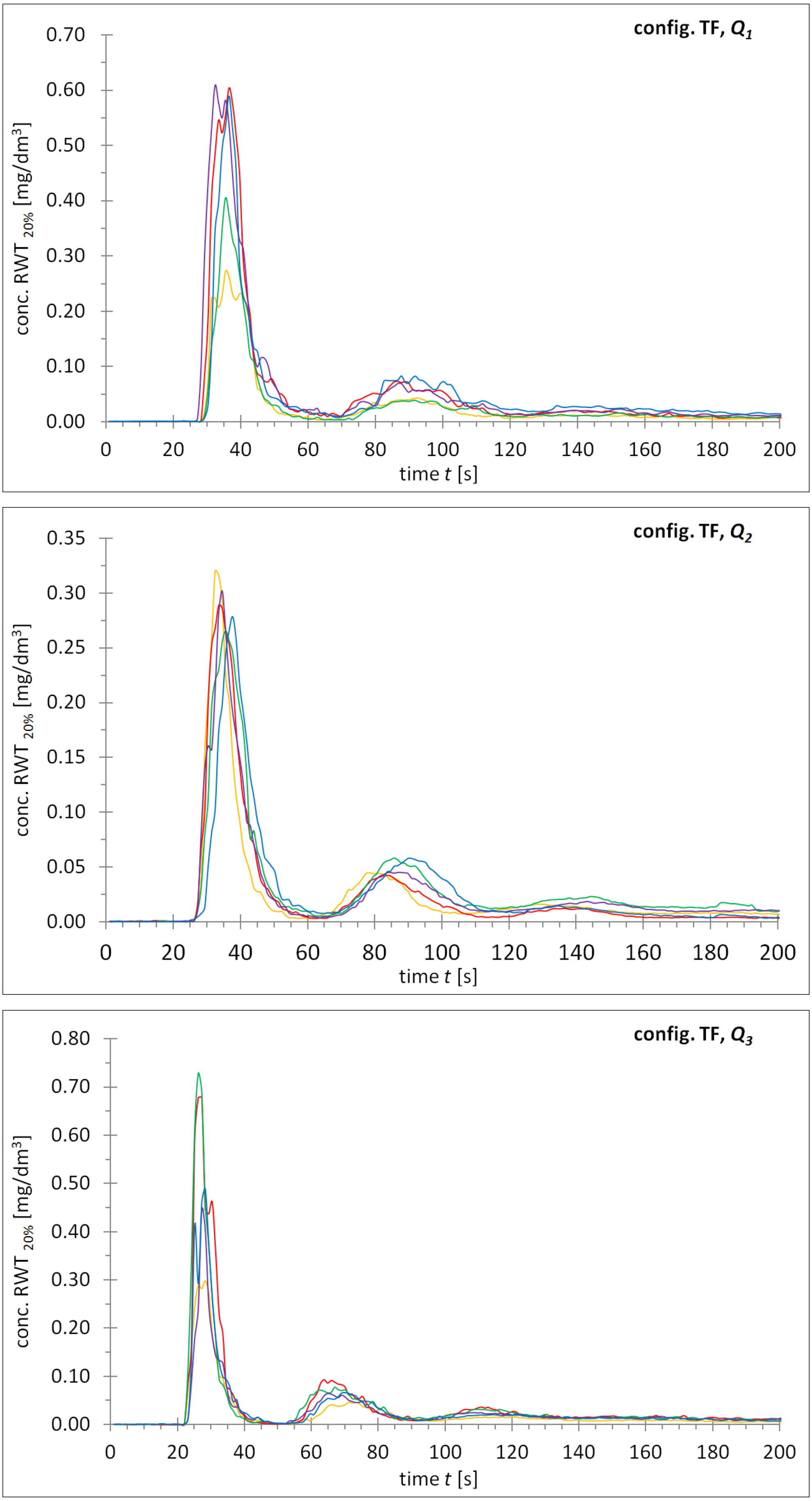

Fig. App2.8. Residence time distribution curves $E(t)$ for configuration “TF”

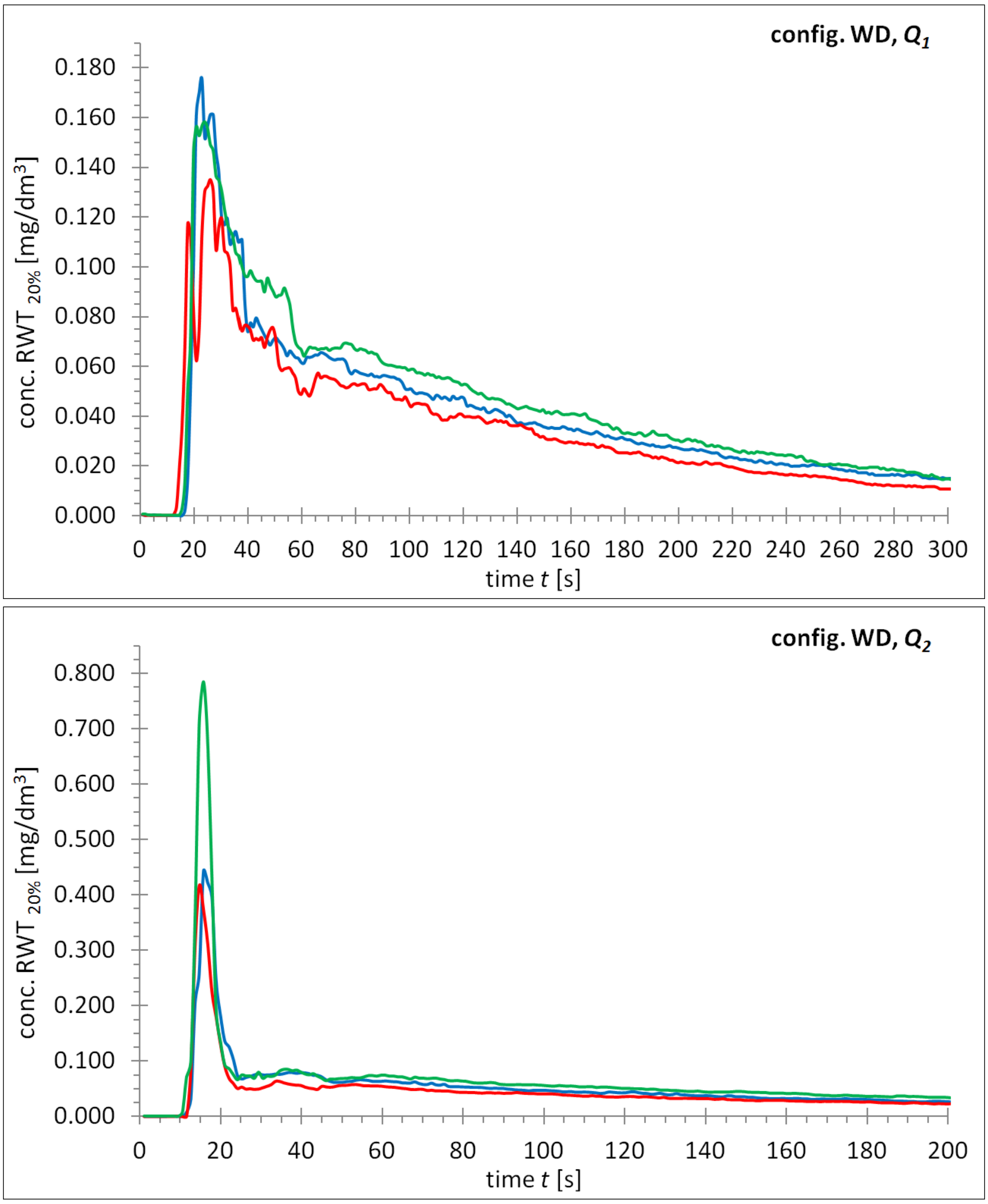

Fig. App2.9. Residence time distribution curves $E(t)$ for configuration "WD"

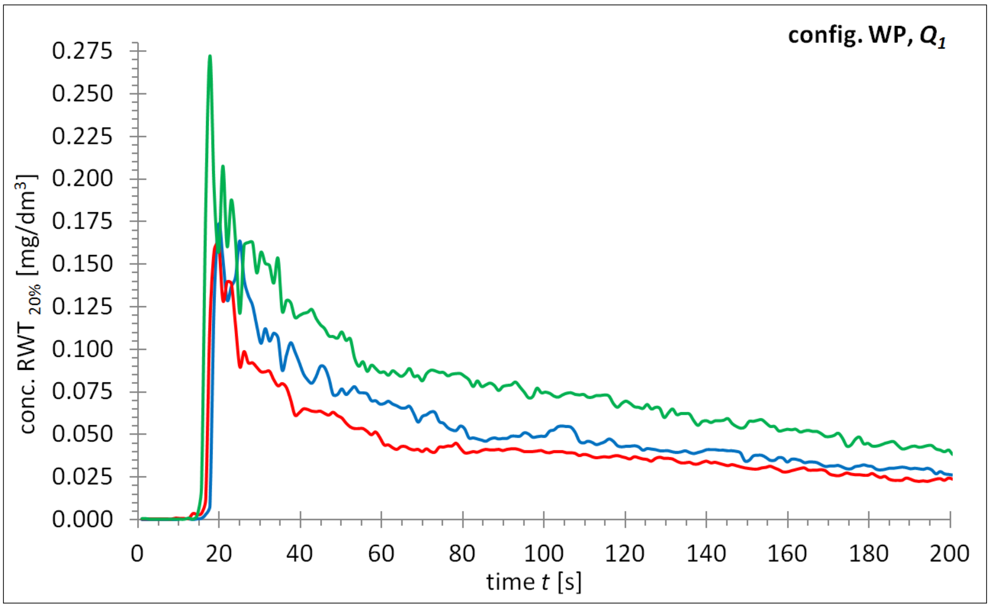

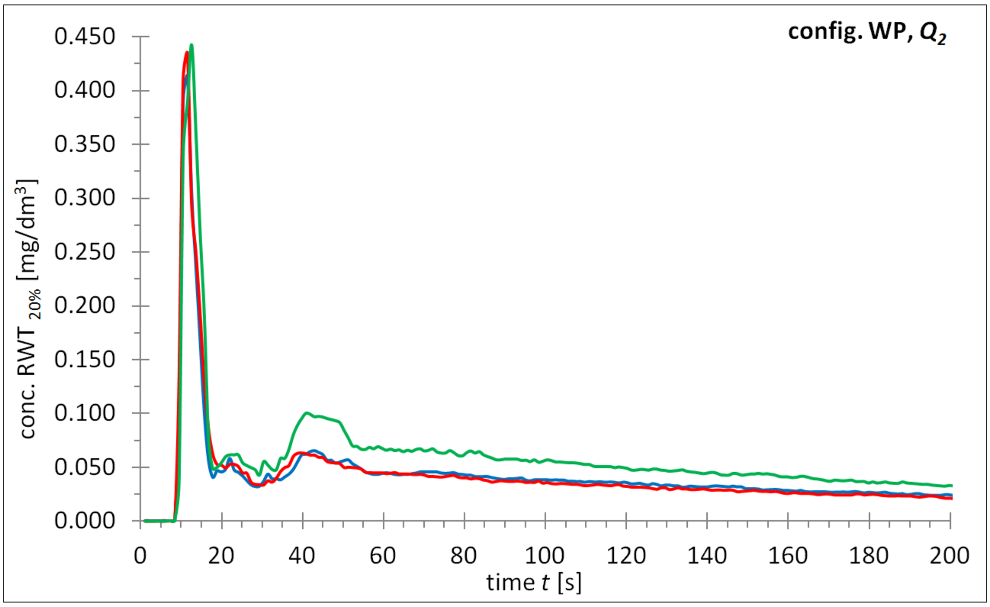

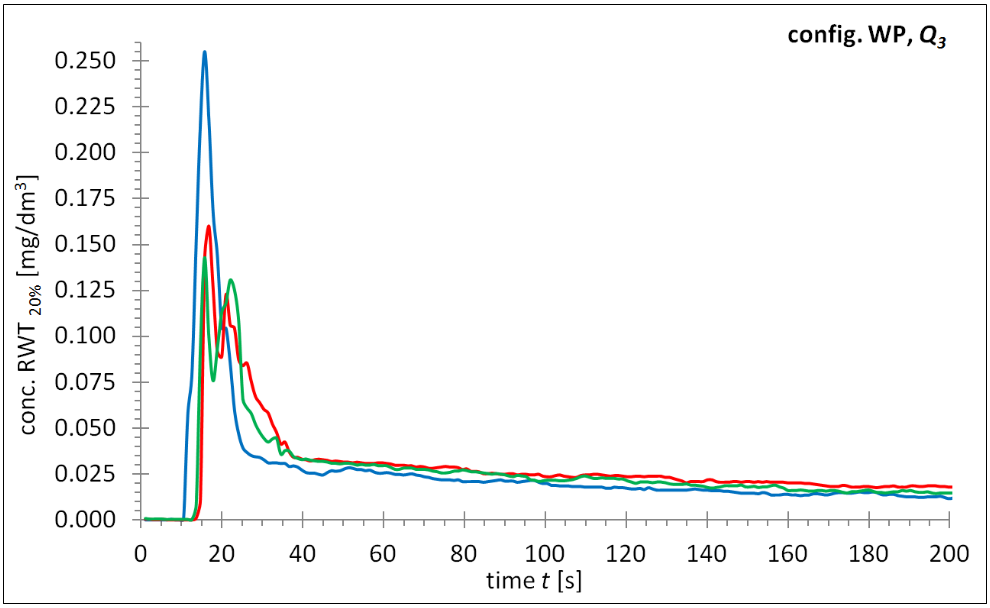

Fig. App2.10. Residence time distribution curves $E(t)$ for configuration “WP”

Appendix No. 3

Photographs of the laboratory test stand and the prototype of vortex separator.
Films demonstrating operation of laboratory separator and tracer measurements on a DVD.